Title	Synthesis of new organic optical materials for micro-optical devices(Dissertation_)
Author(s)	Kawatsuki, Nobuhiro
Citation	Kyoto University ( )
Issue Date	1994-07-23
URL	http://dx.doi.org/10.11501/3077516
Right	
Type	Thesis or Dissertation
Textversion	author

SYNTHESIS OF NEW ORGANIC OPTICAL MATERIALS FOR MICRO-OPTICAL DEVICES

NOBUHIRO KAWATSUKI

1994

Synthesis of New Organic Optical Materials for Micro-Optical Devices

Nobuhiro Kawatsuki

1994

Preface

The work described in this thesis has been carried out at Central Research Laboratories, Kuraray Co. Ltd. during 1986-1989 and at the Materials Department, University of California, Santa Barbara during 1990-1992 under the direction of Professor Hans-Werner Schmidt. This thesis is concerned with the synthesis of new passive and active optical polymers and their applications for micro-optical devices.

The author wishes to express his sincere gratitude to Professor Hans-Werner Schmidt and Dr. Masao Uetsuki for valuable suggestions and hearty encouragement throughout this work. The author's grateful acknowledgment is due to Professor Isao Saito for his precious comments and suggestions for this thesis.

Grateful acknowledgment is also due to Professor Paul Smith and Professor Alan J. Heeger for their comments and experimental suggestions. The author is grateful to Dr. Junji Nakagawa for his constant advises and discussions for optical materials and applications. The author deeply thanks to Emeritus Professor Teruo Matsuura, Professor Isao Saito and Dr. Yoshikatsu Ito who had instructed him on basic photochemistry.

The author is greatly indebted to Dr. Khashayer Pakbaz, Mr. Michael Dörr, Mr. Rikuji Watanabe, Mr. Toshiaki Tokuhara, Dr. Shiro Nagata and Mr. Hidejiro Ichimura for their active collaborations. Special thanks are also due to Dr. Reiner Giesa, Dr. Wilfried Hatke, Mr. Kevin Becker, Ms. Jackie S. Uhm, Ms. Petra Eiselt, Mr. Andy Hays, Mr. Craig Halvorson and all of members of Professor Schmidt's, Professor Smith's and Professor Heeger's laboratories for their goodwill and kindness.

CONTENTS

General Introduction

Organic optical materials are of great interests as optical elements for integrated devices such as optical switching, photonic transmissions, and memory applications. [1,2] Because of low cost, easy fabrication and variability of materials, polymeric materials have a great advantage compared to inorganic materials. Many kinds of polymeric materials have been synthesized and applied as passive and active integrated optical elements. [1,2] In fabricating optical devices from thin polymer films that are usually prepared on a substrate by means of spin-coating technique, it is frequently required to draw precise patterns on the films. The patterning has been achieved by surface structure modification or by refractive index modification of the film. The most important feature of organic materials is that they can utilize light beams to induce, selectively and with high resolution, substantial changes of the physical properties of the material.

Photochemical reactions cause a considerable change in the diffusion rate of dopants or the solubility of polymers. Chandross *et al* [3] proposed a photolocking process shown in figure 1, in which a photochemical reaction was used to lock or fix a dopant in a polymer film with a lower refractive index and the unreacted dopant was then removed by heating. They prepared a photoreactive polymer film from a 1:1 copolymer of methyl methacrylate (MMA) and glycidyl methacrylate doped with ethyl 2-(1-naphtyl)-acrylate. The inherent refractive index of the dopant was ~1.60, well above that of the copolymer (N=1.515). After exposure to ultraviolet beams followed by heating, they found that the exposed portion was ~15% greater in thickness and 1.3% higher in refractive index than the unexposed portion.[3] Using naphthalenethiol as the dopant in the preceding process, they

1
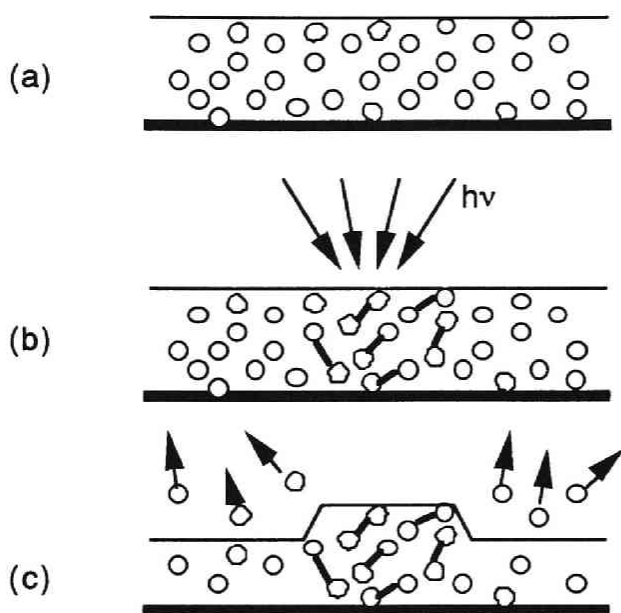
Figure 1. Schematic representation of the photolocking process, using dimerization of the dopant as the photosensitive process.

(a) A polymer film doped with photosensitive species (circles)
(b) Selective dimerization is initiated by UV light.
(c) Heating removes unreacted monomer.

confirmed that the exposed portion was ~10% thicker and 1.3% higher in refractive index than the unexposed portion.[4] Franke observed a refractive index change of ~3% in a photoreactive film of poly-(methyl methacrylate) (PMMA) doped with 2,2-di-methoxy-1,2-diphenyl-ethanone. [5] Combining the photoreactive copolymer of Chandross *et al* [3] with the dopant studied by Franke, [5] Driemeier and Brockmeyer [6] recorded optically a phase grating in the copolymer film to attain a resolution better than 1200 lines/mm and a refractive index change of 1.2%. These materials can be applied to passive optical devices.

There is also a great potential in the use of these organic materials as optically active systems such as nonlinear optical (NLO) devices. [2] As compared with inorganic materials, organic materials have unique possibilities, such as high nonlinear coefficients and higher frequency capacity due to their low dielectric constant, and a higher flexibility which is very important for device fabrications. In the case of polymeric non-linear optical materials, nonlinear optically active moieties should be polymerized or co-polymerized in a polymer side-chain or a main-chain. Because second order NLO polymers are usually aligned the NLO chromophores by an external electric field, stable alignment of them, which tends to relax, must be essentially required for the practical use. Many kinds of NLO side-chain and/or main-chain polymers have been studied, some of which are applied to a waveguide switching, modulation or second harmonic generation (SHG) prototype devices. [7-25]

The principal problem with second-order NLO polymers is a relaxation of the non-centrosymmetric structure. One approach for solving this problem is the formation of a chemically crosslinked network during or after the poling process. Thermally crosslinkable NLO polymers were first reported a few years ago by an *IBM group* on the basis of multifunctional epoxy monomers and nitrophenylamine chromophores. [17,18] Other thermally crosslinkable NLO polymer systems have been reported subsequently. [19,20] In the case of photocrosslinkable NLO-polymers, the crosslinking can be performed by irradiation at various temperatures during and/or after the poling process. Photocrosslinking additionally offers patternability by photolithographic techniques as follows: Tripathy *et al* [21,22] studied photocrosslinkable host-guest NLO systems, based on the photoreaction of cinnamoyl esters. The same crosslinking reaction

was also used in NLO side chain polymers. [23] Another approach to keep a stable non-centrosymmetric alignment is to synthesize high Tg NLO materials. An aromatic polyester derivative is one of the candidates to achieve high Tg NLO materials if they possess a NLO chromophore in their structure. Because of low solubility in organic solvents, it is difficult to apply the aromatic polyesters to the NLO materials. Hall *et al* [24] obtained soluble aromatic NLO polyesters containing *p*-oxy-α-cyanocinnamate units by incorporating small amount of methylene units into them. Stenger-Smith *et al* [25] also found that NLO polyesters having methylene units in their main-chain were soluble in chloroform and that their Tg was around 100 °C.

Following conditions are required in order to utilize polymer materials for passive or active optical elements such as waveguides, optical gratings or nonlinear optical devices:

1. Polymer materials are soluble in solvents to fabricate a thin polymer film, which is usually formed on a substrate by spin-coating.
2. Some physical or chemical change of the polymer materials are needed to draw a pattern useful for waveguide or grating devices.
3. Patterned structure and optical properties of the polymer materials should be stable under high temperature and humidity.
4. NLO chromophore can be aligned by the external electric field and the aligned structure does not relax.

Photochemical reaction is a useful tool in patterning because it often causes large change in properties of polymer materials such as refractive index, thickness or absorption spectrum. If the

4

patterning photoreaction takes place intermolecularly, photo-crosslinking reaction can occur to raise Tg of the patterned portion forming a stable structure. Furthermore, when the crosslinking reactions are carried out under the electric field, alignment of the chromophore would be very stable in the case of NLO polymers.

From these points of view, new photoreactive copolymer materials for optical elements were synthesized and applied to optical devices such as the phase grating. These materials are gradually changing in refractive index and in thickness by UV light irradiation and showing a stable structure. The phase gratings made from the photoreactive materials have been practically used for an optical pick up head and other optical elements. [25] Side-chain and main-chain modified NLO polymers were also synthesized in order to achieve stable chromophore alignment. These polymers were studied from the following two points of view: One was to synthesize crosslinkable NLO copolymers based on a concept of photo- and thermal-crosslinking reactions. Another was to synthesize aromatic polyesters with strong acceptor group which was soluble in organic solvents enough to be useful to fabricate thin films. This thesis consists of the following three parts:

Part 1.
Synthesis and characterization of new photoreactive methacrylic copolymers for optical elements.

Part 2.
Optical grating elements made from photoreactive polymers and their applications to an optical pickup head.

Part 3.
Synthesis of new second order nonlinear optical polymers based on poly-methacrylic esters and aromatic polyesters.

Part 1 contains 2 chapters and deals with the synthesis of new photoreactive copolymers for optical elements and the reaction mechanism. Chapter 1 describes synthesis and optical properties of photo-patternable optical copolymers stable at high temperature and their photo-patterning processes. Chapter 2 deals with the mechanistic study of the photoreaction of typical photo-patternable materials in solution and solid states.

The photoreactive copolymers in Part 1 are based on methyl methacrylate and methacrylic ester which comprises olefinic double bonds in its side chain. A film of this copolymer doped with aromatic ketone derivatives can react photochemically and shows changes of refractive index and thickness after exposure to UV light followed by removal of unreacted aromatic ketones, according to the photolocking system. Reaction mechanism is mainly based on the photoreaction between excited benzophenone and olefinic derivatives as shown in figure 2. Refractive index change and thickness change of this system were 3 % and 100 %, respectively, and the patterned structure made from the materials have been very stable as a result of crosslinking.
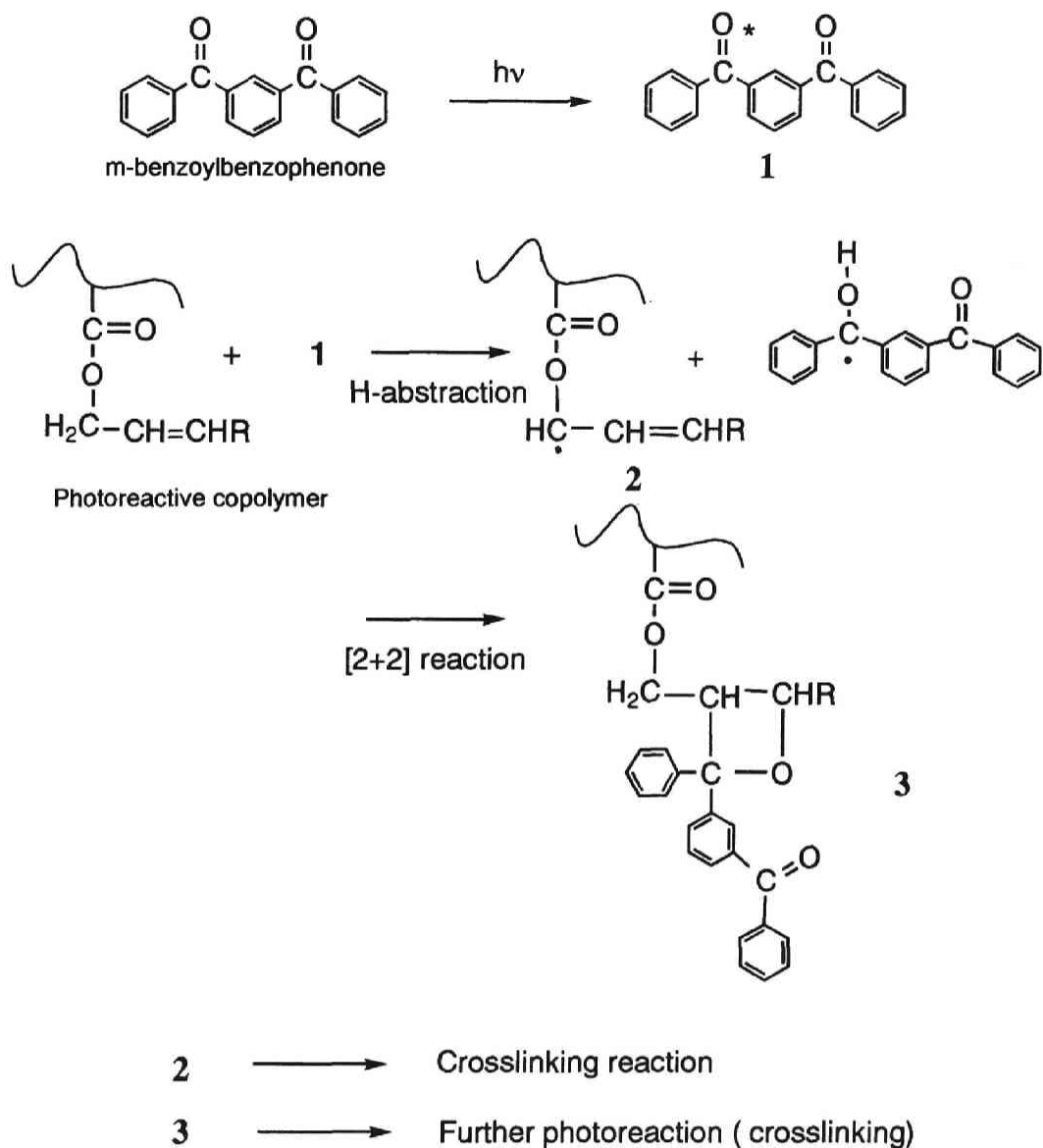
Figure 2. Photoreaction of *m*-benzoylbenzophenone with photoreactive polymers.

7

Part 2 is consisted of two chapters and deals with the application of organic materials to optical elements. As an application of photoreactive polymer materials in part 1, chapter 3 describes an optical phase grating for a three-beam optical pick-up head in CD (compact disc) or LD (laser disc) players. Due to a trapezoid structure of the phase grating made from photoreactive polymers, total intensity of non-usable light beam (> 2nd order diffraction light beams) was much less than that of a rectangular shape phase grating which was usually made from inorganic materials.

In the case of magneto-optical (MO) pick-up head, several polarizing beam splitters (PBS's) are needed to read out a slight change of polarization angle of signal laser beam reflected from a MO disk. It has been practically required that the PBS is replaced by a high-density holographic grating in a form of a planar phase grating. [27] Chapter 4 describes new multifunctional holographic grating and demonstrats that it can be used for MO pick-up head.

Part 3 contains three chapters and deals with second order nonlinear optical materials. Chapters 5 and 6 describe crosslinkable side-chain modified NLO copolymers and corona poling studies. For the application of photoreactive polymer materials described in part 1 to NLO materials, 4'-[(2-hydroxyethyl)-ethylamino]-4-nitroazobenzene (DR1) was attached to the methacrylate backbone as shown in figure 3.

Chapter 5 describes corona poling and SHG studies for NLO copolymers crosslinked by thermal reaction at high temperature and photo-reaction with m-benzoylbenzophenone prior to the corona poling step. The alignment and relaxation of the chromophores will be optimized by the pre-crosslink density. The SHG intensity during the corona poling and stability in the NLO

8

copolymers with different pre-crosslinking conditions were discussed.

Chapter 6 describes new photo-crosslinkable copolymers based on the similar reaction as described in part 1, which are based on methyl methacrylate, a photo-excitable benzophenone
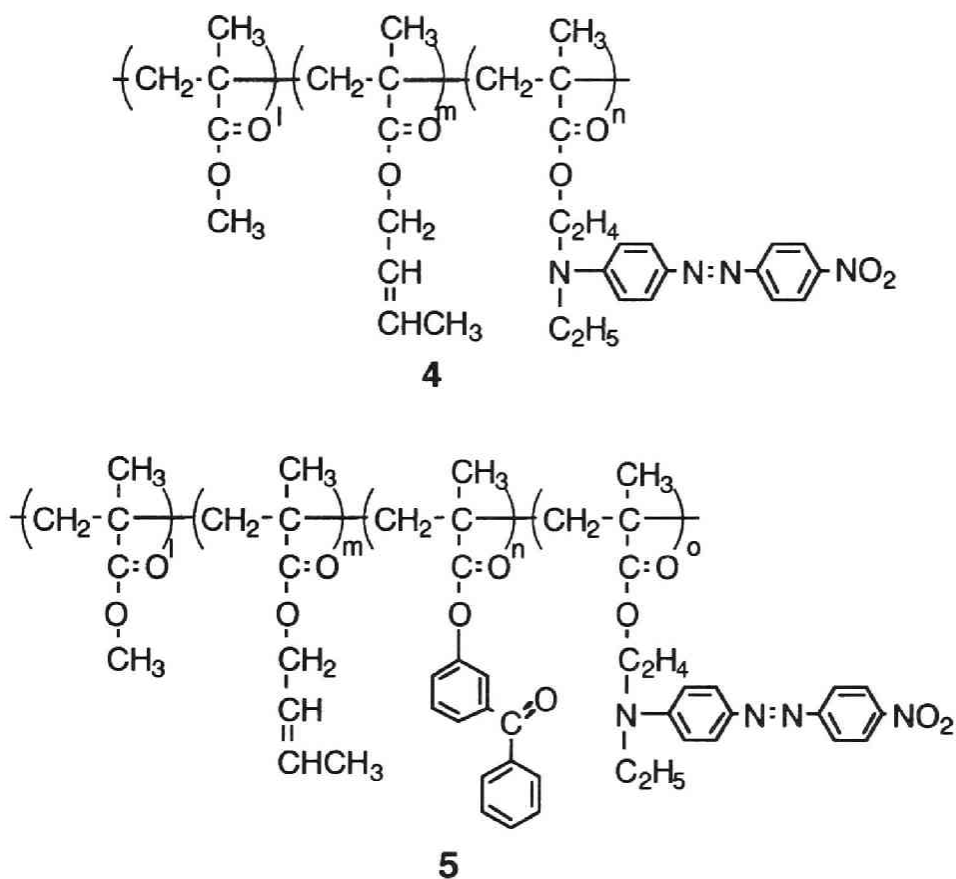
Figure 3. Chemical structures of thermally and photochemically crosslinkable NLO copolymer **4** described in chapter 5 and photochemically crosslinkable copolymer **5** described in chapter 6.

monomer, a crosslinkable 2-butenyl monomer and a nonlinear optical active DR1 side chain monomer. The copolymers can be crosslinked by UV light at 366 nm under the corona poling and show a stable alignment of NLO chromophore.

Chapter 7 presents a synthetic aspect and characterization of aromatic polyesters possessing dicyanovinyl substituents. The dicyanovinyl substituent has been utilized as an alternative group to nitro and cyano substituents in designing donor-π-acceptor chromophores for nonlinear optical effects.[2] Two structurally comparable polyester series based on two catechol derivatives with dicyanovinyl substituents were prepared (figure 4).

Figure 4. Chemical structure of dicyanovinyl substituted aromatic polyesters based on catecol units and terephthalic acid or isophthalic acid units.

References

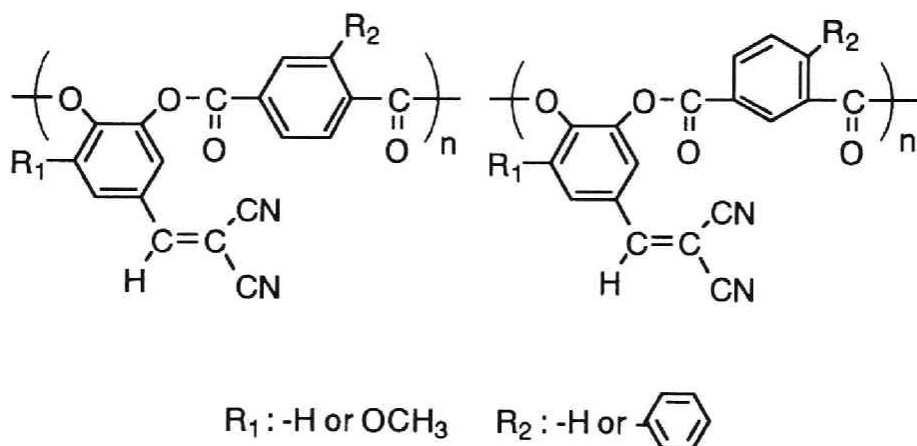1) Reviews, see for example : a) L. A. Hornak ed., *"Polymers for Lightwave and Integrated Optics "*, Marcel Dekker, New York, (1992), b) C. B. McArdle ed., *"Applied Photochromic Polymer Systems"*, Blackie, New York (1992), c) H. P. Weber, W. J. Tomlinson, and E. A. Chandross, *Opt. Quantum Electron.,* **7**, 465 (1975).

2) Reviews for NLO materials, see for example : a) P. N. Prasad and D. R. Urich (Eds.) *"Nonlinear Optical and Electroactive Polymers"* Plenum Press (1988), b) P. N. Prasad and D.J. Williams (Eds.) *"Nonlinear Optical Effects in Molecules and Polymers"* John Wiley & Sons (1991), c) R. Lytel, G. F. Lipscomb, M. Stiller, J. I. Thackara, and A. J. Ticknor, *Nonlinear Optical Effects in Organic Polymers,* J. Messier et al. eds., Kluwer Academic Publishers (1989), p.277, e) S. R. Marder, J. E. Sohn, and G. D. Stucky (Eds.) " Materials for Nonlinear Optics" ACS Symposium Series 455 (1990), f) D. R. Ulrich, *Mol. Cryst. Liq. Cryst.,* **189**, 3 (1990).

3) E. A. Chandross, C. A. Pryde, W. J. Tomlinson, and H. P. Weber, *Appl. Phys. Lett.,* **24**, 72 (1974).

4) W.J.Tomlinson, H. P. Weber, C. A. Pryde, and E. A. Chandross, *Appl. Phys. Lett.,* **26**, 303 (1975).

5) H. Franke, *Appl. Opt.,* **23**, 2729 (1984).

6) W. Driemeier and A. Brockmeyer, *Appl. Opt.,* **25** 2960 (1986).

7) S. Ducharme, J. C. Scott, R. J. Twieg, and W. E. Moerner, *Phys. Rev. Lett.,* **66**, 1846 (1991).

8) H. L. Hampsh, J. Yang, G. K. Wong, and J. M. Torkelson, *Macromolecules,* **21**, 526 (1988).

9)   K. D. Singer, M. G. Kuzyk, W. R. Holland, J. E. Sohn, S. J. Lalama, R. B. Comizzoli, H. E. Katz, and M. L. Schilling *Appl. Phys. Lett.,* **53**, 1800 (1988).

10)   M. L. Schilling, H. E. Katz, and D.I. Cox , *J. Org. Chem.,* **53**, 5538 (1988).

11)   Z. Ni, T. M. Leslie, A. Buyle Padias, and H. K. Hall, Jr., *Macromolecules,* **24**, 2100 (1991).

12)   G. Gadret, F. Kajzar and P. Raimond, *Proceedings SPIE* **1560**, 26 (1991).

13)   Y. Shuto, M. Amano and T. Kaino, *Proceedings SPIE* **1560**, 184 (1991).

14)   H. E. Katz, K. D. Singer, J. E. Sohn, C. W. Dirk, L. A. King and H. M. Gordon, *J. Am. Chem. Soc.,* **109**, 6561 (1987).

15)   K. D. Singer, M. G. Kuzyk, W. R. Holland, J. E. Sohn, S. J. Lalama, R. B. Comizzoli, H. E. Katz, and M. L. Schilling, *Appl. Phys. Lett.,* **53**, 1800 (1988).

16)   E. Eich, A. Sen, H. Looser, G. C. Bjorklund, J. D. Swalen, R. Twieg, and D. Y. Yoon, *Appl. Phys. Lett.,* **66**, 2559 (1989).

17)   M. Eich, B. Reck, D. Y. Yoon, C. Grant, and G. C. Bjorklund, *J. Appl. Phys.,* **66**, 3241 (1989).

18)   D. Jungbauer, B. Reck, R. Twieg, D. Y. Yoon, C. G. Willson, and J. D. Swalen, *Appl. Phys. Lett.,* **56**, 2610 (1990).

19)   K. D. Singer, M. G. Kuzyk, T. Fang, W. R. Holland and P. A. Cahill, *Organic Molecules for Nonlinear Optics and Photonics,* J. Messier, F. Kazyar and P. Prasad. eds., NATO ASI Series E. **Vol 194** 105 (1991).

20)   S. Allen, D. J. Bone, N. Carter, T. G. Ryan, R. B. Sampson, D. P. Devonald and M. G. Hutchings, *Organic Materials for Nonlinear Optics II.* R. A. Hann and D. Bloor eds., Redwood Press Ltd, Melksham, Wiltshire (1991), p235.

21)   B. K. Mandal, J. Kumar, J.-C. Huang, and S. Tripathy, *Makromol. Chem., Rapid Commun.,* **12**, 63 (1991).

22) B. K. Mandal, J. Kumar, J.-C. Huang, and S. Tripathy, *Appl. Phys. Lett.*, **58**, 2459 (1991).

23) H. Müller, I. Müller, O. Nuyken, and P. Strohriegel, *Makromol. Chem., Rapid Commun.*, **13**, 289 (1992).

24) H. K. Hall Jr., *J. Macromol. Sci.- Chem.* **A25**, 5-7, 729 (1988).

25) J. D. Stenger-Smith, J. W. Fischer, R. A. Henry, J. M. Hoover, G. A. Lindsay, and L. M. Hayden, *Makromol. Chem., Rapid Commun.*, **11**, 141 (1990).

26) M. Uetsuki, *"Small Optical Elements"*, Optronics Co. p129,1991.

27) M. G. Moharam, T. K. Gaylord, G. T. Sincerbox, H. Werlich, and B. Young, *Appl. Opt.*, **23**, 3214 (1984).

Part 1.

Synthesis and Characterization of
New Photoreactive Methacrylic Copolymers for
Optical Elements

Chapter 1

Photo-Patternable Copolymers with High Thermal Stability: Synthesis, Optical Properties, and Photo-Patterning Process Studies

Abstract : Photopatternable copolymers and photo-patterning processes for optical elements with high thermal stability have been studied. The photo-patternable copolymers were synthesized from methyl methacrylate and methacrylic ester comprising non-conjugate carbon-carbon double bond side chain and epoxy side chain, and their optical properties were investigated on film samples doped with m-benzoylbenzophenone (BBP). After irradiating with UV light, insoluble polymer was formed in a high yield at higher temperature, resulting in changes in thickness and refractive index, which were precisely controlled by the exposure energy of UV light. The two steps photo-patterning processes were carried out by means of UV irradiations with and without a photomask bearing a grating pattern followed by removal of unreacted BBP to draw an optical pattern on the polymer material with crosslinking. Further photoreaction was also performed to cure the polymer by exposure with a high energy UV lamp containing shorter wavelength light after the patterning process. By a combination of the patterning process and the post-curing process, an optical grating fabricated from these copolymers showed a heat-stability up to 160 °C.

Introduction

Because of the great potential of organic polymer materials for integrated optics and photonics, a lot of functionalized polymeric materials have been studied. [1] Optical patterning is often useful for fabricating waveguides and/or grating elements. Usually, wet process of UV-lithography procedure requires to develop UV-patterned photoresist. To fabricate a patterned structure on the materials directly, Chandross *et al* proposed a photolocking process in which a photochemical reaction was used to fix a dopant in a polymer film with a lower refractive index and the unreacted dopant was then removed by heating. [2] The photo-locking has been studied on methacrylate copolymers doped with photoreactive dopants. [3-7] The advantage of this method is that the optically patterned structure can be directly formed on a polymer material by a photoreaction with UV irradiation. We developed a photoreactive polymer composite composed of copolymers of methyl methacrylate and a methacrylic ester comprising carbon-carbon double bond doped with an aromatic ketone. [6,7] Film thickness and refractive index can be changed with UV irradiation followed by removal of the unreacted aromatic ketone. The photoreaction was applied to fabricate optical phase gratings and they showed heat-stability up to 85 °C. [7]

In the semiconductor industry, optical elements are sometimes put in a high temperature atmosphere such as a thin inorganic film coating or an assembling process. In the case of organic optical elements, the structure of the optical pattern tends to deform at a high temperature because of their mobility above the glass transition temperature (Tg). Optical elements fabricated from our materials [7] did not have enough heat-stability for these

processes at 150 °C. Photo-patternable organic materials with higher thermal stability are required in practical use.

One of the factors for hardness of a polymer is attributed to a crosslinking of the material, so that higher Tg and less mobility of the material could be expected. Photochemical reaction is effective for crosslinking as well as changing in optical properties if the reaction undergoes not only between a polymer and a dopant but also between polymers. The patterning process of photoreactive materials should be designed to achieve a crosslinked structure for whole patterned area.

This chapter will describe new photopatternable optical materials and a new patterning process of those with UV light to accomplish a high temperature stable patterned structure. The materials consist of methacrylate copolymers comprising carbon-carbon double bond and epoxy side chain, and *m*-benzoylbenzophenone (BBP). Glycidyl methacrylate have been co-polymerized to the copolymer previous reported [7] to achieve higher crosslinking. Insoluble polymer was formed by irradiating UV light and its amount was changed with reaction temperature. Optical properties of the materials and optical patterning processes comprising a few irradiation steps have been studied. Optical phase grating made from a new copolymer doped with BBP and a new process showed a high temperature stability at 160 °C for several hours without change in optical properties and the structure.

Experimental

Materials :

Methyl methacrylate, glycidyl methacrylate and methacryloyl chloride were used after distillation to remove the reaction inhibitor. Geraniol was supplied by Kuraray Co., Ltd.

and used without further purification. *m*-Benzoylbenzophenone was synthesized as described previously. [8] All other solvents and chemicals were commercially available and used as received.

Monomer synthesis :

2-Butenyl methacrylate (1a)

Under nitrogen atmosphere, a mixture of 28.0 g (0.389 mol) of 2-butenol, 39.2 g of triethylamine, 20 mg of 2,6-di-*t*-butyl-4-methyl-phenol (inhibitor) and 300 ml of dry ether was cooled to 5 °C. 40.6 g (0.4 mol) of methacryloyl chloride was added dropwise with stirring. The reaction mixture was stirred for 2 h at 0 °C and kept overnight at room temperature. After adding 300 ml of ether into the reaction mixture, the solution was poured into 300 ml of water and extracted with diethyl ether (3 X 100 ml). The combined ether extracts were washed with saturated aqueous sodium chloride (300 ml) and water (300 ml) and dried over sodium bicarbonate. The solvent was removed at reduced pressure and the raw product was distilled under vacuum. Finally the product was further purified by column chromatography over silica gel using dichloromethane as eluent.
Yield : 24 g (45%) ; b.p. 70 - 72 °C/22 - 24 mmHg.
^{1}H-NMR: (CDCl$_3$): δ (ppm) = 1.70 (brs, 3H), 1.94 (s, 3H), 4.54 (brs, 2H), 5.51 (brs, 1H), 6.10 (brs, 1H), 5.58-5.80 (m, 2H).
IR (neat): 1718 (C=O), 970 (C=C) cm^{-1}.

2-Methyl-2-butenyl methacrylate (1b)

1b was synthesized by the same procedure as **1a** from 91.4 g (1.02 mol) of 2-methyl-2-butenol and 107 g (1.02 mol) of methacryloyl chloride. The raw product was purified by distillation followed by column chromatography over silica gel using dichloromethane as eluent.

20

Yield : 56.6 g (36%) ; b.p. 55 - 59 °C/3 - 6 mmHg.
^{1}H-NMR: (CDCl$_3$): δ (ppm) = 1.70 (brs, 3H), 1.92 (s, 6H), 4.55 - 4.70 (m, 2H), 5.24 - 5.50 (m, 2H), 6.08 (brs, 1H).
IR (neat): 1712 (C=O), 970 (C=C) cm^{-1}.

2-Methyl-2-propenoyl methacrylate (1c)

1c was also synthesized by the same procedure as **1a** from 2-methyl-2-propene-1-ol and methacryloyl chloride. The raw product was purified by column chromatography over silica gel using a mixture of hexane and ethyl acetate (19 : 1) as eluent.
Yield : 35 % ; viscous oil .
^{1}H-NMR: (CDCl$_3$): δ(ppm) = 1.76 (brs, 3H), 1.95 (s, 3H), 4.56 (brs, 2H), 4.92 (brs, 1H), 4.99 (brs, 1H), 5.56 (brs, 1H), 6.62 (brs, 1H).
IR (neat): 1715 (C=O), 965 (C=C) cm^{-1}.

Geranyl methacrylate (1d)

1d was also synthesized by the same procedure as **1a** from 31 g (0.201 mol) of geraniol and 20 g (0.191 mol) of methacryloyl chloride. The raw product was purified by column chromatography over silica gel (hexane : ethyl acetate = 5 : 1 as eluent).
Yield : 15.9 g (37.5%) ; viscous oil.
^{1}H-NMR: (CDCl$_3$): δ(ppm) = 1.58 (s, 3H), 1.62 (s, 3H), 1.68 (s, 3H), 1.90 (s, 3H), 2.00 - 2.11 (m, 4H), 4.64 (brs, 2H), 5.06 and 5.35 (s, 2H), 5.51 (s, 1H), 6.09 (s, 2H).
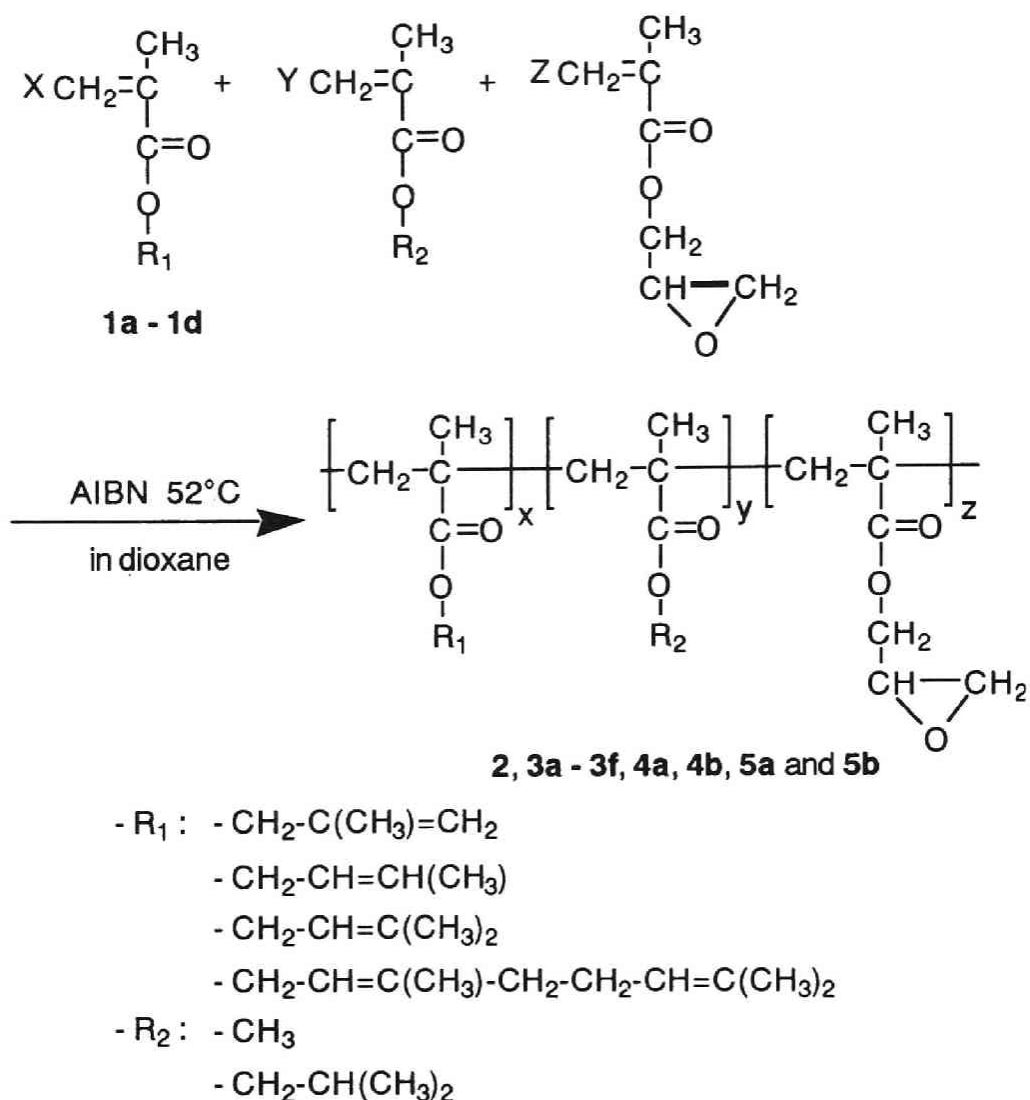IR (neat): 1718 (C=O), 970 (C=C) cm^{-1} .

Figure 1. Synthesized photoreactive methacrylate copolymers.

Polymer synthesis :

The copolymers **2** , **3a - 3f** , **4a** , **4b**, **5a** and **5b** (figure 1) were obtained by a free radical solution polymerization in a dioxane with AIBN as an initiator. The concentration of

monomers was 30 - 40 %(w/v) and the [monomers]/[AIBN] molar ratio was about 1000. Monomer feed ratio, yield and copolymer composition are summarized in Table 1. Poly(methyl methacrylate) (PMMA) and copolymer of methylmethacrylate-co-glycidyl methacrylate (1/1 : mol/mol) were also synthesized from methyl methacrylate by the same procedure and the number

Table 1. Monomer feed ratio, yield and copolymer composition of copolymers **2, 3a - 3f, 4a, 4b, 5a** and **5b**.

No.	Copolymer[a] X - Y - Z	Feed ratio (mol%) X	Y	Z	Yield (%)	Composition(mol%)[b] x	y	z
2	MAMA-MMA	52.0	48.0	-	36	52.8	47.2	-
3a	BMA-MMA	50.0	50.0	-	26	48.2	51.8	-
3b	BMA-MMA	25.1	74.9	-	52	24.1	75.9	-
3c	BMA-MMA	4.8	11.7	-	57	8.7	91.3	-
3d	BMA-iBuMA	25.5	74.5	-	66	24.5	75.5	-
3e	BMA-MMA-GMA	25.0	37.5	37.5	47	24.3	37.1	38.6
3f	BMA-MMA-GMA	24.9	50.2	24.9	48	24.4	49.1	26.5
4a	PMA-MMA	56.5	43.5	-	53	55.1	44.9	-
4b	PMA-MMA	30.8	69.2	-	50	27.5	72.5	-
5a	GeMA-MMA	58.5	41.5	-	44	54.7	45.3	-
5b	GeMA-MMA	26.5	73.5	-	44	23.2	76.8	-

a) Feed monomers : MAMA: 2-methyl-2-propene-1-ol, MMA: methyl methacrylate, BMA: 2-butenyl methacrylate, iBuMA: isobutyl methacrylate, GMA: glycigyl methacrylate, PMA: 3-methyl-2-butenyl methacrylate, GeMA: geranyl methacrylate.

b) Co-polymerization ratio, determined by NMR.

average of molecular weight was about 300,000. As an example for the general copolymerization procedure the synthesis of copolymer **3b** is described as follows:

Copolymer 3b

15.0 g (0.107 mol) of 2-butenyl methacrylate **1a**, 32.0 g (0.32 mol) of methyl methacrylate and 47 mg of AIBN were dissolved in 135 ml of dioxane. The reaction mixture was treated with a gentle stream of nitrogen. After sealing, the mixture was heated to 52 °C for 24 h. The resulting homogeneous viscous solution was cooled and added dropwise into 400 ml of methanol to precipitate the polymer. After two additional precipitations from dichloromethane solution into methanol, the copolymer was extracted under reflux with methanol for 1 day. The polymer was dried at room temperature under vacuum for 48 h.
Yield: 25 g (53 wt %).
^{1}H-NMR (CDCl$_3$): δ (ppm) = 0.81 (brs), 0.98 (brs), 1.1~1.4 (m), 1.6~1.9 (m), 3.60 (brs, OC$\underline{H}_3$), 4.42 (brs, O-C$\underline{H}_2$-CH=CHCH$_3$), 5.57 (brs, O-CH$_2$-CH=C$\underline{H}$CH$_3$), 5.78 (brs, O-CH$_2$-C$\underline{H}$=CHCH$_3$).
IR (film on NaCl): 1730 (ester C=O), 1149, 967 (trans C=C) cm^{-1}.

Characterizations:

Differential scanning calorimetry (DSC) data were obtained on a Mettler DSC 30 using a heating rate of 10 °C/min. The molecular weight and its distribution were measured by using tetrahydrofuran as eluent on a Waters 150-C gel-permeation chromatography (GPC) system calibrated with polystyrene standards. NMR spectra of the samples dissolved in duterated chloroform were measured with a JEOL GX-500 NMR spectrometer operating at 500 and 125 Mz. IR spectra were

measured on a JEOL JMS-DX 300 spectrometer. Copolymer composition was determined from relative intensities of NMR signals of monomeric units.

Refractive indices of thin film samples were measured by a prism coupling method at a wavelength of 632.8 nm on a quartz substrate. Film thickness and surface structure were measured on a Rank-Taylor-Hobson Talystep on the basis of a styrus contact method.

Film preparation :

Thin films were prepared from a solution of approximately 10 wt% of a polymer or a polymer doped with *m*-benzoylbenzophenone (BBP) dissolved in benzene or toluene. The solution was filtered through 0.2 μm Teflon filter, and then spin-coated at 900 - 1000 rpm on a substrate. Quartz substrates were used for measuring refractive index and thickness of the polymer film. IR spectra were measured with thin film samples spin-coated on a plate of a potassium bromide plate.

Irradiation apparatus:

400-W high pressure mercury lamp (Toshiba) with Pyrex filter in a temperature controlled bath was used for preparative photolysis. For evaluating optical and physical properties, photoreactive films were irradiated with a Canon PLA-521 mask aligner equipped with a high pressure mercury lamp with cut filters for IR and deep UV (<300 nm) wavelength lights. Light intensity of this apparatus is 25 mW/cm^2 at 365 nm. This apparatus was also used for fabricating an optical patterning on the film. A high pressure mercury lamp without any filters using a Toshiba Toscure-1000, which contains deep UV wavelength of 254

nm as well as UV wavelength, with a dose rate of 30-60 mW/cm^2 at 365 nm , was also used for post-curing of the film.

Preparative photolysis of the film:

Irradiation procedure was as follows: a solution containing 200 mg of polymer and 120 mg of *m*-benzoylbenzophenone (BBP) in ca. 1 ml of methylene chloride was poured onto a quartz plate. A transparent film was formed after evaporation of the solvent. After baking at 80 °C for 40 min to remove the solvent completely, the film was irradiated for 2 h at various temperatures through a Pyrex filter under a nitrogen atmosphere. Thorough washing of the irradiated film with warm methylene chloride (ca. 100 ml total) left an insoluble polymer, which was collected by filtration. The methylene chloride washings were concentrated under reduced pressure and a soluble polymer was corrected by reprecipitation from methylene chloride solution to methanol. Combined organic solutions were evaporated under reduced pressure and the residue was subjected to preparative TLC (silica gel, methylene chloride as eluent).

It was confirmed that the insoluble polymers isolated above were not contaminated with methylene chloride-soluble substances. Thus, the isolated insoluble polymer was refluxed in methylene chloride overnight. No contaminants were detectable in the methylene chloride layer by HPLC.

Optical properties measurements:

A transparent polymer film doped with 37.5 - 44.4 wt% of BBP on a quartz substrate was irradiated with a Canon PLA-521 mask aligner for 0 - 15 min. After the exposure unreacted BBP was removed by sublimation at 105 °C for 20 h under vacuum of

0.2 mmHg. Thickness and refractive index change of the exposed and unexposed region was then measured respectively.

Fabrication process of optical elements:

Typical fabrication process for the optically patterned elements such as a phase grating is shown in figures 2(a) - (e). Films used for this experiment were 0.1 - 3.0 μm thick and formed on a washed glass substrate. After the film was heated at 80 °C for 40 min to remove a solvent, it was irradiated for 2 - 15 min through a photomask with a grating pattern on a Canon PLA-521 mask aligner. After the first UV irradiation, the film was irradiated again for 0 - 2 min without photomask to react the unexposed region of the first irradiation step. The sample was then heated at 105 °C for 20 h under vacuum of 0.2 mmHg to allow the unreacted BBP to sublime. Thereby an optical phase grating was fabricated. A post-curing process after the patterning process with a Toscure-1000 was performed to the sample without photomasks for 7 - 17 min for a further photoreaction.

IR spectra monitoring:

A thin film containing 44.4 wt% of m-benzoylbenzophenone in a polymer composite on a potassium bromide plate with a thickness of about 0.5 mm was irradiated with a Canon PLA-521 mask aligner and a Toshiba Toscure-1000 UV lamp apparatus. IR-spectrum was monitored at each step of the fabrication process of a phase grating as shown in figures 2(a) - 2(e).
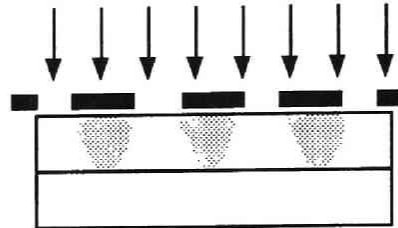
Film coating process

- Copolymer/dopant
  spin-coating.
  thickness : 1 - 3 µm.

- Prebaking, 60 -80 °C
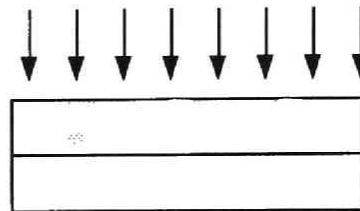 40 min.

(a)
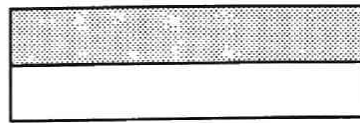
Patterning process

- UV light irradiation
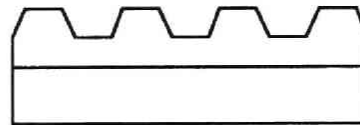 through a photomask
  (on PLA-521)

(b)

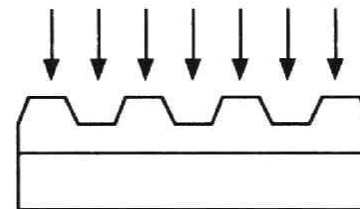- UV light irradiation
  without the photomask

(c)

- Heating to remove
  unreacted BBP

(d)

Post-curing process

- Post-curing without
  any masks.
  (on Toscure-1000)

(e)

Figure 2. Optical patterning process for fabricating optical elements
from the photoreactive copolymers.
(a) Toluene solution of copolymer/m-benzoylbenzophenone was spin-coated on a
washed substrate (thickness; 1 - 3 µm), and pre-baking at 60-80 °C for 40 min.
(b) Optical patterning through a photomask.
(c) Additional UV irradiation without the photomask.
(d) Optical pattern development by removing un-reacted m-benzoylbenzo phenone
by sublimation at 150 °C under 0.2 mmHg for 20 h .
(e) Post-curing irradiation without photomasks on Toscure-1000.

28

Durability measurements:

Durability of diffraction efficiency was measured before and after heating for 7 h at 160 °C on the phase gratings made from photoreactive copolymers. Three gratings from different copolymers (**3b** and **3f**) with different fabrication processes were fabricated and measured.

Results and discussions

Polymer synthesis:

The methacrylate copolymers **2**, **3a - 3f**, **4a**, **4b**, **5a** and **5b** studied in this paper are based on methyl methacrylate, methacrylic ester comprising non-conjugate carbon-carbon double bonds, and glycidyl methacrylate (figure 1). The copolymers were synthesized by a free radical polymerization using AIBN as an initiator. All synthesized copolymers were completely soluble in organic solvents such as benzene or chloroform, indicating that no crosslinking occurred during copolymerization. Polymerization was carried out at 52 °C after purification of the monomers prior to mixing in order to prevent gelation of the reaction mixture, which took place above 60 °C and even below 60 °C without purifying the monomers by column chromatography before the polymerization reaction. The gelation occurred during the reaction when used the monomer purified only by distillation, especially in copolymers **3a - 3f** and highly concentrated comonomers **1a - 1d**. Very small amount of methacryloyl chloride could cause gelation and crosslinking of monomers. The results of GPC, DSC and refractive index investigations of copolymers **2**, **3a - 3f**, **4a**, **4b**, **5a** and **5b** are summarized in Table 2. The molecular weight and its distribution was measured by GPC calibrated with polystyrene standards. All copolymers showed a mono-modal

distribution. The number average molecular weights were in the order of 230,000 - 400,000 g/mol and the weight average molecular weights in the order of 450,000 - 870,000 g/mol. All polymers were amorphous. The glass transition temperature (Tg) varied with a copolymer composition which was dominated by the number of non-conjugate carbon-carbon double bond. Tg decreased with increasing amount of the methacrylic ester of **1a** - **1d**. The copolymers were slightly higher in refractive index than PMMA (n=1.485 at 632.8 nm) with increasing content of comonomers **1a** - **1d**, suggesting the effect of the π-electron located on side chains of the comonomers.

Photoreaction of copolymers doped with m-benzoylbenzo- phenone (BBP):

The photochemical reaction of copolymers **3b** or PMMA doped with BBP was studied in the solid film at various temperatures. The reaction was carried out at a composition of 37.5 wt% BBP doped in a polymer film. Product yields are summarized in Table 3. In the case of copolymer **3b**, an insoluble polymer is a main product as previously reported . [6)]   The yield of the insoluble polymer became larger above 55 °C, whereas recovered copolymer **3b** decreased with raising a reaction temperature. A very small amount of pinacol was formed at lower temperature and the yield of recovered BBP decreased with increasing temperature. These results show that the photoreaction is influenced by the glass transition temperature (Tg) of the matrix. [9)] Photoreaction is faster at the higher temperature because the Tg of the film is about 30 ~ 50 °C by the effect of doped BBP as a plasticizer in the polymer matrix. A small amount of insoluble polymer was also formed in the case of PMMA. This

Table 2. Molecular weight Mw(weight-averaged) and Mn (number-averaged), glass transition temperature (Tg) and refractive index of copolymers **2**, **3a-3f**, **4a**, **4b**, **5a** and **5b**.

No.	Molecular weight[a]			Tg[b] (°C)	Refractive Index[d]
	Mw	Mn	Mw/Mn		
2	c)	c)	-	79.9	1.500
3a	746,000	355,000	2.10	c)	1.499
3b	456,300	278,500	1.63	92.9	1.498
3c	513,500	241,300	2.13	110.2	c)
3d	870,000	398,000	2.19	54.1	1.486
3e	756,000	344,000	2.20	74.2	1.505
3f	724,800	354,800	2.04	81.3	1.505
4a	632,500	273,200	2.32	56.8	1.499
4b	523,600	233,300	2.24	78.9	1.497
5a	728,000	325,000	2.24	c)	1.508
5b	756,000	353,000	2.14	55.4	1.503

a) Determined by GPC, polystyrene standards, THF as eluent.

b) Determined by DSC, second run at heating rate 10°C/min.

c) Not measured.

d) Measured at 632.8 nm.

shows that a hydrogen atom of PMMA was abstracted by an excited BBP to form a crosslinkage. This reaction was very slow compared to the reaction with the carbon-carbon double bond side chain. A more insoluble polymer (~ 10 mg in the same reaction condition at 20 °C) than PMMA was formed when used poly(methyl methacrylate-co-glycidyl methacrylate). This means that the hydrogen atom abstraction from glycidyl group is slightly faster than that from MMA.

Table 3. Yields(mg) of products from preparative photolysis of copolymer **3b** and PMMA doped with m-benzoylbenzophenone (BBP) at various temperatures.

Polymer[a]	Reaction temp.(°C)	Insoluble polym.(mg)	Recovered polym(mg)	Recovered BBP(mg)[b]	Pinacol (mg)[b]
3b	7	170	62	82	<1
	20	199	40	72	<1
	40	205	12	75	<1
	55	242	1	64	1
	70	239	<1	75	1
	85	241	<1	63	2
PMMA	20	2.5	180	89	3
	70	3.5	178	78	2.6

a) A film, which was prepared by evaporation of solvent from methylene chloride solution of polymer 200 mg and BBP 120 mg, was irradiated under nitrogen.

b) Isolated by preparative TLC.

Photoreaction rate of different copolymers was monitored by measuring an insoluble fraction of photoreacted polymer film doped with BBP at various irradiation times. Figure 3 shows an insoluble polymer fraction of copolymers **3a** - **3c** and PMMA doped with 33.3 wt% of BBP as a function of the irradiation time. Reaction is faster with increasing the molar ratio of photoreactive comonomer **1b** as a result of the concentration of the reaction site restricted in the polymer matrix film. [10]
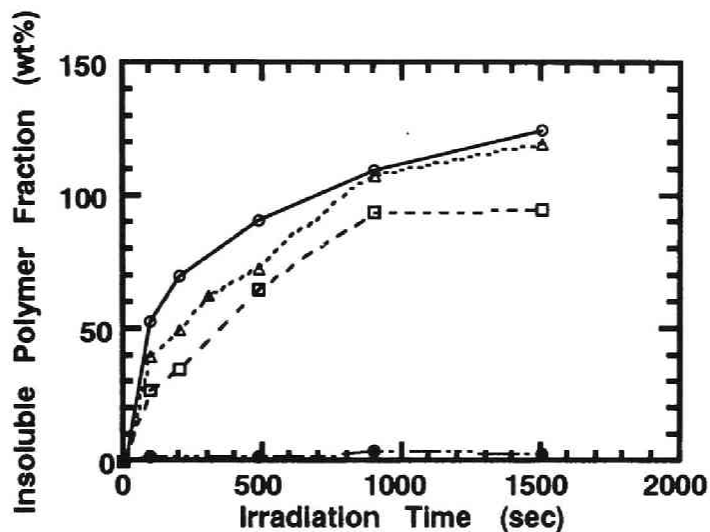
32

Figure 3. Insoluble polymer fraction in the film of *m*-benzoyl-
benzophenone (BBP) and photoreactive copolymers **3a** - **3c**
and PMMA as a function of irradiation time.
The content of BBP in the film was 33.3 wt%. O : **3a**, △ : **3b**,
▫ : **3c**, ● : PMMA.

Optical properties of photoreacted copolymers:

Copolymers used are composed of methacrylic ester with
non-conjugate carbon-carbon double bonds that can
photochemically react with *m*-benzoylbenzophenone (BBP),
resulting in a refractive index change as well as a thickness change
after irradiating UV light. [7]   Table 4 shows photochemical
changes in thickness and refractive index of the photoreactive
copolymer films doped with 44.4 wt% of BBP. Each film was
exposed about 15 J/cm^2 (10 min) at 365 nm on a PLA-521 mask
aligner. It can be seen that values of ΔN and ΔD were around 3 %
and 60 - 88 %, respectively, and these values were slightly

Table 4. Photochemical changes in thickness (ΔD) and refractive index (ΔN) of copolymers **2**, **3a**, **3b**, **3d** - **3f**, **4a**, **4b**, **5a** and **5b** doped with m-benzoylbenzophenone.

Copolymer[a]	Refractive index[b]		ΔD (%)[d]
	After exposure	ΔN (%)[c]	
2	1.545	3.0	60
3a	1.548	3.2	80
3b	1.547	3.2	78
3d	e)	e)	70
3e	1.552	3.1	77
3f	1.551	3.1	75
4a	1.547	3.2	79
4b	1.546	3.2	68
5a	1.557	3.2	88
5b	1.552	3.2	85

a) Copolymer/dopant=1/0.8, film thickness before exposure 1.2 - 1.5 μm. Unreacted BBP was removed by sublimation after exposure.

b) Measured at 632.8 nm.

c) $(N_{exposed}-N_{initial})/N_{initial} \times 100$.

d) $(D_{exposed}-D_{initial})/D_{initial} \times 100$.

e) Not measured. The film surface was not uniform because of phase separation between polymer and BBP.

increased with increasing the portion of non conjugate carbon-carbon double bonds in the copolymers. The effect of side chains, such as methyl, isopropyl, or glycidyl group, might be very small because a hydrogen abstraction reaction by the excited BBP would be very slow compared to that of non conjugate carbon-carbon

double bonds containing side chain. ΔN and ΔD are more influenced by a proportion of BBP and an exposure time. Figures 4 and 5 show that the thickness and the refractive index of the copolymer **3f** were changed with the amount of BBP. Both ΔN and ΔD became larger with increasing the proportion of BBP or the exposure time. These phenomena suggest that the change of optical properties of the film can be regulated by adjusting the exposure energy and the content of BBP. Other copolymers showed similar results. With increasing the proportion of BBP, the photoreaction was accelerated in the initial stage to be saturated earlier as shown in figures 4 and 5, suggesting an increase in number of reaction sites. Table 5 shows the molar ratio of BBP and carbon-carbon double bond constituting the main reaction site in each case of figures 4 and 5. Excess BBP to the carbon-carbon double bond could react slowly with other reaction sites such as MMA monomer unit and glycidyl side chain unit as a result of crosslinking.

Table 5. Molar ratio of *m*-benzoylbenzophenone (BBP) and 2-butenyl group of copolymer **3f**.

BBP wt%[a]	dopant / double bond[b] mol / mol
33.3	0.865
44.4	1.385
52.4	1.904

a) Copolymer **3f** doped with *m*-benzoyl-benzophenone (BBP).
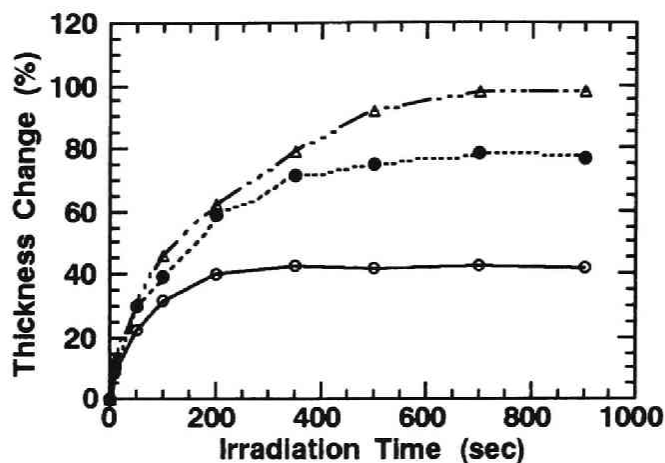b) Molar fraction of 2-butenyl group in copolymer **3f**.

Figure 4. Change in film thickness of copolymer **3f** doped with BBP as a function of irradiation time. The content of BBP in the film was ; O : 33.3 %, ● : 44.4 %, Δ : 52.4 %.
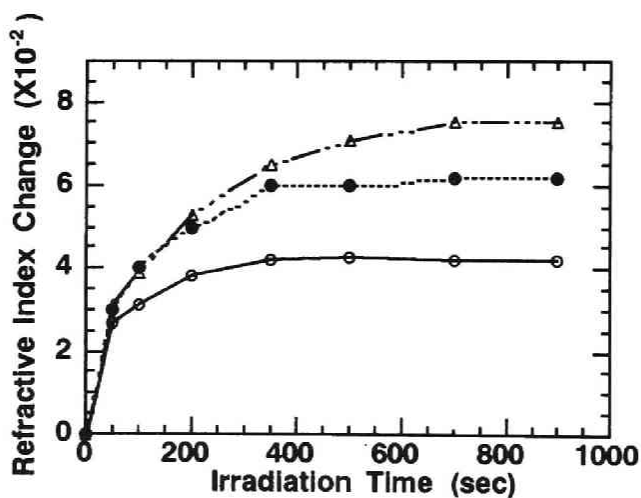

Figure 5. Change in refractive index of copolymer **3f** doped with BBP as a function of irradiation time. The content of BBP in the film was; O : 33.3 %, ● : 44.4 %, Δ : 52.4 %.

Optical patterning processes:

Optical patterning process for fabricating optical elements in this study is depicted in figure 2. Photoreactive polymer, in general, needs high resolution to achieve a precise patterned optical element. The optical patterning should be carried out at temperature lower than Tg because high temperature above Tg might cause motion of polymer matrix as a result of a low resolution in spite of high reactivity at the temperature above Tg as described above section. For this reason UV light with filters to cut IR and deep-UV lights was used for a patterning process to keep the film temperature below its Tg during the photoreaction. After the first exposure step with a photomask (figure 2(b)), the film was irradiated without a photomask to react an unexposed portion at the first exposure step (figure 2(c)). This step allows that whole region of the film was photoreacted and crosslinked with different crosslinking density according to the optical pattern. Sublimation of unreacted BBP revealed an optically patterned structures shown in figure 2(d). If the crosslinking density of the whole exposed area was sufficient, the optical element could have a high temperature stability. In order to achieve the higher crosslinked structure of the film, post-curing process shown in figure 2(e) was also carried out in addition to the patterning process. The crosslink reaction could take place in residual benzoyl group attached to the copolymer, olefinic side chain and/or glycidyl group (**3e** and **3f**) by the post-curing. A strong energy UV light such as a Toscure-1000 was used to accelerate the reaction in the solid state. The optical pattern was not affected by IR heating.

Figures 6 (a) - (d) show IR spectra of the film of copolymer **3f** doped with 37.5 wt% of BBP at each step of the patterning

process. As shown in figure 6 (a), copolymer **3f** exhibited absorption bands 1740 cm^{-1} for C=O, 970 cm^{-1} for carbon-carbon double bond of 2-butenyl group and 910 cm^{-1} for epoxy ring of glycidyl group, while BBP exhibited those of 1660 cm^{-1} for C=O, 1600, 720, and 640 cm^{-1} for phenyl ring, respectively. After UV light irradiation of 10 J/cm^2 at 365 nm with a Canon PLA-521 mask aligner, the absorption of carbon-carbon double bond at 970 cm^{-1}, epoxy group at 910 cm^{-1} and carbonyl group of BBP at 1660 cm^{-1} was decreased, while other peaks little changed (figure 6(b)). After removing an unreacted BBP at 105 °C for 20 h under 0.2 mmHg, the absorption of BBP and epoxy ring displayed further decrease, though the carbonyl bond of BBP at 1660 cm^{-1} still remained (figure 6(c)). These results indicate bonding of the phenyl carbonyl group to the polymer and thermal ring-opening reaction of epoxy group. The absorption intensities of residual carbonyl group of BBP, carbon-carbon double bond, and epoxy group of the polymer film decreased in the course of post-curing process as shown in figure 6 (d). This is a consequence that the further photoreaction occurred at the post-curing process with high energy UV light. The photoreacted film was very hard, brittle and non-swerable in organic solvents. In addition, films of **2, 3a - 3f, 4a, 4b, 5a** and **5b** were crosslinked without BBP and became insoluble in organic solvents by a high energy UV light of a Toscure-1000 lamp generating deep-UV light at 254 nm as a result of reaction of [2+2] reaction by deep UV light. [11]
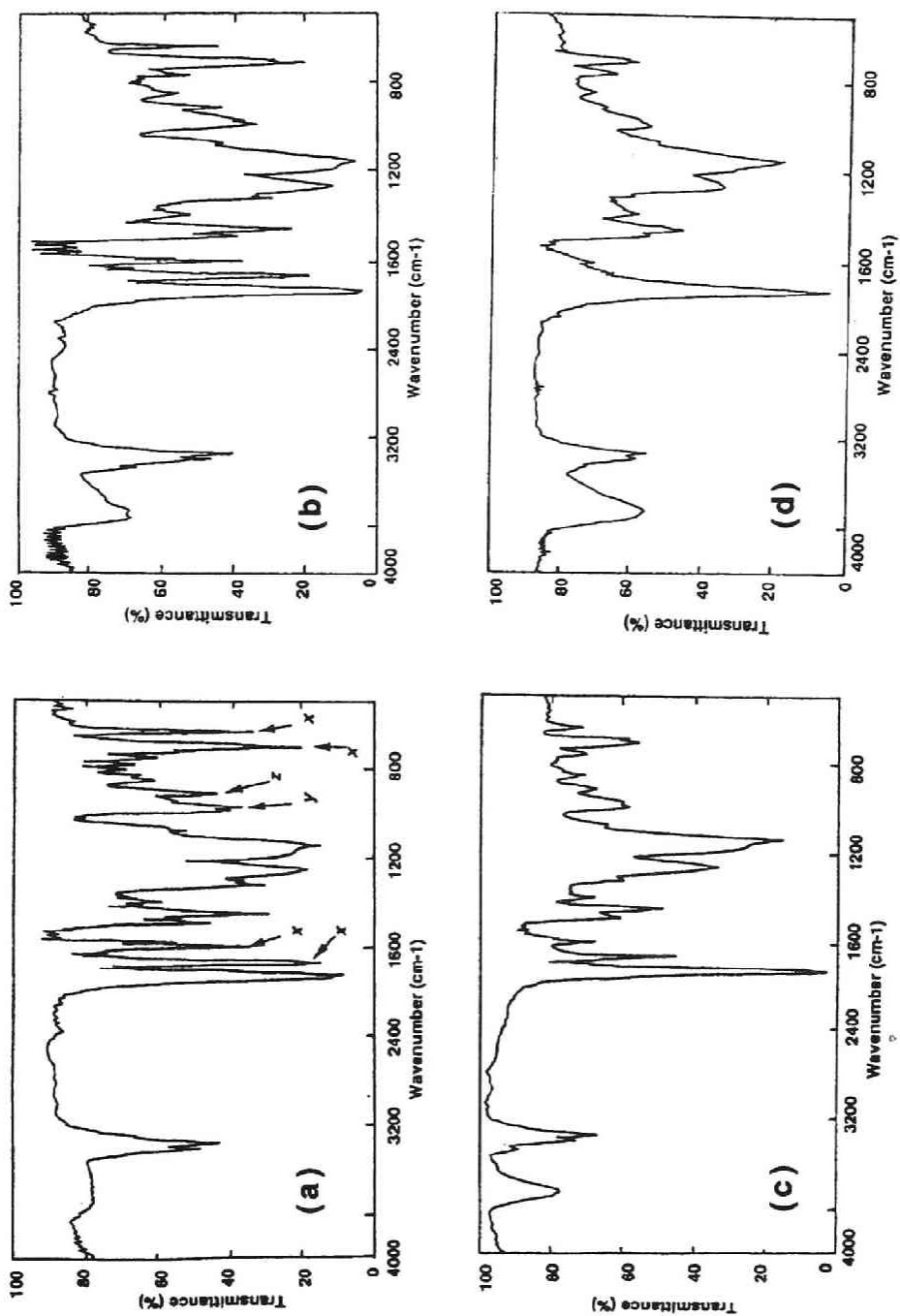
Figure 6. (see. next page)

Figure 6. IR spectra of the photoreacted polymer film formed on a KBr plate. Film before exposure contained 44.4 wt% of *m*-benzoylbenzophenone (BBP) in copolymer **3f** :

> (a) Before irradiation. *x* designates absorption of BBP, *y* absorption bond of carbon-carbon double bond of 2-butenyl group of **3f**, *z* epoxy ring bond absorption of **3f**.
> (b) After irradiation for 10 J/cm^2 on a Canon PLA-521 mask aligner.
> (c) After removing unreacted BBP by heating at 105 °C for 20 h under 0.2 mmHg.
> (d) Post-cured sample irradiated for 17 min on a Toshiba Toscure-1000 UV lamp.

Stabilities:

Stability test was carried out with respect to phase grating samples made from photoreactive copolymers (**3b** and **3f**) with high diffraction efficiencies. To compare the effects of copolymers and the fabrication processes, three samples were prepared using photoreactive copolymers doped with 37.5 wt% of BBP to form ca. 3μm thickness films before exposure. Sample *A* was irradiated 10 min with a photomask and successively irradiated 1 min without the photomask followed by removing unreacted BBP at 105 °C for 20 h using copolymer **3b**. Sample *B* was fabricated in the same way as sample *A* and additional post-curing for 7 min. Sample *C* was fabricated from copolymer **3f** in the same way as sample *B*. It can been seen from figure 7 that the grating sample *B* was greater in heat stability than a sample *A* when the same copolymer **3b** was used. Because of higher crosslinking density of the glycidyl group, the sample *C* showed excellent heat stability than those of samples *A* and *B*.
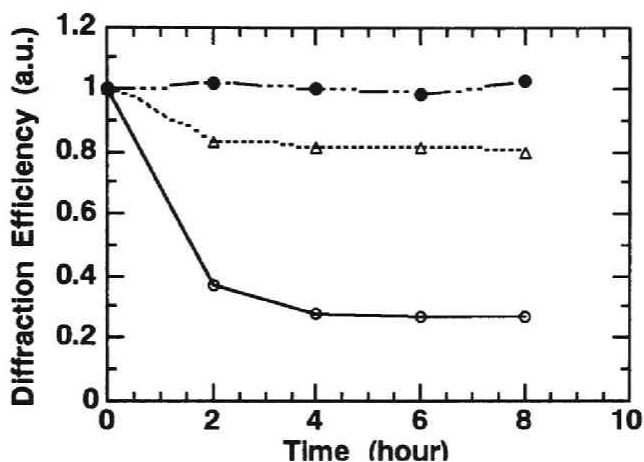
Figure 7. Stability test of the phase gratings fabricated from photoreactive copolymers. Grating pitch was 60 μm and the copolymer was doped with 37.5 wt% BBP. Each film was exposed with UV light with a photomask for 10 min. and without it for 2 min. Ratio of the first order and the zero-order diffraction efficiencies at wavelength 632.8 nm were monitored in the course of heating at 160 °C.

O: Sample A, copolymer **3b** without post-curing. Initial diffraction efficiency (η) was 173 %.

Δ: Sample B, copolymer **3b** with post-curing for 7 min. Initial η was 164 %.

●: Sample C, copolymer **3f** with post-curing for 7 min. Initial η was 165 %.

Conclusions

Photoreactive copolymers were synthesized from methacrylic esters comprising non-conjugate carbon-carbon double bond and epoxy ring. Photoreaction of the photoreactive film of copolymers doped with *m*-benzoylbenzophenone (BBP) resulted in formation of insoluble polymer and its reaction rate was faster at higher temperature because of motion of the polymer matrix film. Insoluble polymer was formed even in the case of PMMA, though the reaction was very slow. Optical properties of the photoreactive film after irradiation of UV light showed the film thickness change of ~100% and the refractive index change of ~3.2%, respectively, depending on the concentration of BBP and the exposure time.

The two step exposures in patterning process with and without a photomask followed by removing unreacted BBP were performed to achieve crosslinking of whole portion of the polymer material. After the patterning process, residual photoreactive moieties such as phenyl carbonyl groups of BBP attached to the polymer, carbon-carbon double bonds, and epoxy groups, can be also photochemically reacted, resulting in a highly crosslinked pattern. With the aid of monitoring IR spectra of each step in the exposure process, it was found that high crosslinking was caused by the photoreaction of residual reactive groups at the post-curing. A phase grating fabricated from the photoreactive film followed by the post-curing showed a high temperature stability up to 160 °C.

References

1) For review information: L. A. Hornak ed., *Polymers for lightwave and integrated optics*, Mercel Dekker, New York, 1992.

2) E. A. Chandross, C. A. Pryde, W. J. Tomlinson, and H. P. Weber, *Appl. Phys. Lett.*, **24**, 72 (1974).

3) W. J. Tomlinson, H. P. Weber, C. A. Pryde, and E. A. Chandross, *Appl. Phys. Lett.*, **26**, 303 (1975).

4) H. Franke, *Appl. Opt.*, **23**, 2729 (1984).

5) W. Driemeier and A. Brockmeyer, *Appl. Opt.*, **25**, 2960 (1986).

6) Y. Ito, Y. Aoki, T. Matsuura, N. Kawatsuki, and M. Uetsuki, *J. Appl. Polym. Sci.*, **42**, 409 (1991).

7) N. Kawatsuki, and M. Uetsuki, *Appl. Opt.*, **29**, 210 (1990).

8) Y. Ito, N. Kawatsuki, B. J. Giri, M. Yoshida, and T. Matsuura, *Org. Chem.*, **50**, 2893 (1984).

9) E. Dan, and J. E. Guillet, *Macromolecules*, **6**, 230 (1970).

10) P. L. Egerton, E. Pitts, and A. Reiser, *Macromolecules*, **14**, 95 (1981).

11) N. J. Turro, *Modern Molecular Photochemistry*, Benjamin/Cummings, New York, 1978.

Chapter 2

Mechanistic Study on Photocrosslinking of Methacrylates Copolymers by Benzophenones

Abstract : The types of photochemical reactions that will occur in the photoreactive materials for optical devices, poly(methyl methacrylate-co-2-butenyl methacrylate) (PMMA-CMA) doped with benzophenone (BP) and *meta*-benzoylbenzophenone (BBP), were investigated. Oxetane formation, hydrogen abstraction followed by radical coupling, and pinacol formation were found to occur. The quantum yield for disappearance of BP in the PMMA-CMA films was estimated as 0.68. The pendant 2-butenyl group seems to be a major photoreaction site of this system.

Introduction

Photoreactive polymer composite which consists of copolymers of methyl methacrylate and methacrylic ester bearing non-conjugate carbon-carbon double bond in its side chain, and benzophenone derivatives can crosslink and become insoluble in organic solvents. These composite are useful for organic optical devices because of its high transparency and ease of optical patterning on their surface. A copolymer (PMMA-CMA) of methyl methacrylate (MMA) and 2-butenyl methacrylate (crotyl methacrylate: CMA), which is the typical photoreactive copolymers for optical devices as described in chapter 1, are easily

44

soluble in various organic solvents. UV irradiation of a thin film of this copolymer doped with *meta*-benzoylbenzophenone (BBP) as light-absorber hardens rapidly, resulting in changes in the film thickness and refractive index of the film. Because of these changes in its physical properties, for example, a mixture of BBP and PMMA-CMA (BBP/copolymer = 0.3-1 in weight ratio) is practically utilized, for example, as a plastic phase grating for the optical head of CD and LD players. [1]

Photochemistry of carbonyl compounds in solution is very well studied. [2] They are also photoreactive in the solid state [3] and are frequently employed as photoinitiators or photosensitizers of photopolymerization and for modification of polymer structure.[4] The mechanism of photocrosslinking in the above photosensitive materials, PMMA-CMA + BBP are unknown. Recently there are increasing interests in the solid state photochemistry. [5]

In this chapter photoreaction of PMMA-CMA and BBP were employed both in solution and in the solid state. By synthesizing a model monomer of this reaction, the photoreaction mechanism of PMMA-CMA and BBP was investigated.

Experimental

General :

NMR spectra were recorded with a Varian Gemini-200 or a GEOL GX-500 spectrometer. IR spectra were measured on a JASCO FT/IR-5M or a JEOL JIR-5500 spectrometer. UV and mass spectra were taken with JASCO UVIDEC-610 and JEOL JMS DX 300 spectrometers, respectively. Analytical and preparative TLC's were done on Merck precoated TLC (or PLC) plates (silica gel 60 F254). HPLC analyses were performed with a

Shimazu LC-5A chromatograph by using a Cosmosil 5C18 column.

Irradiations were done with a 400-W high pressure mercury lamp through suitable filters. Quantitative photolyses were carried out on a Riko RH-400-10W merry-go-round apparatus.

Materials :

Copolymers were synthesized as described in chapter 1. PMMA is commercially available (Ardrich, MW = 12,000) and use as received. *meta*-Benzoylbenzophenone (BBP) was prepared by Friedel-Crafts reaction between isophthaloyl chloride and benzene. [6]

Crotyl pivalete (**1**) was prepared from a reaction of pivaloyl chloride and 2-butenyl alcohol in the presence of pyridine. [7] **1**: colorless liquid, yield 46%, b.p. 62-64°C (20 mmHg) ; nmr (CDCl$_3$) δ (ppm) 5.9-5.5 (2H, m, CH=CH), 4.49 (2H, dd, J=5.0 and 1.2 Hz, CH$_2$O), 1.72 (3H, dd, J=6.2 and 1.2 Hz, CH=CH-C$\underline{H}$3), 1.20 (9H, s, *t*-Bu) ; IR (neat) 1729 (C=O), 1156, 966 (*trans* CH=CH) cm^{-1}.

Anal: Calcd for C$_9$H$_{16}$O$_2$: C, 69.19%;H, 10.32%. Found: C,68.94%, H, 10.42%.

Preparative Photolyses :

Photolysis of crotyl pivalate (1) and BBP

A solution containing 200 mg (1.3 mmol) of **1** and 100 mg (0.35 mmol) of BBP in 10 ml of benzene was irradiated (Pyrex filter) for 2 h under bubbling nitrogen through the solution. During the irradiation, the solution was cooled by circulation of

PMMA-CMA   BBP

BP
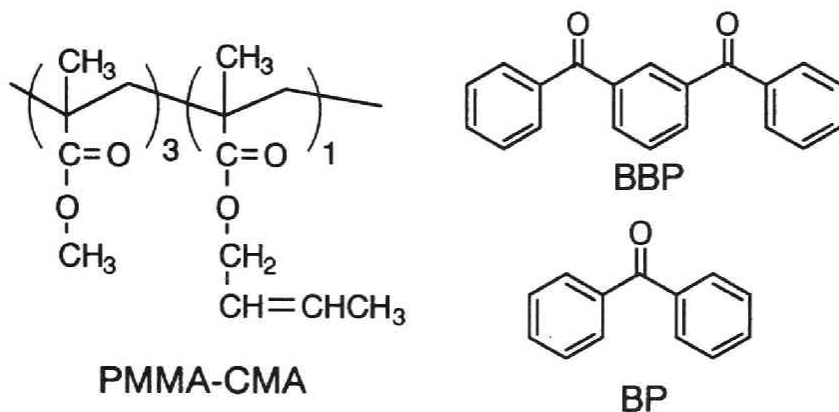
the tap water. The reaction mixture was rotary-evaporated under reduced pressure and the residue was separated by repeated preparative TLC (hexane-ethyl acetate 2:1 v/v or hexane-acetone 2:1 v/v). The following compounds were isolated and listed in the order of increasing Rf values : uncharacterized products **X** 15mg, pinacol **2** 32mg (32%), uncharacterized products **Y** 17mg, recovered BBP 25mg (25%), oxetane **3** 29mg (19%). Pinacol **2** was characterized by NMR, TLC, and HPLC, which were identical with those of the authentic sample. [8]   Oxetane **3** was assigned from its spectral data: NMR (CDCl3) δ 7.9-7.0 (aromatic protons), 5.0-3.4 (methylene and methyne protons), 1.45-0.8 (methyl and t-Bu protones) (figure 1) ; IR (KBr) 1729 (ester C=O), 1660 (benzoyl C=O), 1282, 1156, 759, 717, 702 cm^{-1} for strong peaks and 1003 cm^{-1} (oxetane ring) for a medium peak; MS m/e(re. intensity) 442 (M^{+}, 0.4), 298 (15), 287 (50), 156 (100). Three deferent *tert*-butyl peaks are observable at δ 1.11, 1.00, and 0.97 ppm in figure 1, indicating that **3** is a mixture of at least three stereoisomers. The mass spectrum of **3** gave a major peak at m/e 298, which correspond to [PhC(O)C6H4(Ph)=CHCH3]$^{+}$. This support that the structure of the oxetane is **3** rather than **3**'. (Scheme 1)
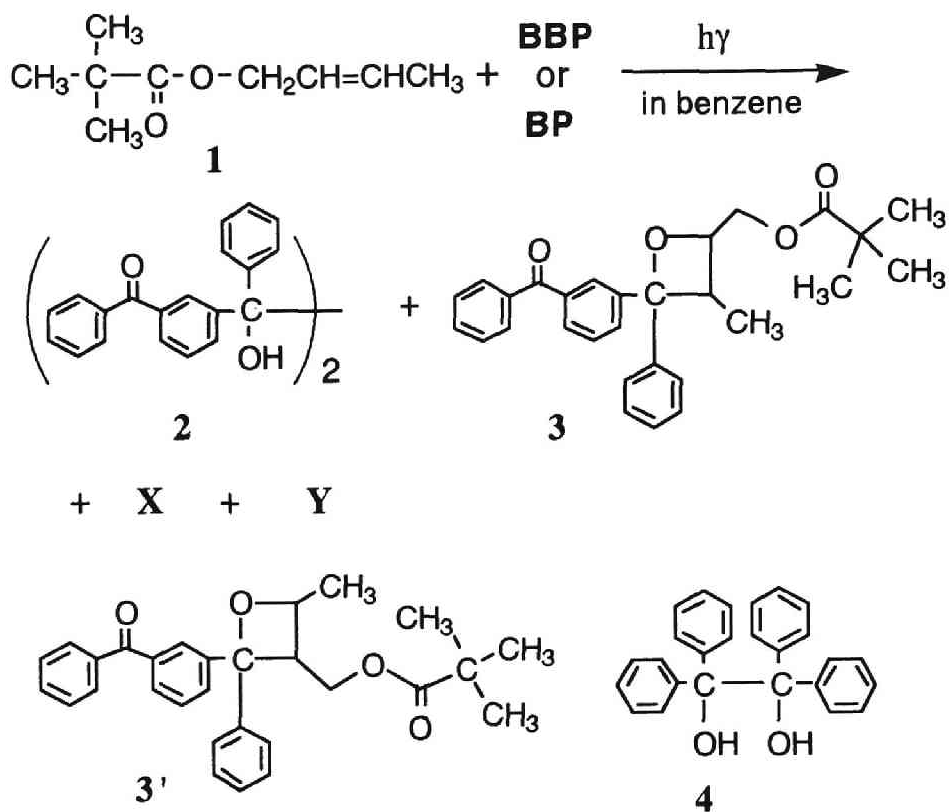
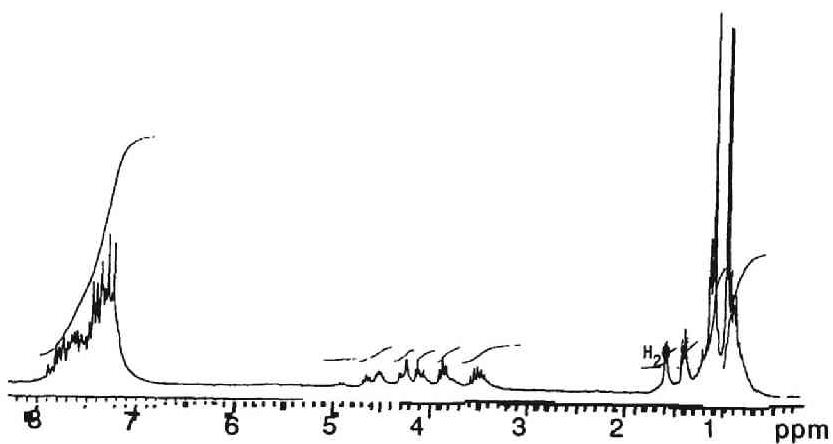**Scheme 1.** Photoreaction of crotyl pivalate **1** and **BBP** or **BP**

Figure 1. The 200-MHz NMR spectrum of oxetane **3** in CDCl3.

48

Photolysis of PMMA-CMA and BBP (or BP) in solution

A mixture of 170 mg of copolymer and 100 mg of BBP (or BP) in 10 ml of benzene was irradiated as described above. After the photolysis (2 h), an insoluble polymer formed was collected by filtration and was thoroughly washed with warm methylene chloride (ca. 100 ml total). The combine benzene and methylene chloride solution was evaporated under reduced pressure and the residue was separated by preparative TLC (hexane-acetone 3:2 v/v) to give pinacol **2** (or **4**), recovered BBP (or BP), and a recovered copolymer.

Photolysis of PMMA-CMA and BBP (or BP) in the solid state

A solution containing 170 mg of PMMA-CMA and 100 mg of BBP (or BP) in ca. 1 ml of methylene chloride was poured onto a Pyrex disk (9 cm diameter). A transparent film was formed after evaporation of the solvent on a hot plate or an oven. After drying overnight, the film was irradiated for 2 h at 0 °C through a Pyrex filter under a nitrogen atmosphere. Thorough washing of the irradiated film with warm methylene chloride (ca. 100ml total) left an insoluble polymer, which was collected by filtration. The methylene chloride washings were evaporated under reduced pressure and the residue was subjected to preparative TLC as outlined above.

It was confirmed that the insoluble polymers isolated above were not contaminated with methylene chloride-soluble substances. Thus, the isolated insoluble polymer was refluxed in methylene chloride overnight. No contaminants were detectable in the methylene chloride layer by HPLC.

UV monitoring :

A small amount of a solution containing 18.2 mg of BP and 20.0 mg of PMMA-CMA in methylene chloride was dripped on

the interior sidewall of a quartz UV cell. A thin film was obtained by evaporation of the solvent with a hair dryer. The film was further dried *in vacuo* (1 mmHg) at ambient temperature for 2 h and was then irradiated through Pyrex at 0 °C. The reaction was followed by UV spectroscopy over 2 h.

Quantum yield measurements :

Quantitative photolyses in the solid state were carried out in a similar manner to that described previously. [9] Thus, a solution of 18.2 mg of BP (or 20 mg of BBP) and 20.0 mg of PMMA-CMA in methylene chloride (ca. 1 ml) was placed in a 180 x 17 mm Pyrex tube. The outside of the tube was heated with a hair dryer to evaporate the solvent. By this manipulation the interior wall of the tube was coated with a transparent film, the top of which was adjusted as precisely as possible to be amount 2 cm from the bottom. After air-drying overnight and then vacuum drying (1 mmHg) at 0 °C for 2 h, the tube was degassed at 0.01 mmHg at 0 °C for 5 min. Several other sample tubes were prepared in the same manner and all the tubes simultaneously irradiated on a merry-go-round apparatus at 20 °C through a Riko U-360 glass filter (maximum transmittance around 366 nm). After the photolysis, the film was dissolved by addition of methylene chloride (ca. 2 ml) and the solution was added dropwise to 200 ml of methanol under stirring. A small amount of an insoluble polymer remaining in the tube was washed with further addition of methylene chloride, which was then similarly added to the above methanol solution. This procedure was repeated several times, until no BP (or BBP) was detectable by HPLC in the methylene chloride washings. The analysis of BP (or BBP) involved in the methanol solution was done by HPLC (methanol-H_2O, 3-4 : 1 v/v), using 2,6-dimethylnaphthalene as the internal standard. The amount of reacted BP (or BBP) thus determined

may be subject to considerable errors at low conversions but careful experiments gave reproducible and consistent results.

Quantitative photolyses in degassed benzene solution and chemical actinometry, where photocyclization of 2,4,6-triisopropylbenzophenone was used, were carried out as described previously. [10]

Results and discussion

Photoreaction of crotyl pivalate and BBP :

As a model for the photoreaction of PMMA-CMA and BBP, the photoreaction between crotyl pivalate (**1**) and BBP (Scheme 1) was first studied. A complex reaction occurred from photolysis of 200 mg of **1** and 100 mg of BBP in benzene. The reaction mixture was separated by repeated preparative TLC on silica gel to afford pinacol **2** (32mg, 32 %), oxetane **3** (29 mg, 19%), recovered BBP (25 mg, 25%), and uncharacterized products **X** (15 mg) and **Y** (17 mg). (Judging from their NMR spectra, it appears that **X** is a mixture of BBP oligomers which are presumably formed by consecutive pinacol formation and that **Y** is a mixture of certain coupling products between BBP and **1**.

Photoreaction of PMMA-CMA and BBP :

The photochemical reaction of BBP or BP with PMMA-CMA was studied in both the solution phase (benzene) and the solid phase (film). The reactions were carried out at a composition similar to that of the industrially used resin, *i.e.*, PMMA-CMA : BBP (or BP) = 1 : 0.6 in weight ratio. Product yields are summarized in Table 1. The main product is a polymer that is

Table 1. Yields (mg) of products from photolysis of *m*-benzoyl-benzophenone (BBP) or benzophenone (BP) with a copolymer of methyl methacrylate and 2-butenyl methacrylate (PMMA-CMA).

		Insoluble polymer[c]	Recoverd PMMA-CMA	Pinacol	Recovered BBP or BP
BBP	Benzene[a]	170	45	16	49
	Solid[b]	199	0.6	2	41
BP	Benzene[a]	155	28	13	44
	Solid[b]	214	13	3	26

a) A mixture of 100mg BBP (or BP) and 170mg PMMA-CMA in 10 ml of benzene was irradiated (Pyrex) under nitrogen atmosphere for 2 h.
b) A film, which was prepared by evaporation of the solvent from the CH_2Cl_2 solution of 100mg BBP (or BP) and 170mg PMMA-CMA, was similarly irradiated.
c) Insoluble in all organic solvents tested.

insoluble in all kinds of organic solvents tested (benzene, chloroform, methylene chloride, carbon tetrachloride, carbon disulfide, acetone, methanol *etc.*). It was soluble only in concentrated sulfuric acid. A small amount of pinacol **2** or **4** was also formed and was isolated by preparative TLC, but its yield was much lower in the solid state than in the benzene solution. The uncharacterized products **X**, which are presumably oligomers of BBP as aforementioned, were not formed in a sufficient amount to be isolated, unlike the photolysis of **1** and BBP (scheme 1).

The insoluble polymers exhibited the IR absorption of a phenyl ring at 700-800 cm^{-1} as shown in figures 2(a)-2(d), which indicate that they are an adduct between PMMA-CMA and BBP or BP. Furthermore, a prominent shoulder peak is visible around 990 cm^{-1}, probably indicative of the presence of the oxetane

structure.[11]) Therefore, oxetane formation seems to be at least partly responsible for the adduct formation, resulting in the production of the insoluble polymer. In figure 2(d), the IR absorption of a residual benzolyl carbonyl group is visible at 1660 cm^{-1}, while it is not visible in figure 2(c). This result suggests that both of the two carbonyl groups in the BBP molecule are capable of reacting easily in the benzene solution, but in the solid state the photoreactivity of the second carbonyl group is considerably less after the first one reacted.
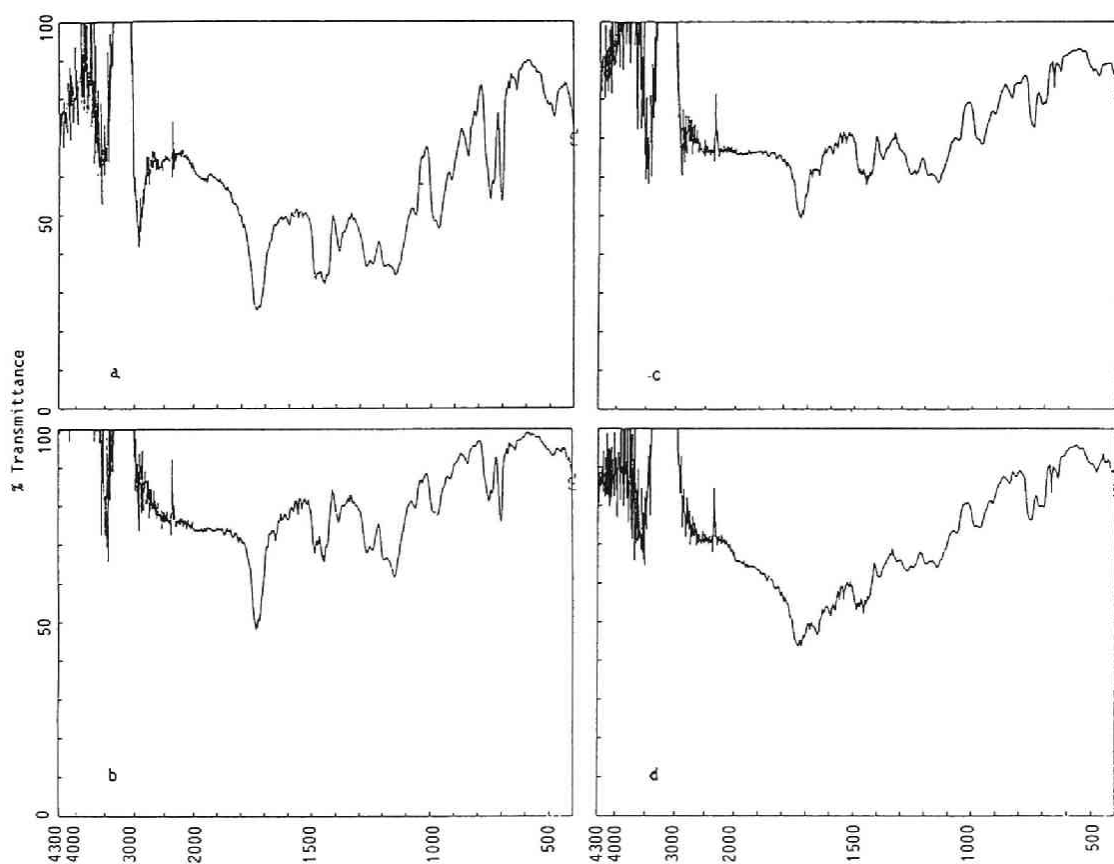

Figure 2. The FT-IR spectra of the photochemically formed insoluble polymer (KBr): (a) BP+PMMA-CMA in benzene, (b) BP+PMMA-CMA in the solid state, (c) BBP+PMMA-CMA in benzene, (d) BBP+PMMA-CMA in the solid state.

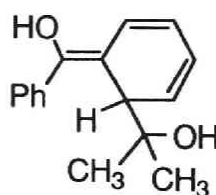### UV monitoring of the photolysis of BP in PMMA-CMA film :

UV monitoring of the photoreaction of PMMA-CMA and BP in the solid state was performed. Figure 3 demonstrates that, although the π,π^* absorption of BP at 253 nm decrease with the irradiation time, the absorption around 310 nm increases with it. The PMMA-CMA doped with BBP system showed also a similar absorption spectral change upon photolysis.

It is known that irradiation of BP in isopropyl alcohol induces hydrogen abstraction from the solvent *via* its n,π^* excited state and leads to radical coupling to form enols such as 5 and 6: these products are called "light absorbing transient (LAT)". [12] The compound 5 has the absorption maxima at 315 nm and 6 at 360 nm. The formation of LAT in a PMMA film containing BP was also reported. [13]
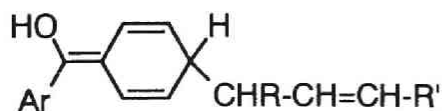
The observed increase in the absorbance near 310 nm in figure 3 should correspond to production of a new species with the structure similar to 5, *e.g.*, 7. Such a product may be formed most probably through allylic hydrogen abstraction from pendant crotyl groups of PMMA-CMA, followed by radical coupling.
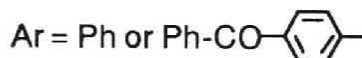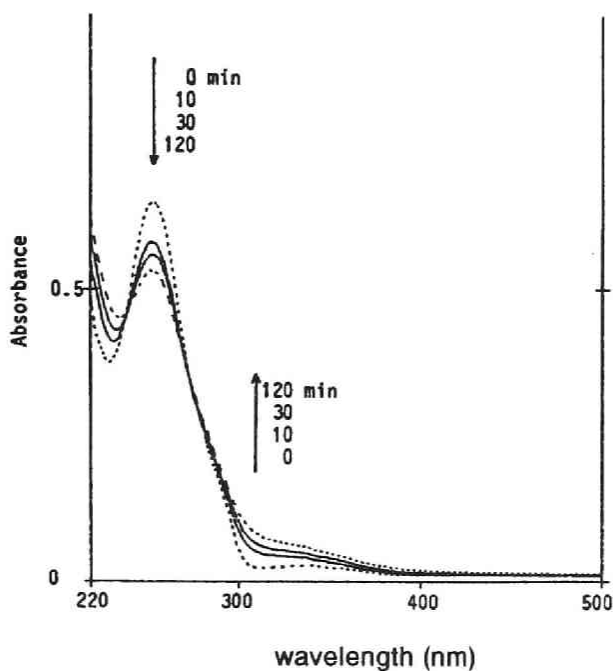

5

6

7

Ar = Ph or Ph-CO-⟨⟩-
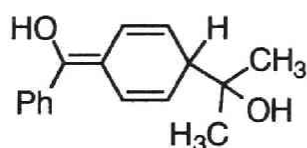
Figure 3. UV monitoring of the photolysis of BP in the PMMA-CMA film (BP/PMMA-CMA = 0.9 in weight ratio) :irradiation time, 0, 10, 30 and 120 min.

Possible photoreactions :

From the above results, main possible photoreaction occurring in the photosensitive resin of industrial usage, PMMA-CMA doped with BBP, are oxetane formation, allylic hydrogen abstraction followed by radical coupling, and pinacol formation. As a result of first two photoreactions, PMMA-CMA becomes insoluble in organic solvents.

Quantum yields :

Quantum yields are basic criteria not only for discussing mechanisms of photoreactions but also for evaluating practical utilities of various functional photopolymers. For solid-state photoreactions, however, quantum yield measurements are not

done very often. [3,9] This is probably because of difficulties in doing the experiment. Convenient procedures for measuring solid-state quantum yields have recently reported. [9] The method is very simple: A film is prepared by evaporation of a sample solution and irradiated on a merry-go-round apparatus. This method is now applied to measure quantum efficiencies for disappearance of BP or BBP in polymer films.

The photochemical conversion rate of BP or BBP in the PMMA-CMA film decrease with the irradiation time as shown in figure 4. This is attributable to an internal filter effect by enol such as **7**, which accumulates with extended irradiation. In the case of BBP, the conversion tends to level off at much shorter irradiation times. Therefore, quantum yields were measured only for BP (Φ_{-BP}) in a polymer film (PMMA-CMA film or PMMA film) or in a benzene solution containing PMMA-CMA are summarized in Table 2.
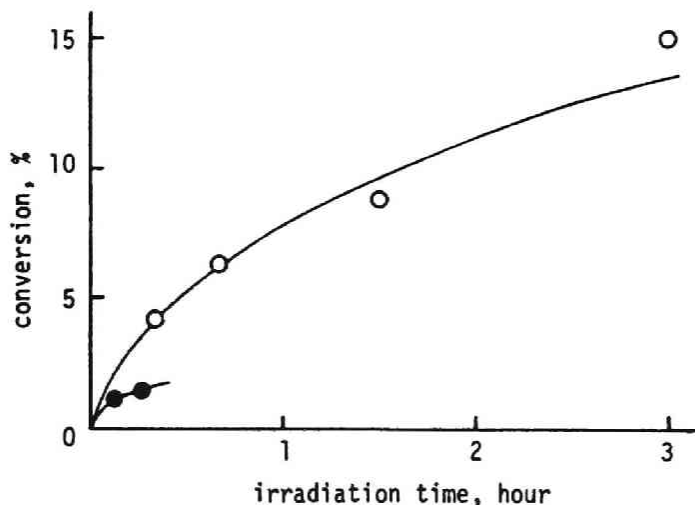

Figure 4. The photochemical conversion of BP(O) or BBP(●) in the PMMA-CMA film. The film consists of BP 18.2 mg (or BBP 20.0 mg) and PMMA-CMA 20.0 mg.

As readily seen from Table 2, Φ_{-BP} is higher in the PMMA-CMA film (0.68) than the PMMA film (0.26). This result may be explained in two ways. (1) A pendant 2-butenyl group of PMMA-CMA bears one olefinic double bond and five allylic hydrogens, which are very reactive toward the n,π^* triplet state of BP. [15] (2) PMMA-CMA (Tg = 93°C) possesses a lower glass transition temperature than that of PMMA (Tg = 105°C). Addition of a large amount of BP to PMMA-CMA has been found to reduce Tg near room temperature. It is known that quantum yields for certain photochemical reactions in polymer materials depend on their Tg. [13,14]

Table 2. Quantum yields for the disappearrance of benzophenone (BP)

Medium	Φ_{-BP}
PMMA-CMA film[a]	0.68[b]
PMMA film[a]	0.26
Benzene solution containing PMMA-CMA[c]	0.17

a) A film was prepared by evaporation of the solvent from a CH_2Cl_2 solution containing 18.2 mg BP and the polymer 20 mg. After degassing the film, it was irradiated at 366 nm at 20 °C for 20 min.
b) An analogous experiment employing a larger quantity of BP(27.3 or 36.4 mg) gave the same Φ_{-BP} value within an experimental error (±10%).
c) A degassed benzene solution (2.0 ml) containing 18.2 mg BP and 20.0 mg PMMA-CMA was irradiated under the same conditions as mentiond above (footnote a).

Table 2 also shows that Φ_{-BP} in the PMMA-CMA film (0.68) is much higher than that in the benzene solution of PMMA-CMA (0.17). This result is somewhat unexpected, since molecular and atomic motions are more restricted in polymer matrices as compared with those in solution. [14] However, it may be understood by considering the concentration effect of the 2-butenyl group. In the benzene solution the concentration of the 2-butenyl group is about 0.023M under the reaction conditions, whereas in the solid state it should be very high. Thus, BP triplet may be trapped more efficiently in the solid state than the benzene solution.

Conclusions

Three main photoreactions occurring in the photosensitive resin of industrial usage, PMMA-CMA doped with BBP, have been found, *i.e.*, (1) oxetane formation, (2) hydrogen abstraction followed by radical coupling, and (3) pinacol formation. The quantum yield for disappearance of BP in the PMMA-CMA film is unexpectedly high (0.68). The pendant 2-butenyl group in the copolymer seems to be a major photoreaction site.

References

1)   (a) M. Uetsuki and N. Kawatsuki, *Microoptics News,* **6**, 165
      (1988), (b) N. Kawatsuki and M. Uetsuki, *Appl. Opt.,* **29**, 210
      (1990).

2)   N. J. Turro, *Modern Molecular Photochemistry,* Benjamin
      /Cummings, Menlo Park, CA, 1978.

3)   Y. Ito, *in Photochemistry on Solid Surfaces,* S. Anpo and T.
      Matsuura Eds., Elsevier, Amsterdam, 1989, p469.

4)   J. Guillet, *Polymer Photophysics and Photochemistry,*
      Cambridge University Press, Cambridge, 1985.

5)   V. Ramamurthy and K. Venkatesan, *Chem. Rev.,* **87**, 433
      (1987).

6)   Y. Ito, N. Kawatsuki, B. J. Giri, M. Yoshida, and T. Matsuura, *J.
      Org. Chem.,* **50**, 2893 (1985).

7)   R. E. Ireland, R. H. Muellar, and A. K. Willard, *J. Am. Chem.
      Soc.,* **98**, 2868 (1976).

8)   Y. Ito, N. Kawatsuki, and T. Matsuura, *Tetrahedron Lett.,* **25**,
      2801 (1984).

9)   (a) Y. Ito and T. Matsuura, *J. Photochem. Photobiol. A: Chem.* to
      be appear; (b) *Tetrahedron Lett.,* **29**, 3087 (1988).

10)   (a) Y. Ito, H. Nishimura, Y. Umehara, Y. Yamada, M. Tone, and
      T. Matsuura, *J. Am. Chem. Soc.,* **105**, 1590 (1983). (b) Y. Ito, B.
      P. Giri, M. Nakasuji, T. Hagiwara, and T. Matsuura, *ibid.,* **105**,
      1117 (1983).

11)   D. R. Arnold, R. L. Hinman, and A. H. Glick, *Tetrahedron Lett.,*
      1425 (1964).

12)   A. Demeter and T. Berces, *J. Photochem. Photobiol. A: Chem.,*
      46, 27 (1989) and references cited therein.

13)   F. W. Deeg, J. Pinsl, and C. Braushle, *J. Phys. Chem.,* **90**, 5715
      (1986).

14)   (a) A. D. Gudmundsdottir and J. Scheffer, *Tetrahedron Lett.,* **30**, 419 (1989), (b) **30**, 423 (1989).

15)   M. V. Encias and J. C. Scaiano, *J. Am. Chem. Soc.,* **103**, 6393 (1981).

Part 2.

Optical Grating Elements Made from Photoreactive Polymers and Their Applications to an Optical Pickup Head

Chapter 3.

Optical Phase Gratings Made from Photoreactive Copolymers

Abstract : Based on a combination of surface structure and refractive index modifications, an optical phase grating was fabricated from a thin film of photoreactive optical copolymers, which had been synthesized from methyl methacrylate and a methacrylic ester including non-conjugate carbon-carbon double bonds, and doped with an aromatic ketone. After exposure to ultraviolet light beams through a photomask with a grating pattern, the exposed portion of the polymer film was up to ~110% thicker and ~3% higher in refractive index than the unexposed portion. Diffraction efficiencies of light beams passing through the optical phase grating was varied with its cross-sectional shape. Measured values of diffraction efficiencies were in good agreement with calculated values from Fraunhofer's diffraction theory.

Introduction

Because organic materials possess interesting feature for the fabrication of integrated optical circuits and devices, they have been studied directed toward practical use. [1] In fabricating optical devices from thin polymer films, which are usually prepared on a substrate by spin-coating technique, it is frequently

required to draw precise patterns on the thin polymer film. The patterning has been achieved by surface structure modification or by refractive index modification of the film. The most important feature of organic materials is that they can use light beams to introduce, selectively and with high resolution, substantial changes in the physical properties of the material.

Photochemical reactions can cause large change in diffusion rates of dopants or polymer solubilities, so that Chandross *et al* [2] proposed a photolocking process in which a photochemical reaction was used to lock or fix a dopant in a polymer film with a lower refractive index and the unreacted dopant was then removed by heating. They prepared a photoreactive polymer film from a 1:1 copolymer of methyl methacrylate (MMA) and glycidyl methacrylate doped with ethyl 2-(1-naphtyl)-acrylate. The inherent refractive index of the dopant was ~1.60, well above that of the copolymer (N=1.515). After exposure to ultraviolet beams followed by heating, they found that the exposed portion was ~15% greater in thickness and 1.3% higher in refractive index than the unexposed portion. [2] Using naphthalenethiol as the dopant in the preceding process, they confirmed that the exposed portion was ~10% thicker and 1.3% higher in refractive index than the unexposed portion. [3] Franke observed a refractive index change of ~3% in a photoreactive film of poly-(methyl methacrylate) (PMMA) doped with 2,2-di-methoxy-1,2-diphenyl-ethanone. [4] Combining the photoreactive copolymer of Chandross *et al* [2] with the dopant studied by Franke, [4] Driemeier and Brockmeyer [5] recorded optically a phase grating in the copolymer film to attain a resolution better than 1200 lines/mm and a refractive index change of 1.2%. These results support the fact that both the surface structure modification and the refractive index modification cause a phase shift in light beams traveling through the polymer film.

The object of this chapter is to make an optical phase grating for practical use, with hybrid characteristics of the surface structure modification type and the refractive index modification type, by using a photoreactive copolymer of MMA and a methacrylic ester doped with an aromatic ketone having a large molecular volume and a high refractive index compared with monomeric components of the copolymer, as described in chapters 1 and 2. Diffraction efficiencies of light beams that pass through the phase grating are represented in terms of their cross-sectional shape and refractive index. In addition, various shapes of phase gratings made by these materials were also represented.

Experimental

### *Synthesis of photoreactive materials :*

Geraniol was manufactured by Kuraray Co., and all the other source compounds and catalysts used were commercially supplied by Wako Pure Chemical Industries. The compounds 2-propenyl methacrylate (PMA), 2-butenyl methacrylate (BMA), and geranyl methacrylate (GMA) were synthesized by an esterification reaction of methacryloyl chloride with 2-propene-1-ol, 2-buten-1-ol, and geraniol, respectively, in the presence of triethylamine as described in chapter 1. Photoreactive copolymers were synthesized from MMA and a methacrylic ester bearing a substituent group R with non-conjugate carbon-carbon double bonds in dioxane adding 2,2'-azobisisobutyronitrile (AIBN) as a reaction initiator (Scheme 1).

The compounds, 3-benzoylbenzophenone (BBP) and 4-benzoylbenzophenone (BBP') were synthesized by an ordinary Friedel-Crafts reaction on benzene with isophthaloyl chloride or terephthalolyl chloride, respectively, in the presence of aluminum
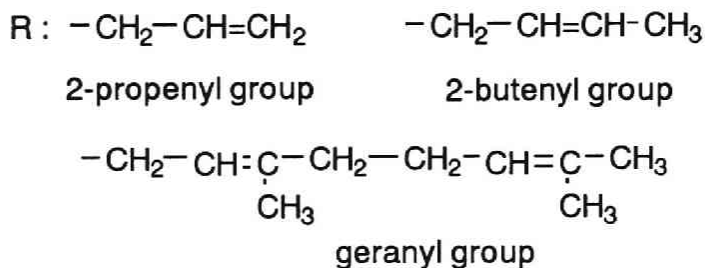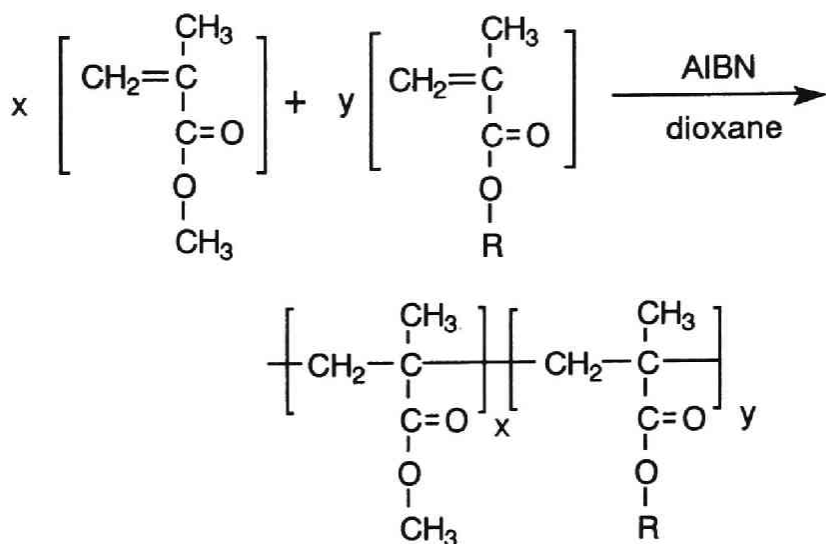
Scheme 1. Synthesis of photoreactive copolymers.

trichloride. [6] Their molecular structures were determined from ^1H NMR spectra and IR spectra. Molecular weight of the photoreactive copolymers was measured in a tetrahydrofuran solution with a Waters 150-C gel-permeation chromatograph. Benzophenone (BP), BBP, and BBP' was used as a dopant in a photoreaction system in this chapter.
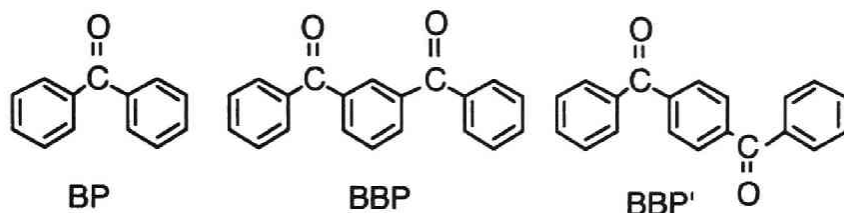
Scheme 2. Photosensitive benzophenone derivatives.

Fabrication of phase gratings :

Typical fabrication process of phase grating is shown in figure 1. For example a 4-wt.% toluene solution of the photoreactive copolymer was prepared by adding the dopant equimolar with the methacrylic ester component and methyl-silicone of 0.0004 wt.%, and filtered through a 0.2-μm membrane filter. The solution was then spin-coated 0.1 ~ 3.0 μm thick on a washed glass substrate with a Mikasa H-700 spinner to form a transparent film, when methylsilicone raised film uniformity. After the film was heated at 60 - 80 °C for 40 min to remove toluene, it was exposed to ultraviolet light with a dose rate of 17 mW/cm^2 at 365 nm wavelength for 1 ~ 15 min through a photomask with a grating pattern using a Canon PLA-521 mask aligner. After irradiation the sample was heated at 95 °C for 4 h under vacuum of 0.2 mmHg to allow the unreacted dopant to sublime, thereby an optical phase grating with combined characteristics of a surface structure modification and a refractive index modification was fabricated. The cross-sectional shape of the grating was controlled by regulating distance between the photomask and the film surface in the course of exposure to ultraviolet light beams.

Evaluation of photochemical and optical properties :

Photochemical parameters for the dopants and aromatic ketones were measured with a Hitachi 330 spectrophotometer. Film thickness was measured at the exposed and unexposed portions with Mizojiri dual-beam interference microscope. A convex - concave surface structure of the phase grating was

•Substrate washing

•Copolymer/dopant
  spin-coating
•Prebaking

•UV light irradiation
  through aphotomask

•Heating to remove
  unreacted dopant

Figure 1. Process to fabricate phase gratings.
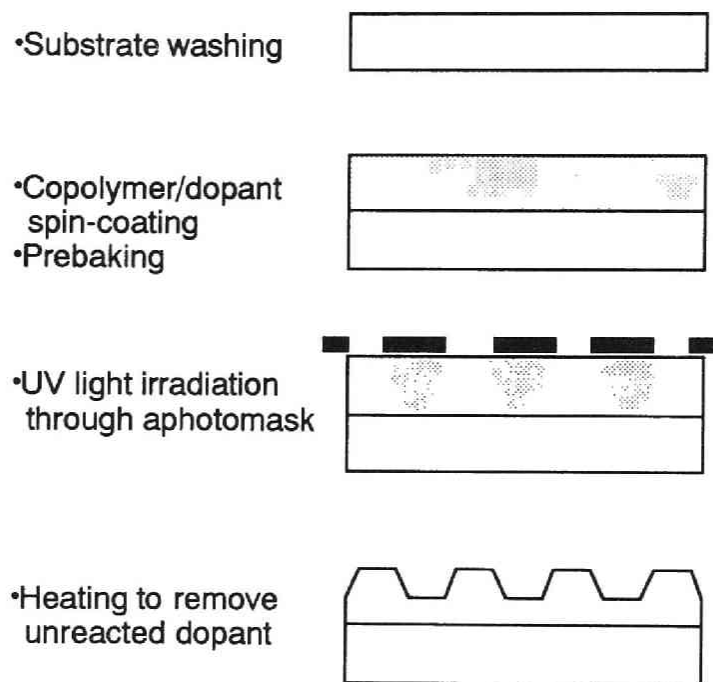
recorded on a Rank-Taylor-Hobson Talystep on the basis of a stylus contact method. Refractive index of the copolymer films was measured at the exposed portion as well as the unexposed portion with a prism coupling method using a laser diode of 780 nm wavelength. The intensity of the light beams diffracted by the phase grating was measured with the laser diode and a light power

meter. Wavefront aberration of light beams passing through the phase grating at a right angle was measured with a Zygo Mark III interferometer system.

Durability tests :

A Tabai PL-1G temperature- humidity chamber was used to study effects of temperature and humidity on diffraction efficiencies of light beams passing through the phase grating before and after heating 1000 h at 60 °C and 95% RH, and before and after ten cycles of heating at 85 °C for 2 h followed by cooling at -30 °C for 2 h.

Results and discussion

Photoreaction systems :

It has been known that a ketone in an excited state reacts with a carbon-carbon double bond in a ground state when the ketone is lower in an excited energy level than the carbon-carbon double bond. [7] In general, aromatic ketones and non-conjugate carbon-carbon double bonds have triplet energies 270 - 300 and ~330 kJ/mol, respectively, while the triplet energy of conjugate carbon-carbon double bonds is smaller than that of the aromatic ketones. When the aromatic ketone is in an excited state which arises from $n\pi^*$ electron transition, it undergoes a photoreaction with the non-conjugate carbon-carbon double bond to form an oxetane ring as illustrated in Scheme 3 with a regard to typical reaction of BP with 2,3-dimethyl-2-butene (DMB). In a similar manner, the aromatic ketone will be photochemically added to the non-conjugate carbon-carbon double bond of the photoreactive copolymer as described in chapters 1 and 2. On the other hand,
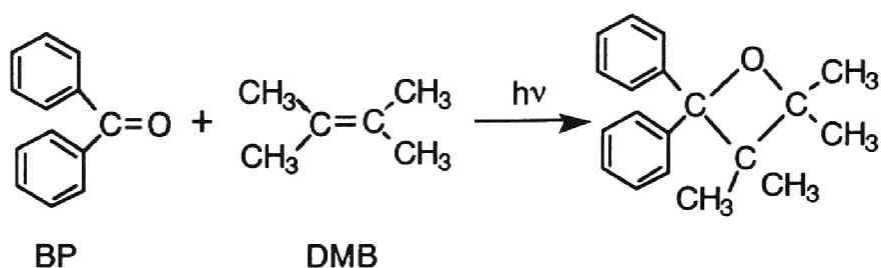
Scheme 3.

Table 1. Composition of photoreactive polymers

Polymer number	Methacrylic ester (ME)	Content of ME (mol%)
1	PMA	50
2	BMA	56
3	BMA	50
4	BMA	25
5	GMA	45
6	GMA	23

physical characteristics of the aromatic ketones are represented by a large molecular volume and a high refractive index of the aromatic groups compared with PMMA and methacrylic esters which have none of the aromatic groups. PMMA has been commonly employed for manufacturing optical products because of its high transparency.

Based on such a background, a photoreaction system for making a phase grating was designed by adopting a combination of an aromatic ketone and a copolymer synthesized from MMA and a methacrylic ester comprising of non-conjugate carbon-carbon double bonds. Content of the methacrylic ester component in the photoreactive copolymer was set at 23 ~ 56 mol% as listed in Table 1. The photoreactive copolymer took on weight-average molecular weight of ~740,000, number-average molecular weight of ~380,000, and refractive index of 1.505 ~ 1.510. The aromatic ketone was added to the photoreactive copolymer with weight ratios of 0.8 : 1.0 ~ 1.5 : 1.0 . Values of photochemical parameters for the dopants are listed in Table 2 where it can be seen that BBP' is inferior to BP and BBP in photoreactivity because of the dominant $\pi\pi^*$ character.

Table 2. Photochemical parameters of dopants.

| Dopant | UV absorption[a] | | | | Triplet energy[b] (kJ/mol) |
| | $n\pi^*$ | | $\pi\pi^*$ | | |
	λmax(nm)	ε	λmax(nm)	ε	
BP	346	120	244	19400	288
BBP	345	230	247	36800	287
BBP'	348	360	260	35100	277

a) Measured in cyclohexane at r.t.
b) reference 6.

Photoreactive films :

By measuring film thickness of the exposed portion D_a and that of the unexposed portion D_b, a rate of change in film

thickness was determined from a value of $\Delta D = (D_a - D_b)/D_b$. A rate of change in the refractive index of the polymer film $\Delta N = (N_a - N_b)/N_b$ was obtained from the refractive index of the exposed portion N_a and that of the unexposed portion N_b. When the photoreactive polymer composite was spin coated ~1.5 μm thick on a glass substrate followed by irradiation to ultraviolet light beams for 14 min, ΔD and ΔN varied with a molecular species and the prepared content of the dopants as listed in Table 3. Within the experimental range, the maximum values of ΔD and ΔN were ~30% and ~1.5%, respectively, when BP was used, while those of ΔD and ΔN were ~110% and ~3%, respectively, when BBP was used. However, BBP' was of no use as dopant. The maximum value of ΔD when BBP was used is exceptionally larger than the

Table 3. Photochemical changes in thickness and refractive index of photoreactive polymer films.

Polymer number	Dopant	Dopant/ polymer [a]	$\Delta D(\%)$ [b]	Refractive index [c] exposed	Refractive index [c] unexposed	$\Delta N(\%)$
3	BP	0.8	27	1.527	1.505	1.5
4	BP	0.8	25	1.526	1.505	1.5
1	BBP	0.8	40	1.542	1.505	2.3
2	BBP	0.8	65	1.547	1.505	2.8
2	BBP	1.5	110	1.550	1.505	3.0
4	BBP	0.8	60	1.547	1.505	2.8
5	BBP	0.8	100	1.555	1.510	3.0
6	BBP	0.8	93	1.551	1.509	2.8

a) Weight ratio

b) Film thickness before exposure was 1.4 - 1.5 μm.
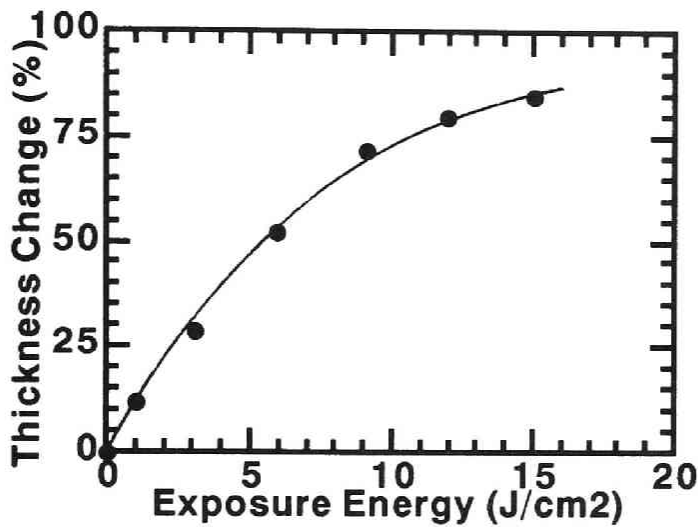
c) Measured at wavelength 780 nm.

Figure 2. Variation of a change rate in film thickness ΔD with exposure energy. Experimental conditions were as follows; Copolymer number 2, BBP/copolymer (weight ratio) 0.8/1.0, film thickness before exposure 1.2 μm, and effective wavelength of UV light 365 nm.
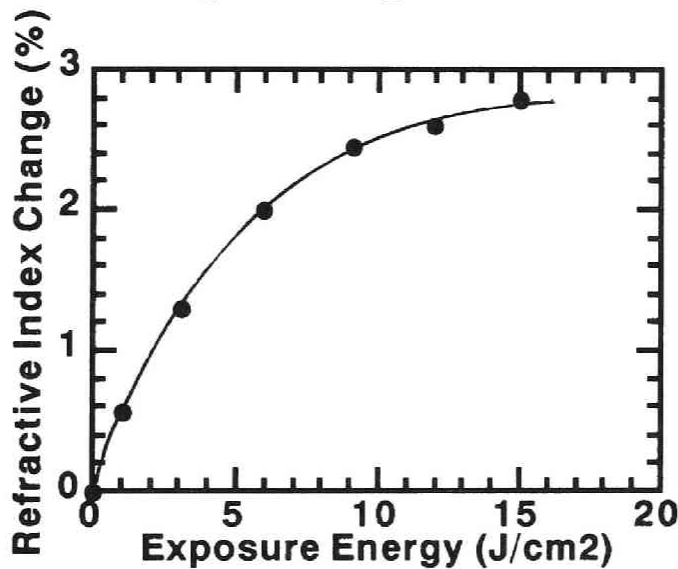

Figure 3. Variation of a change rate in refractive index ΔN with exposure energy. The refractive index was measured at wavelength 780 nm, and the other conditions are the same as those in figure 2.

known data. It can be seen from these results that ΔD and ΔN increase in proportion to the number of aromatic groups in the dopant molecule as well as the contents of the non-conjugate carbon-carbon double bond and the dopant. As shown in figures 2 and 3, both ΔD and ΔN increased to a plateau with increasing exposure energy, which was proportional to the exposure time and measured at 365 nm wavelength. These phenomena suggest that most of the aromatic ketone molecules would undergo a stoichiometric reaction with the photoreactive copolymer, which is regulated by controlling the contents of the methacrylic ester component and the aromatic ketone as well as by the exposure time.

The exposed portion of the photoreactive film doped with BBP was hardly soluble in organic solvents, reflecting that a few BBP molecules formed an intermolecular cross-link with a couple of carbon-carbon double bonds attached to different polymer molecules. The photoreaction was available for fabricating micro-patterns with high resolution of ~ 3000 lines/mm with irradiation by interference beams from He-Cd laser of 325 nm wavelength.

Formulation of diffraction efficiencies :

A phase change P, which is caused when light beams of wavelength λ travel a distance D within a light medium with a refractive index N, is shown by an expression $P=(2\pi/\lambda)DN$. When a periodic distribution of P is caused on an outlet plane of the light medium due to variations in D and N, the light beams are diffracted in such a direction that light beam components with different P values are mutually amplified by phase matching.

On the basis of Fraunhofer's diffraction phenomenon, it is conducted to formulate diffraction efficiencies of light beams with a wavelength λ which passes through a phase grating at an
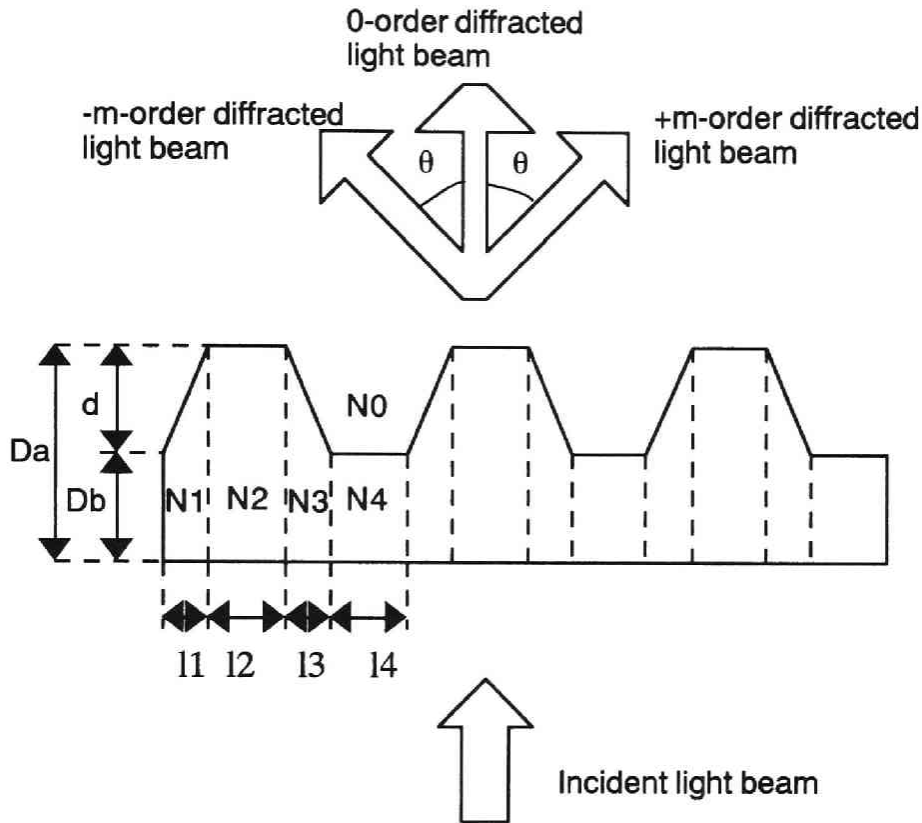
Figure 4. Schematic drawings of cross-section of the phase grating.

incident angle of $0°$ and a diffraction angle of θ as depicted in figure 4, where the phase grating has a cross sectional shape of trapezoids periodically arranged on a transparent plane. A unit of the phase grating is composed of a convex portion, a convex portion and a couple of intermediate portions. Parameters of each portion are expressed as follows: a convex portion with a thickness D_a, a width l_2, and a refractive index N_2; a concave portion with a thickness D_b, a width l_4, and a refractive index N_4; a couple of intermediate portions with widths l_1 and l_3, and refractive indices N_1 and N_3, respectively. The surrounding space has a refractive

index N_0. As a result of the phase matching among light beam components, the zero-order diffraction efficiency η_0 and the m-order diffraction efficiency η_m are expressed by equations (1) and (2), respectively, where m is an integer other than zero:

$$\eta_0 = (U_0 + V_0)^2 - 4(W_0 + X_0 + Y_0 + Z0), \tag{1}$$

$$\eta_m = (U_m + V_m)^2 - 4(W_m + X_m + Y_m + Z_m), \tag{2}$$

where

$$U_0 = \frac{\alpha_1}{\delta_1}\sin\delta_1 + \frac{\alpha_3}{\delta_3}\sin\delta_3, \tag{1-1}$$

$$V_0 = \alpha_2 + \alpha_4 \tag{1-2}$$

$$W_0 = \frac{\alpha_1\alpha_3}{\delta_1\delta_3}\sin\delta_1\sin\delta_3\sin^2\delta_{13}, \tag{1-3}$$

$$X_0 = \alpha_2\alpha_4\sin^2\delta_{24}, \tag{1-4}$$

$$Y_0 = \frac{\alpha_1}{\delta_1}\sin\delta_1(\alpha_2\sin^2\delta_{12} + \alpha_4\sin^2\delta_{14}), \tag{1-5}$$

$$Z_0 = \frac{\alpha_3}{\delta_3}\sin\delta_3(\alpha_2\sin^2\delta_{23} + \alpha_4\sin^2\delta_{34}), \tag{1-6}$$

$$U_m = \alpha_1\frac{\sin(m\pi\alpha_1 + \delta_1)}{m\pi\alpha_1 + \delta_1} + \alpha_3\frac{\sin(m\pi\alpha_3 - \delta_3)}{m\pi\alpha_3 + \delta_3}, \tag{2-1}$$

$$V_m = \frac{1}{m\pi}[\sin(m\pi\alpha_2) + \sin(m\pi\alpha_4), \tag{2-2}$$

$$W_m = \alpha_1\alpha_3\frac{\sin(m\pi\alpha_1 + \delta_1)\sin(m\pi\alpha_3 - \delta_3)}{(m\pi\alpha_1 + \delta_1)(m\pi\alpha_3 - \delta_3)}$$

$$\text{x }\sin^2\left[\frac{m\pi}{2}(1 + \alpha_2 - \alpha_4) - \delta_{13}\right] \tag{2-3}$$

$$X_m = \frac{\sin(m\pi\alpha_2)\,\sin(m\pi\alpha_4)}{(m\pi)^2}$$

$$\times\ \sin^2\left[\frac{m\pi}{2}(1 - \alpha_1 + \alpha_3) - \delta_{24}\right] \qquad (2\text{-}4)$$

$$Y_m = \alpha_1\,\frac{\sin(m\pi\alpha_1 + \delta_1)}{(m\pi\alpha_1 + \delta_1)}$$

$$\times\ \left\{\sin(m\pi\alpha_2)\sin^2\left[\frac{m\pi}{2}(1 - \alpha_3 - \alpha_4) + \delta_{12}\right]\right.$$

$$\left.+\ \sin(m\pi\alpha_4)\sin^2\left[\frac{m\pi}{2}(1 + \alpha_2 + \alpha_3) + \delta_{14}\right]\right\} \qquad (2\text{-}5)$$

$$Z_m = \alpha_3\,\frac{\sin(m\pi\alpha_3 - \delta_3)}{(m\pi\alpha_3 - \delta_3)}$$

$$\times\ \left\{\sin(m\pi\alpha_2)\sin^2\left[\frac{m\pi}{2}(1 - \alpha_1 - \alpha_4) + \delta_{23}\right]\right.$$

$$\left.+\ \sin(m\pi\alpha_4)\sin^2\left[\frac{m\pi}{2}(1 - \alpha_1 - \alpha_2) + \delta_{34}\right]\right\} \quad \cdot \quad (2\text{-}6)$$

Parameters used in equations (1) and (2) are defined as follows: $\alpha_1 = l_1/l$, $\alpha_2 = l_2/l$, $\alpha_3 = l_3/l$, $\alpha_4 = l_4/l$, $l = l_1 + l_2 + l_3 + l_4$, $\delta_1 = (\pi d/\lambda)(N_1 - \mu N_0)$, $\delta_3 = (\pi d/\lambda)(N_3 - \mu N_0)$, $\delta_{12} = (\pi D_a/\lambda)(N_2 - N_1) + \delta_1/2$, $\delta_{13} = (\pi/\lambda)(D_a - d/2)(N_1 - N_3)$, $\delta_{14} = (\pi/\lambda)(D_a - d)(N_4 - N_1) - \delta_1/2$, $\delta_{23} = (\pi D_a/\lambda)(N_2 - N_3) + \delta_3/2$, $\delta_{24} = (\pi/\lambda)[D_a(N_2 - N_4) + d(N_4 - \mu N_0)]$, $\delta_{34} = (\pi/\lambda)(D_a - d)(N_4 - N_3) - \delta_3/2$, $d = D_a - D_b$, and $\mu = 1/\cos\theta = \{1 - [m\lambda/(N_0 l)]^2\}^{-1/2}$.

Characteristics of phase gratings :

Conventional phase gratings are divided into the following two categories. One is a surface structure modification type phase grating, named "an S-type phase grating", having regularly arranged convex-concave portions with a uniform refractive index. Another is a refractive index modification type phase grating, named "an R-type phase grating", comprised of regularly arranged layers with uniform thickness and alternately different
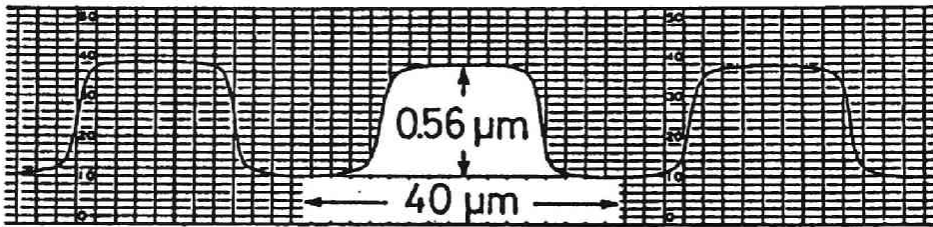
(a)
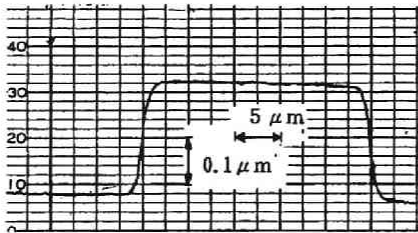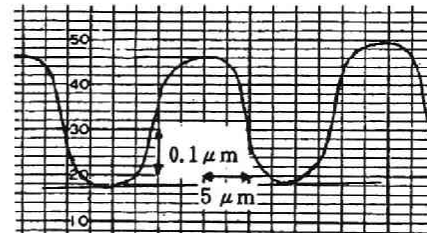
(b)   (c)

Figure 5. Talystep spectrum of the phase grating surface. (a) Trapezoidal shape: Experimental conditions are the same as those in figure 2, except that film thickness before exposure was 1.42 μm. (b) Near -rectangular shape: Print gap ~0 μm. (c) Sinusoidal shape: Light dispersing plate was used on a photomask.

refractive indices. A phase grating, named "an H-type phase grating", was investigated in this work to make use of hybrid characteristics of S-type and R-type phase gratings. The cross-sectional shape of the H-type phase grating varied with a print gap g, distance between the photomask and the photoreactive film in the course of exposure to ultraviolet light beams, forming rectangles or trapezoids on a smooth plate when $g = 0$ or $g \neq 0$, respectively. In the case of long print gap or use of light dispersing plate on a photomask to disperse the irradiation light, the grating structure can be a sinusoidal shape. Figure 5(a)-(c) shows various cross-sectional shape of phase gratings. When $g = 30$ μm, the H-type phase grating had a trapezoid profile as shown in figure 5(a) and listed in Table 4. Observed values of diffraction efficiencies appeared to be in fairly good agreement with the values calculated from equations (1) and (2) when $l_1 = l_3 = l_t$, $l_2 = l_4 = l_f$, $N_1 = N_2 = N_3 = N_a$, and $N_4 = N_b$.

Table 4. Feature of the phase grating made by photo-reactive polymer composites.

BBP/ polymer	l_t (μm)	l_f (μm)	Da (μm)	Db (μm)	ΔD (%)
0.8	3.0	17.0	1.42	0.86	65

Na	Nb	ΔN (%)	λ (μm)	$\eta 0/\eta \pm 1$ cal.	obs.
1.547	1.505	2.8	0.78	5.2	5.3±0.2

Fabrication conditions of this grating were the same as shown in figure 5.

The H-type phase grating consists of an S-type phase grating with thickness d and refractive index N_a, and R-type phase grating with thickness D_b and refractive indices N_a and N_b, so that the optical phase shift caused by the H-type phase grating is larger than that caused by either of the other two. Although the S-type phase grating is in a common use for diffraction gratings, light branching elements, Fresnel lens, and the like, it is necessary to increase the difference in level of convex-concave portions to amplify η_m, so that a high degree of precision working is required when a diffraction angle is increased by reducing a grating pitch. With respect to the R-type phase grating, a method for amplifying η_m is to increase the difference in refractive index between alternately arranged layers or thickness of the layers. However, an increasable range of difference in refractive index is comparatively limited in practice, so that the R-type phase grating is disadvantageous in that its thickness should be extremely increased in comparison with the S-type phase grating. The H-type phase grating, therefore, may be easier to manufacture and more suitable for amplify η_m than either the S-type or R-type phase gratings.

Use of trapezoidal phase gratings :

Recently, a number of optical pickup heads for laser disk and CD player systems utilize optical phase gratings with a cross-sectional shape of rectangles periodically arranged on a flat plate as a light branching element. In such a case, the zero-order and the ± 1st-order diffracted light beams are used for focusing, tracking, and signal detection, although the higher order diffracted light beams $|m| > 1$ are lost in vain. The H-type phase grating with a cross-sectional shape of periodically arranged trapezoids is of great use for selective amplification of diffracted light beams suppressing useless diffracted light beams. Such a property of the

H-type phase grating is verified by use of a simplified model as follows. When the relations that $l_1 = l_3 = l_t$, $l_2 = l_4 = l_f$, $N_1 = N_2 = N_a$, and $N_4 = N_b$ hold in equations (1) and (2), the *H*-type phase grating takes a cross-sectional shape of symmetric trapezoids which are periodically arranged on a smooth plate.

A shape factor $\alpha = l_t/(l_t + l_f)$ is introduced to express cross-sectional shapes of a rectangle, a trapezoid, and a triangle when $\alpha=0$, $0<\alpha<1$, and $\alpha=1$, respectively. Since η_m is equal η_{-m} in such a symmetric grating, the sum total of higher-order diffraction efficiencies η_m for $|m|>1$ is shown by an expression by equation (3),

$$S_\alpha = \sum_{|m|>1} \eta_m = 1 - \eta_0 - 2\eta_{\pm 1}, \qquad (3)$$

where $\eta_{\pm 1} = \eta_1 = \eta_{-1}$. For example, when $\gamma = \eta_0/\eta_1$, S_α for the rectangle grating is shown by an expression $S_0 = (\pi^2 - 8)/(\pi^2 - 4\gamma)$, independent of refractive indices N_a and N_b, taking a value of $S_0 = 0.0626$ when $\gamma=5$ which is a typical value for a phase grating in the optical pickup head. Calculation of S_α for the triangle grating is shown by a rather complicated formula, which is omitted from this chapter, taking a large value of $S_1=0.9883$ when $\gamma=5$. While the calculation of S_α for the trapezoidal grating appeared to take a minimum value of $S_\alpha = 0.013$ at $\alpha=0.50$ when $\gamma=5$ as a result of numeric calculations under practicable conditions that $N_0 = 1.00$, $N_a=1.53$, $N_b=1.50$, $d/D_a=0.40$, and $\gamma=0.78$ mm, so that it was lowered down to ~1/5 of the rectangle case resulting in optimum utilization of light.
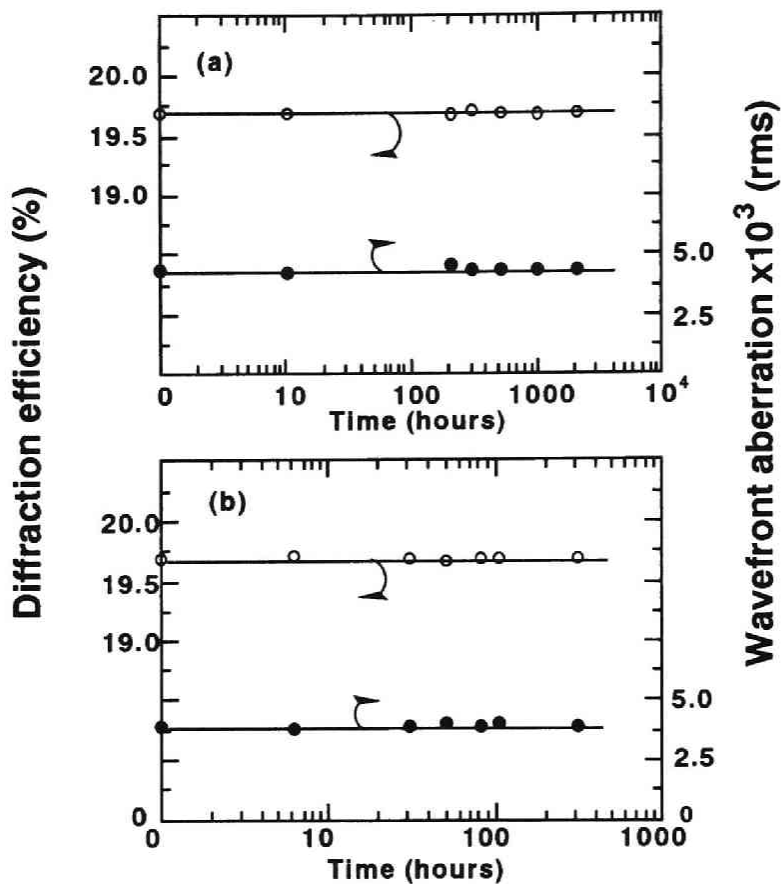
Figure 6. Durability of the phase grating. Two parameters, the ratio of the first order to the zero-order diffraction efficiency at wavelength 780 nm and the wavefront aberration at wavelength 780 nm which was calculated on the observed value at wavelength 632.8 nm, were examined.
(a) In the course of heating under 60°C and 95% RH
(b) In terms of the time elasped after ten cycles of alternate heating at 85 °C for 2 h and cooling at -30 °C for 2 h.

Durability of phase gratings :

Through the customary durability tests, the *H*-type phase grating proved to have stable temperature and humidity, undergoing little changes in diffraction efficiency and wavefront aberration as shown in figure 6. The results presented confirm that the *H*-type phase grating made from photoreactive copolymer composite can be set to practical use.

Conclusions

A copolymer was synthesized from methyl methacrylate and a methacrylic ester comprising non-conjugate carbon-carbon double bonds. A novel photoreactive film was prepared from the copolymer doped with an aromatic ketone with large molecular volume and high refractive index compared with the monomeric components of the copolymer. After the photoreactive film was exposed to ultraviolet light beams through a photomask with a grating pattern, the unreacted dopant was sublimed to fabricate an optical grating. When 2-butenyl methacrylate and 3-benzoylbenzophenone were used as the methacrylic ester and the dopant, respectively, the exposed portion was up to ~110% greater in thickness and ~3% higher in refractive index than the unexposed portion. The rate of change in film thickness was exceptionally larger than the known data.

The phase grating displayed hybrid characteristics of a surface structure modification type and a refractive index modification type phase gratings. Diffraction efficiencies of light beams passing through the phase grating varied with its cross-sectional shape. The shape was regulated by controlling a distance between the photomask and the photoreactive film, that was called

"print gap; g ", to form periodically arranged rectangles, trapezoids or sinusoidal on a smooth substrate when $g = 0$ or $g \neq 0$, respectively. Choosing an optimum cross-sectional shape of trapezoids in practical conditions, the sum of m-order diffraction efficiencies with $|m|>1$ was remarkably lowered in comparison with the rectangle case. Hence, the trapezoidal phase grating is superior to the rectangle one such that zero-order and the ± 1st-order, for example, diffracted light beams are used selectively and effectively at a specially fixed rate. Diffraction efficiencies of the phase grating fabricated from photoreactive polymers were in good agreement with those of calculated value.

The phase grating fabricated in this way was stable at high temperature and humidity and showed little change in diffraction efficiency as well as in wavefront aberration by means of the customary durability tests, suggesting its suitability for a practical use.

References

1) H. P. Weber, W. J. Tomlinson, and E. A. Chandross, *Opt. Quantum Electron.,* **7**, 465 (1975).

2) E. A. Chandross, C. A. Pryde, W. J. Tomlinson, and H. P. Weber, *Appl. Phys. Lett.,* **24**, 72 (1974).

3) W. J. Tomlinson, H. P. Weber, C. A. Pryde, and E. A. Chandross, *Appl. Phys. Lett.,* **26**, 303 (1975).

4) H. Franke, *Appl. Opt.,* **23**, 2729 (1984).

5) W. Driemeier and A. Brockmeyer, *Appl. Opt.,* **25** 2960 (1986).

6) Y. Ito, N. Kawatsuki, B. J. Giri, M. Yoshida, and T. Matsuura, *J. Org Chem.,* **50**, 2893 (1984).

7) N. J. Turro, *Modern Molecular Photochemistry (Benjamin./Cummings, New York,* 1978).

Chapter 4.

Crossed Grating Beam Splitter for Magnetooptical Pickup Head

Abstract : In the form of a crossed grating element (CGE), a novel beam splitter was fabricated by using a pair of holographic surface relief gratings with high spatial frequencies dually formed on a substrate plane. The CGE can act as a beam splitter as well as as a polarized beam splitter. It was experimentally assembled into a magnetooptical pickup head by investigating optical properties.

Introduction

Magnetooptical (MO) disk systems have a great advantage to a conventional magnetic disk because of their large capacity information storage. Information recorded on MO disk is usually read by detecting a slight change in the polarization state of laser beams reflected from a disk. Several beam splitters (BS) are located in MO pickup head to trap laser beams for servo systems of tracking and focusing, while a polarized beam splitter (PBS) separates the laser beam into two polarized light beams to read the information.

It is important for a reduction of access time that the pickup head is small and light. Thus holographic elements have been

proposed. [1,2] Kimura, Sugama and Ono developed a small and light optical head using a holographic optical element, [1] which has three kinds of optical functions: beam splitting, tracking and focusing for error detection. Maeda, Sumi, Ohuchida and Inokuchi proposed a dual-type grating comprising of high density gratings on both of its transparent substrate surfaces, [2] which improved the polarization separation and stability of diffraction angle to wavelength, and evaluated an MO signal detection system using the same element.

When a surface-relief-type grating has a periodicity of less than the wavelength of incident light beams, it causes such interesting phenomena as different diffraction efficiencies in the TE and TM modes, [2-4] wave plates, [5,6] and anti reflection effects. [5-7] Such grating for PBS is of great use of lightening MO pickup head, although it affects only one optical element. Kimura and Ono also proposed a high density holographic optical element with several optical functions to develop a small and light MO pickup head. [8] In making the MO pickup head small and light, it is important to create a new optical element with multiple optical functions.

An object of this chapter is to demonstrate a new type of beam splitter in the form of a crossed grating element (CGE), which plays the role of BS as well as that of PBS, using a couple of holographic surface gratings with high spatial frequencies dually formed on a substrate plane, and to assemble the CGE into a prototype MO pickup head. Until now, CGE have been fabricated from commercially available photoresist. It will be a future work to make a CGE from photoreactive polymer materials described in chapter 1 and 2.

Experimental

Photoresist processing :

In order to prepare a substrate for making a holographic grating, AL glass (Asahi Glass Co.) was washed and driedat 140 °C for 3 h. Micro Posit photoresist MP-1400 was spin-coated on the substrate at 23 °C followed by baking at 80 °C for 40 min to form 1.5 μm thickness layer. Using the 457.9 nm wavelength Ar ion laser, the photoresist layer was illuminated with a couple of plane waves separated angularly by $2X°$ to make a holographic grating with a period of $0.4579/2\sin X$ μm. The exposure energy was varied from 10 to 220 mJ/cm^2 to control the grating height. After exposure to laser light beams, the photoresist layer was developed at 23 °C for 13 sec in Micro Posit MP developer diluted with 1/5 DI water at 23 °C for 1 min.

Figure 1 shows a chemical structure of Micro Posit photoresist which is a positive-type composed of aqueous alkali soluble novolak polymer and naphtodiazoquinone derivative. This mixture cannot dissolve in alkali solvent such as MP developer
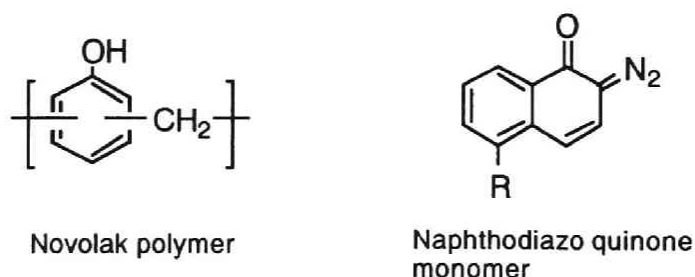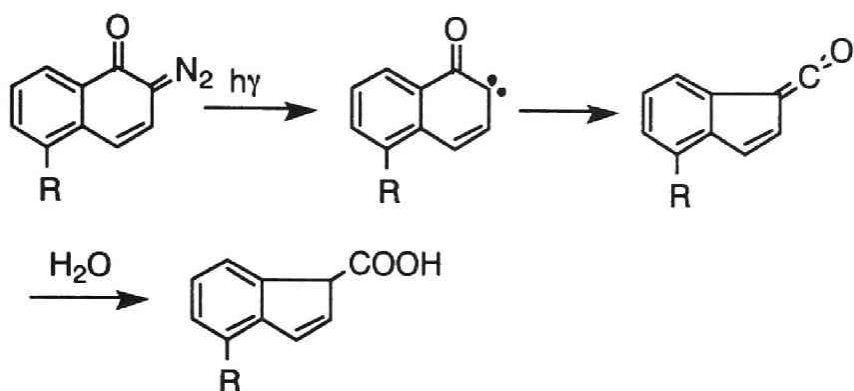

Novolak polymer

Naphthodiazo quinone monomer

Figure 1. Chemical structure of positive type photoresist

Scheme 1

because of the inhibition of novolak dissolution by a photoreactive naphtodiazoquinone derivatives. This monomer is decomposed and become soluble in aqueous alkali by UV light irradiation as shown in Scheme 1, and the polymer can be also soluble in the same solvent.

When holographic crossed grating was made, a 1.8 μm thickness photoresist layer was formed by the above procedure, and dually exposed to the laser light beams in the same conditions, by rotating the sample in the substrate plane by $2T°$. Exposure energy was 170-220 mJ/cm^2 in each case, and the photoresist layer was developed at 23 °C for 9 sec in MP developer.

Extinction ratio :

Constructing an optical system as illustrated in figure 2, polarized/ collimated laser beams passed through a halfwave plate were introduced from the substrate side to the crossed gratings at a calculated angle to obtain two diffraction light beams. The intensity of the light beams diffracted by gratings was measured with a pair of photodiode to determine the extinction ratio. The diffraction efficiency of light beams η was calculated from eq. (1), where I_d, I_{in} and I_r denote the intensity of the diffracted light

89

beam from the unit gratings, the incident light beam and the reflected light beam on the substrate, respectively.

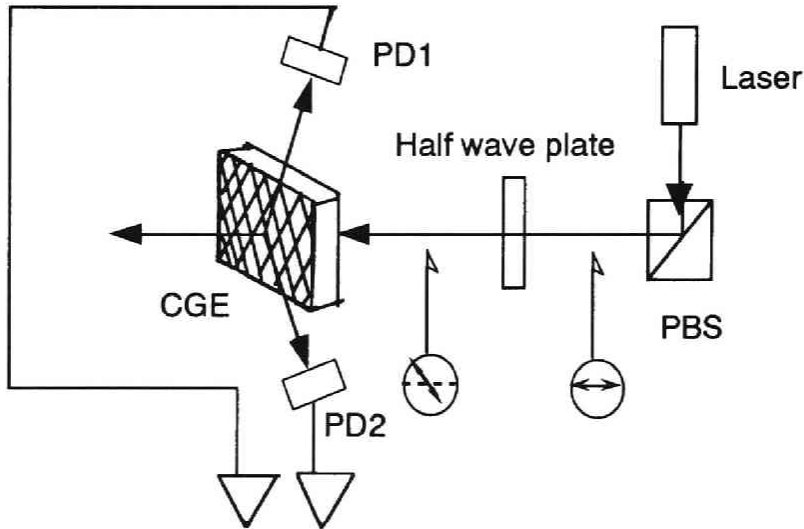$$\eta = \frac{I_d}{I_{in} - I_r} \times 100\ (\%) \qquad (1)$$

Figure 2. Experimental setup of CGE as a PBS

Results and discussion

Line gratings :

Diffraction efficiencies of a pair of light beams diffracted by the line gratings varied with the ratio of grating height h and grating pitch d as shown in figure 3, where the grating pitch and the wavelength were fixed at 0.477 μm and 0.78 μm, respectively. As shown in figure 4, the cross-sectional shape of a grating

observed with a scanning electron microscope (SEM) was an intermediate one between rectangular and sinusoidal. The difference in diffraction efficiencies in the TE and TM incident light beams increased when the cross-sectional areas of the convex portion was not equal to that of the concave portion. [9] In order that the line grating would be effectively applied to a holographic PBS, h should be larger than 0.63 μm, since under these conditions, diffraction efficiency of S-polarized light beams was less than 2% as shown in figure 3.

Design of crossed gratings :

When a pair of line gratings with a high spatial frequency cross each other with a crossing angle $2T°$, light beams passing
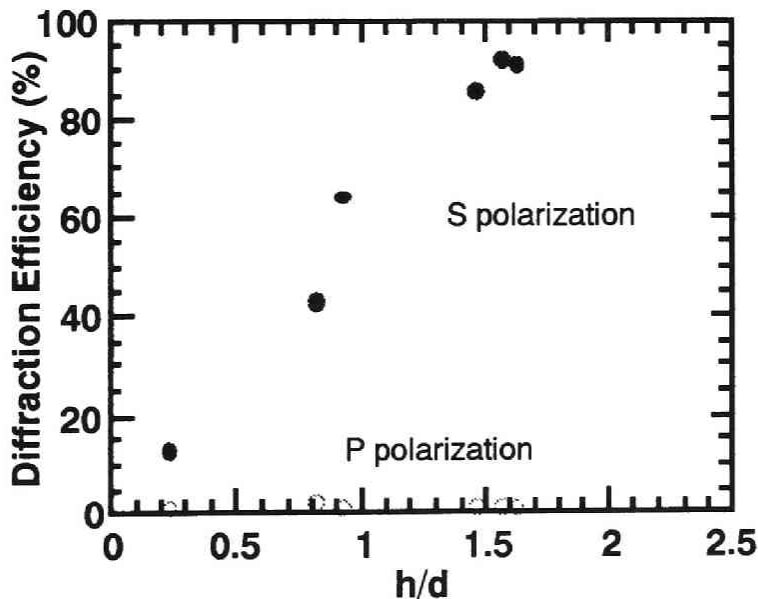

Figure 3. Dependence of η on h/d for polarized light beams of the wavelength of 780 nm introduced to a line grating.
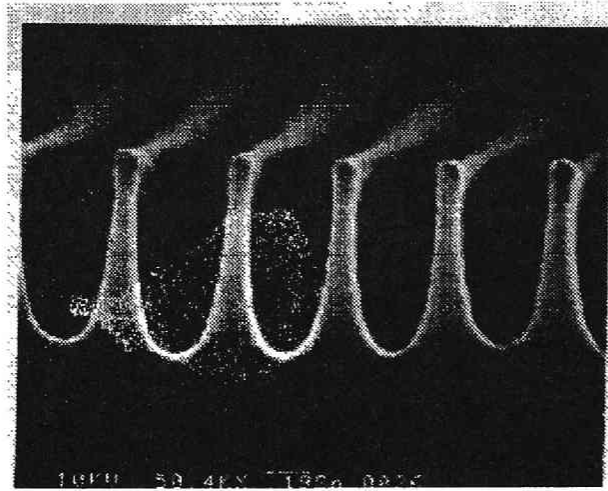
Figure 4. SEM photograph of a line grating showing the side view.

through them are divided into three directions: one is a transmitted light beam Tr, and the other two are light beams D_1 and D_2 diffracted by the component gratings G_1 and G_2, respectively, as shown in figure 5. The optical function of the crossed gratings is schematically depicted in figure 6, where K_1 and K_2 are grating K vectors of G_1 and G_2, respectively, α is a projection angle of K on the x-y plane, m-n is a symmetry line of the crossed gratings, and A and Ψ are inclination angles of the incident light beam from the m-n line and K, respectively.

The theory concerned with the diffraction efficiencies of the surface relief high-density grating [3] is not fully applied to gratings of the CGE, because neither the electric vector (E) nor the magnetic vector (H) is exactly parallel to a vector J, which is perpendicular to K and lies in the grating plane as shown in figure 6. It is impossible to separate the TE and TM incident
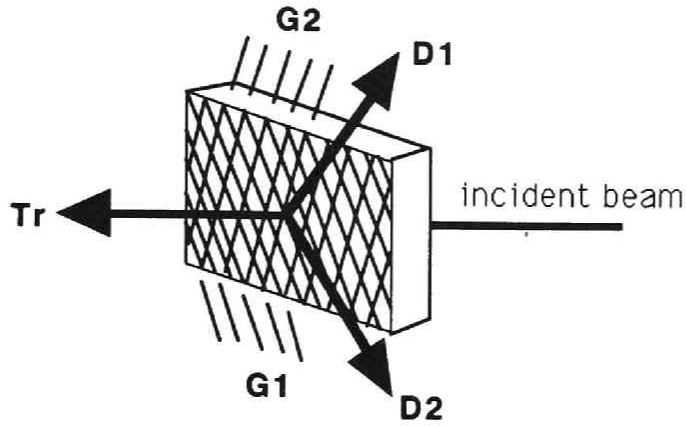
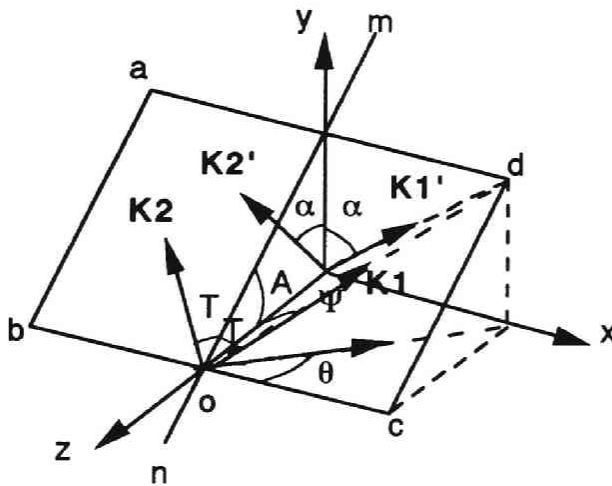**Figure 5.** Behavior of a light beam introduced to CGE

Figure 6. Geometry of the CGE when an incident light
beam travels along the z axis

modes, both of which always arrive simultaneously at the CGE
gratings. When an incident light beam is polarized in a *near*-TE
mode for G_1 and in a *near*-TM mode for G_2, the light beam is
diffracted mainly by G_1 in the following way.

When a vector J_1' perpendicular to a vector K_1' (projection of K_1 to the x-y plane) falls at nearly right angles on the x-y plane with a vector J_2' perpendicular to a vector K_2' (projection of K_2 to the x-y plane), *i.e.*, $\alpha \approx 45°$, a relation that $E // K_1'$ is nearly compatible with a relation that $H // K_2'$ for a polarized light beam. In this conditions, it is predicted that an incident light beam is polarized in a *near*-TE mode for G_1 and in a *near*-TM mode for G_2, so that the CGE divides the incident light beam into three light beams, two polarized and diffracted light beams and a transmitted light beam.

Concerning unit gratings of the CGE, one of a pair will be lower in diffraction efficiency than an ordinary line grating element because of the lack of grating in the crossed region. Since the CGE is about two times larger than in the grating height of its crossed region than the line grating element, as shown in figure 7, the lack of grating lines will have little effect on the diffraction efficiency as compared with a crossed grating whose gratings are fully lacking in the crossed region. The structure in the crossed region will change the polarization state, but the problem is still being studied.

Typical specifications of the CGE are listed in Table 1, where the ratio of wavelength to grating pitch was set 1.57 in order to produce a large difference between diffraction efficiencies of light beams polarized in *near*-TE and *near*-TM polarizations. The α value is forced to shift from its optimum value to assemble the MO pickup head easily.

Characteristics of the CGE :

SEM photographs of a CGE are shown in figure 7 representing (a) top-side view and (b) side view. It can be seen from the photographs that the cross-sectional shape of the grating is not rectangular but sinusoidal, suggesting a deviation of the
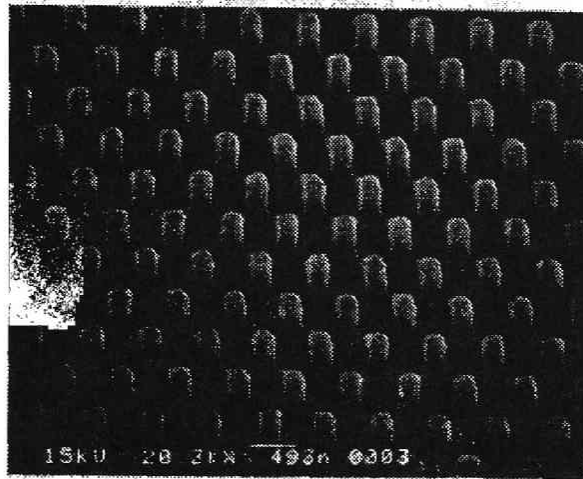
(a)

(b)

Figure 7. SEM photographs of the CGE showing (a) top view
and (b) side view.

Table 1. Design specifications for the CGE

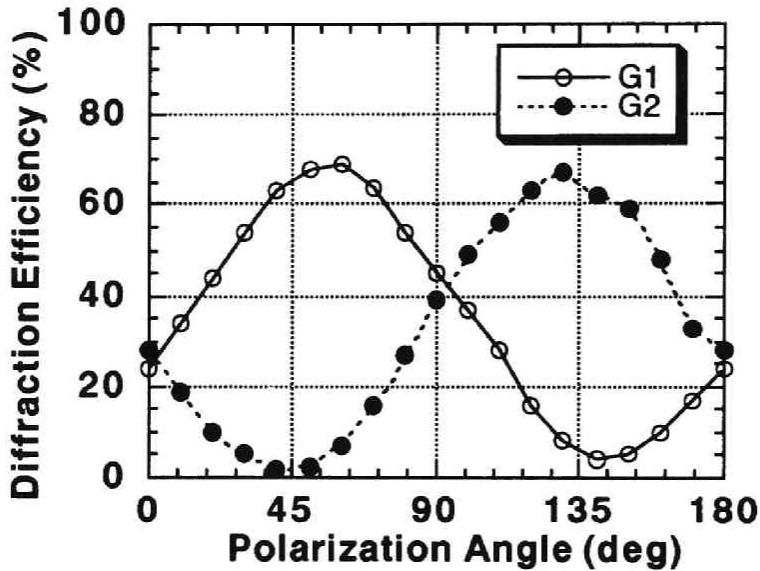| Wavelength	λ	(μm)	0.83
Grating pitch	d	(μm)	0.528
Optical index	λ/d		1.572
Crossing angle	$2T$	(deg)	56
Incident angle	$90-\psi$	(deg)	46.4
Incident angle	A	(deg)	35
Dihedral angle	α	(deg)	42.8

Figure 8. Dependence of η on the polarization angle of an incident beam of the wavelength of 780 nm introduced to the CGE

crossing angle of component gratings from 90°, and that the photoresist remain at the bottom of the cross-sectional grating region.

As shown in figure 8, the observed values of diffraction efficiency η for G_1 and G_2 varied with the polarization angle, which was changed from $0°$ to $180°$ by rotating the half wave plate around the direction of the incident light beam. The η for G_1 reached to the maximum and minimum values at the polarization angles close to $45°$ and $135°$, respectively, which were in practice $48°$ and $138°$, respectively. On the other hand, the η for G_2 reached to the maximum and the minimum values at the polarization angles close to $135°$ and $45°$, respectively. These phenomena are similar to the behaviors of reflected and transmitted light beams caused by use of the ordinary PBS. The crossing angle of the component gratings $2\alpha°$ was forced to be a little different from $90°$ resulting in a little deviation of the polarization angle $45°$ and/or $135°$ at the maximum and the minimum points of the η. The ratio of η values for G_1 and G_2 measured at the polarization angles of $45°$ and $135°$ exhibited small values of 14 dB and 15 dB, respectively, as compared with an extinction coefficient for a PBS. Thus, the CGE is a new type of beam splitter composed of a couple of holographic gratings, which act as a BS as well as a PBS.

Application of the CGE to a MO pickup head :

An optical diagram of the prototype MO pickup head bearing the CGE is illustrated in figure 9. A BS and two PBS's are replaced by a 1-mm-thick CGE as compared with the conventional MO pickup head. In this MO pickup head, the CGE separated a light beam reflected on the MO medium into four light beams, such as two diffracted light beams for reading the recorded information, a transmitted light beam for focusing servo, and a reflected light beam from the reverse plane surface of the CGE substrate for tracking servo.
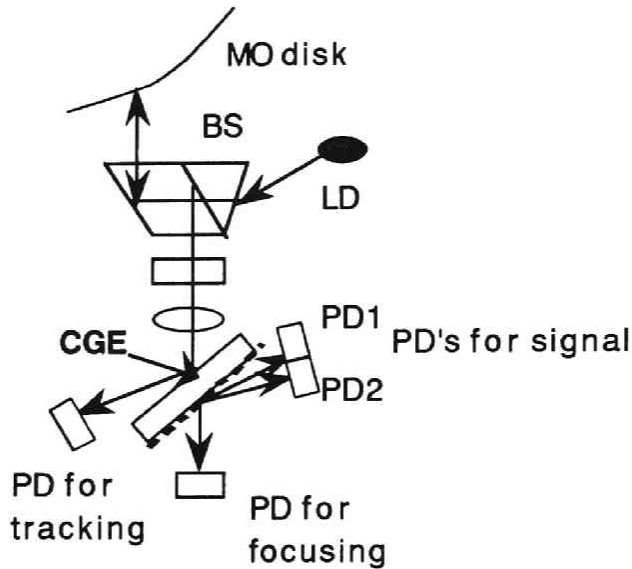
Figure 9. A prototype MO pickup head made from CGE

The reading operation by the prototype MO head was carried out on the basis difference detection in the two diffracted beam intensities. The focusing error signal was derived by an astigmatic method using a transmitted light beam from the CGE mounted diagonally to the incident light beam. The tracking error signal was also derived by a conventional push-pull method using a reflected light beam from the reverse side of the CGE. The polarization angle of the incident light beam to the CGE was set parallel to the plane of figure 9 by rotating a half wave plate mounted in front of the lens.

With the MO pickup head thus prepared, test signals on Te-Fe-Co MO disk at 1 MHz / 900 rpm with a polar Kerr angle of about 0.4° were read out followed by detection of signal beams and their differential signal I_{PD1}-I_{PD2} as shown in figure 10.

In general, the optical grating element for a pickup head has been developed putting stress on sensitivity to wavelength

variation originating in a light source. [1] Since the diffracted light beams were used for signal detection in the present pickup head, the size of each sensor segment of the photodiode covered the movement length of the beam spots on the photodiode owing to wavelength variation.

In order to use the CGE for a practical purpose, holographic grating should be made from optically stable materials as described in chapters 1 and 2 or by the photo-polymerization (2P) method. Holographic experiment using materials in chapter 1 have been underway by an UV-Ar ion laser with a wavelength of 353 nm.
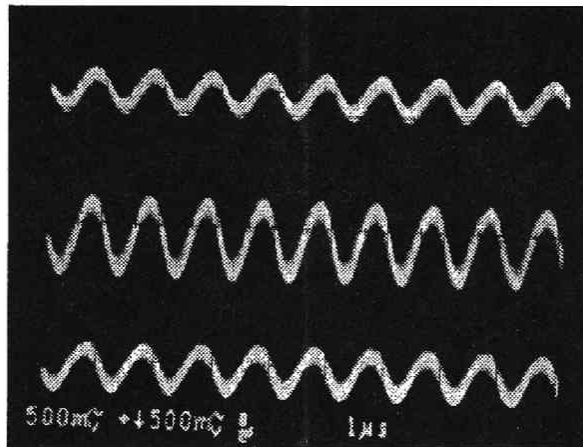
Figure 10. RF signals of the MO disk read by the prototype MO pickup head showing (top) a signal from G_1 (I_{PD1}), (bottom) a signal from G_2 ($-I_{PD2}$) and (middle) a differential signal between G_1 and G_2 ($I_{PD1}-I_{PD2}$).

Conclusions

A crossed grating element (CGE) was holographically made, and a novel magnetooptical (MO) pickup head was experimentally fabricated from the CGE. The CGE exhibited combined properties of a beam splitter (BS) and a polarized beam splitter (PBS) separating the incident light beams into a transmitted light beam and two kinds of diffracted light beams of different phase. The CGE will be useful in producing a small and light MO pickup head.

References

1) K. Kimura, S. Sugama, and Y. Ono, *Appl. Opt.*, **27**, 668 (1988).

2) H. Maeda, Y. Sumi, S. Ohuchida, J. Kitabayashi, and T. Inokuchi, *Proc. Int. Symp. on Optical memory, Kobe, 1989, Jpn. J. Appl. Phys.*, **28** Suppl. 28-3 193 (1989).

3) M. G. Moharam, T. K. Gaylord, G. T. Sincerbox, H. Werlich, and B. Young, *Appl. Opt.*, **23**, 3214 (1984).

4) J. Amako, F. Yamagishi, and H. Ikeda, *Extended Abstracts of 47th Autumn Meeting of Japan Society of Applied Physics*, 30p-v-6 (1986).

5) R. C. Enger, and S. K. Case, *Appl Opt.*, **22**, 3220 (1983).

6) D. C. Flanders, *Appl. Phys. Lett.*, **42**, 492 (1983).

7) Y. Ono, Y. Kimura, Y. Ohta, and N. Nishida, *Appl. Opt.*, **26** 1142 (1987).

8) Y. Kimura, and Y. Ono, Tech. *Digest of 1st Microoptics Conf.*, **F8**, 162 (1987).

9) A. Fukuda, Y. Sakamoto, K. Okada, and J. Tsujiuchi, *Extended Abstracts of 37th Spring Meeting of Japan Society of Applied Physics and Related Societies*, Osaka, April, 29p-b-3 (1990).

Part 3.

Synthesis of New Second Order Nonlinear Optical Polymers Based on Poly-Methacrylic Esters and Aromatic Polyesters

Chapter 5

Processing, Corona-poling and Second Harmonic Generation Studies of Crosslinkable Nonlinear Optical Copolymers

Abstract : Polymethacrylate copolymers, containing nonlinear optically active 4'-dialkylamino-4-nitro-azobenzene side groups and crosslinkable 2-butenyl side groups, have been synthesized and characterized. Films of these copolymers can be thermally crosslinked at elevated temperatures and photochemically crosslinked by exposure to UV light. Both methods allow to control the crosslinking density. A pre-crosslinking step prior to the corona poling step can be applied to optimize the alignment and relaxation of the chromophores. During the corona poling process, the temperature dependence of the second harmonic generation (SHG) of a Nd-YAG laser (1.064 μm) was studied for films with different degrees of pre-crosslinking. Depending on pre-crosslinking conditions, the SHG signal intensity and the alignment stability can be maximized.

Introduction

Second-order nonlinear optical (NLO) polymers are of great interest for use in integrated optical devices, such as modulators, electro-optic (E-O) switches and frequency doublers. [1] Photorefractive applications for these materials are also

emerging. [2] Compared to inorganic molecules, organic molecules generally have large second order hyperpolarizabilities and flat E-O responses well beyond one GHz. [1] Polymeric materials offer additional advantages in device fabrication, such as easy film preparation, which is important for waveguide formation.

In general, non-centrosymmetric order is required for the second order NLO polymers. One of the commercially attractive possibilities to align the chromophores in a non-centrosymmetric order is the application of a strong external electric field. [3-7] In order to prevent relaxation of the chromophores after poling, polymers with high glass transition temperatures or crosslinkable systems have been investigated. [8-19] Even in high Tg NLO copolymers, it was observed that the second order hyper-polarizability decreased after storing for several days at room temperature. [8,9] A more stable alignment can be achieved in chemically crosslinked networks. Thermally crosslinkable NLO polymers were first reported a few years ago by *IBM group*. [10,11] They are based on multifunctional epoxy monomers and nitrophenylamine chromophores. Other thermally crosslinkable NLO polymer systems have been reported subsequently. [12,13] The films with various thicknesses and the crosslinking reaction is usually more difficult to adjust and to control if a monomer mixture is used. Several photocrosslinkable NLO polymers have been also studied. [16-18] In the case of photocrosslinkable NLO-polymers, the crosslinking can be performed by irradiation at various temperatures during and/or after the poling process. Tripathy *et al* studied photocrosslinkable host-guest NLO systems, based on the photoreaction of cinnamoyl esters. [16,17] The same crosslinking reaction was also used in NLO side chain polymers. [18] In these examples, the corona poling step was done prior to photocrosslinking. We reported recently on photocrosslinkable

methacrylate copolymers based on 2-butenyl and benzophenone side-groups. [19] The photocrosslinking reaction and corona poling were done simultaneously.

In this chapter, we explored the concept of using pre-crosslinked NLO polymers prior to the corona poling step. This has the advantage that the alignment and relaxation of the chromophores can be optimized by the pre-crosslink density. Scheme 1 illustrates the various processing steps. A photochemically or thermally crosslinkable NLO-polymer is spin coated on a ITO-glass substrate. In a pre-crosslinking step, the film is partially converted to a desired crosslink density. The non-centrosymmetric alignment is achieved by a corona poling step at elevated temperatures. By optimization of pre-crosslink density and corona poling conditions a stable alignment can be already obtained at this processing stage. It is also possible to further enhance the alignment stability in an additional photochemical crosslinking step.

The experiments reported in this chapter were conducted on a series of polymethacrylate copolymers **1a -1d**, containing non-linear optically active 4'-dialkylamino-4-nitro-azobenzene side groups and crosslinkable 2-butenyl side groups. [20,21] The chemical structure and copolymer composition are shown in figure 1. Films of these copolymers can be thermally crosslinked at elevated temperatures and photochemically crosslinked by exposure to UV light. During the corona poling process, the temperature dependence of the second harmonic generation (SHG) of a Nd-YAG laser (1.064 μm) was studied for films with different degrees of pre-crosslinking.
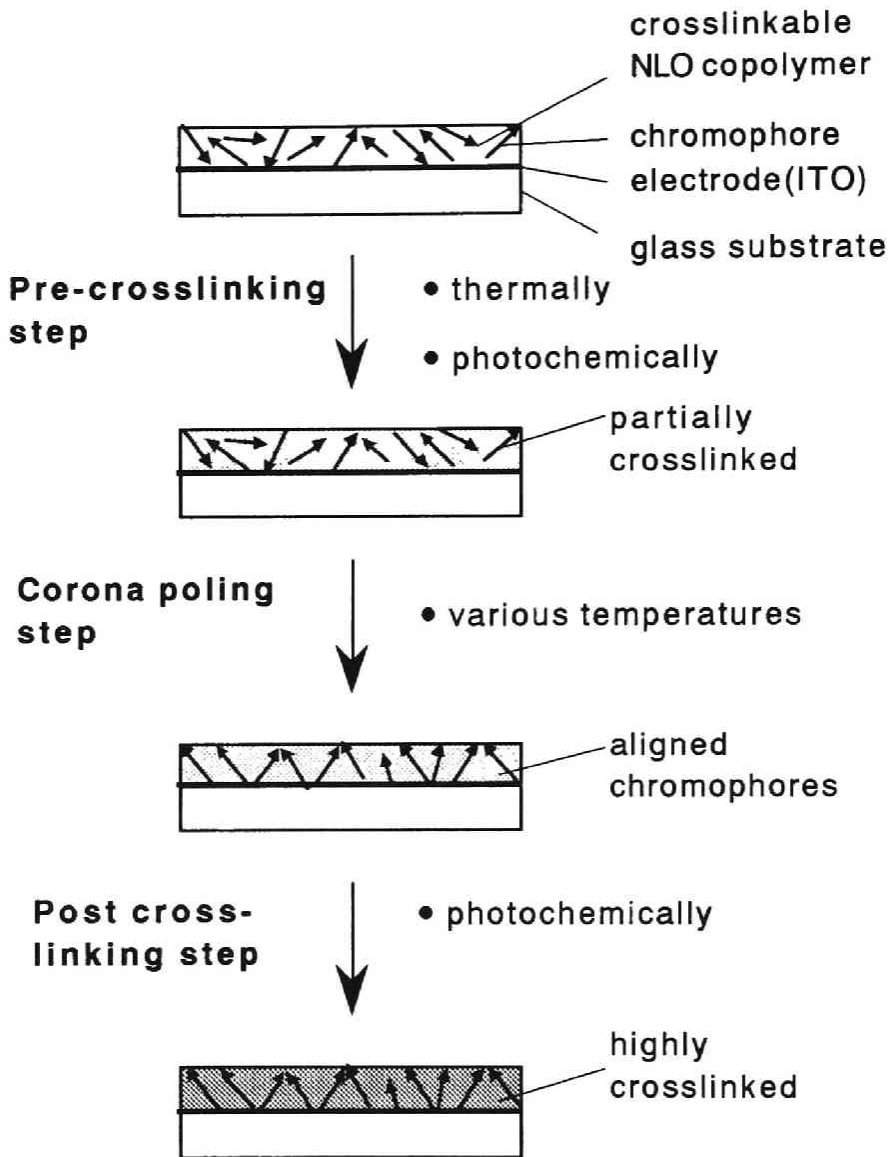
Scheme 1. Representation of processing steps for NLO copolymers.
- Pre-crosslinking step thermally or photochemically.
- Corona-poling step at various temperatures.
- Post crosslinking step photochemically
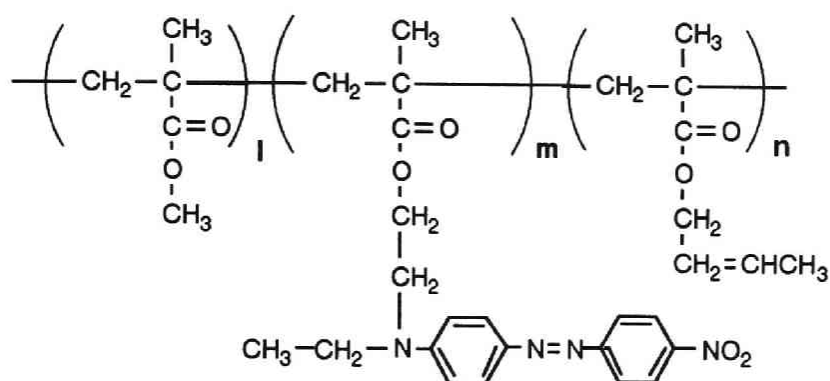
	l	m	n
1a	0.91	0.09	0
1b	0.61	0.09	0.30
1c	0.40	0.11	0.49
1d	0.28	0.11	0.61

Figure 1. Chemical structure of thermally and photochemically crosslinkable NLO copolymers **1a - 1d**.

Experimental

Materials :

Non-stabilized 2-butenyl methacrylate was supplied by Kuraray Co., Ltd. and used without further purification. Methyl methacrylate was used after distillation to remove the inhibitor. 2,2'-Azobis-(2-methylpropionitrile) (AIBN) (Eastman Kodak Co.) was recrystallized from ethanol and stored at 0 °C. *m*-Benzoylbenzophenone was synthesized after the procedure described previously [22] and recrystallized from a hexane and

benzene mixture (1:1). Tetrahydrofuran (THF) was distilled over potassium and stored under argon. All other solvents and chemicals were used as received.

Monomer synthesis :

4'-[(2-Methacryloxyethyl) ethylamino]-4-nitro-azobenzene

Under inert atmosphere, a mixture of 15.7 g (0.05 mol) of 4'-[(2-hydroxyethyl)ethylamino]-4-nitroazobenzene, 5.6 g of triethylamine, 20 mg of 2,6-di-*t*-butyl-4-methyl-phenol (inhibitor) and 300 ml of dry THF was cooled to 5 °C. 5.8 g (0.055 mol) of methacryloyl chloride was added dropwise while stirring. The reaction mixture was stirred for 2 h at 5 °C and 3 h at 50 °C. After cooling, the solution was poured into 200 ml of water and extracted with diethyl ether (3 X 200 ml). The combined ether extracts were washed with saturated aqueous sodium chloride (300 ml) and water (300 ml) and dried over sodium bicarbonate. The solvent was removed at reduced pressure. The resulting red solid was recrystallized from a mixture of hexane/acetone to give 16.2 g (85%) of a raw product. The raw product was purified by column chromatography over silica gel using dichloromethane as eluent. The pure product was obtained as a red crystal.

Yield : 14.1 g (74%) ; m.p. 73-77 °C.

^{1}H-NMR: (CDCl$_3$): δ (ppm) = 1.25 (3H, t, J = 7.0 Hz), 1.92 (3H, s), 3.54 (2H, q, J= 7.0 Hz), 3.73 (2H, t, J= 6.0 Hz), 4.36 (2H, t, J= 6.0 Hz), 5.58 (1H, s), 6.09 (s, 1H), 6.82 (2H, d J= 9.0 Hz), 7.93 (4H, d, J= 9.0 Hz), 8.30 (2H, d, J= 9.0 Hz).

IR (KBr): 1718, 1602, 1512 cm^{-1}.

Polymer synthesis :

The copolymers **1a** - **1d** were obtained by a free radical solution polymerization in dioxane with AIBN as an initiator. The concentration of monomers was about 30 - 40 %(w/v) and the [monomers]/[AIBN] molar ratio was about 1000. Monomer feed ratio, yields and copolymer composition are summarized in Table 1. As an example for the general copolymerization procedure the synthesis of copolymer **1b** is described.

Copolymer 1b

2.0 g (5.24 mmol) of 4'-[(2-Methacryloxyethyl)ethylamino]-4-nitroazobenzene, 2.0 g (14.3 mmol) of 2-butenyl methacrylate, 3.0 g (30 mmol) of methyl methacrylate and 6.5 mg of AIBN were dissolved in 17.5 ml of dioxane. The reaction mixture was treated with a gentle stream of argon. After sealing, the mixture was heated to 52 °C for 24 h. The resulting homogeneous viscous solution was cooled and added dropwise into 400 ml of methanol to precipitate the polymer. After two additional precipitations from dichloromethane solution into methanol, the copolymer was extracted under reflux with methanol until the methanol extracts became colorless. The polymer was dried at 40 °C under vacuum for 48 h.

Yield: 4.0 g (57 wt %)

^{1}H-NMR (CDCl$_3$): δ (ppm) = 0.81 (brs), 0.98 (brs), 1.1~1.4 (m), 1.6~1.9 (m), 3.56 (brs, OC$\underline{H}_3$ + N-C$\underline{H}_2$-CH$_3$), 3.64 (brs, N-C$\underline{H}_2$-CH$_2$-O), 4.13 (brs, N-CH$_2$-C$\underline{H}_2$-O), 4.36 (brs, O-C$\underline{H}_2$-CH=CHCH$_3$), 5.5 (brs, O-CH$_2$-CH=C$\underline{H}$CH$_3$), 5.7 (brs, O-CH$_2$-C$\underline{H}$=CHCH$_3$), 6.83 (brs, aromatic of monomer **1**), 7.92 (brs, aromatic of monomer **1**), 8.29 (brs, aromatic of monomer **1**).

IR (film on NaCl): 1730, 1672, 1600, 1517, 967 cm^{-1}.

Table 1. Monomer feed ratio, yield and copolymer composition of copolymers **1a** - **1d**.

Polymer	Feed ratio (mol%)[a]			Yield(%)	Composition(mol%)[b]		
	L	M	N		l	m	n
1a	90.5	9.5	0	52	91.4	8.6	0
1b	60.5	10.6	28.9	57	60.7	9.3	30.0
1c	44.4	11.2	44.4	35	40.0	11.1	49.3
1d	29.5	11.7	58.8	46	28.1	11.2	60.7

a) Feed ratio of monomers, L : methyl methacrylate, M :

4'-[(2-methacryloxyethyl)ethylamino]-4-nitroazobenzene,

N : 2-butenyl methacrylate.

b) Co-polymerization ratio of a polymer, determined by NMR.

Characterization :

Differential scanning calorimetry data were obtained on a Mettler DSC 30 using a heating rate of 10 °C/min. The molecular weight and molecular weight distributions were measured with chloroform as eluent using a Spectra-Physics LC-GPC systems and Spectra UV-100 detector. The columns (Polymer Standards Service) were calibrated with polystyrene standards. UV-VIS spectra were measured with a Perkin Elmer Lambda-9 spectrometer. NMR spectra were measured with a 400 MHz instrument from General Electric. Duterated chloroform was used as a solvent. Copolymer composition was determined by NMR spectroscopy using separated signals of each monomers. Refractive indices were measured with a Metricon Prism coupler Model-2010 at 632.8 nm. Spin-coated thin films on a silicon substrate were used.

112

Film preparation :

Thin films were prepared from a solution of approximately 10 wt% of copolymer in benzene. The solution was first filtered through 0.2 μm Teflon filter and then spun at 900 - 1000 rpm. Quartz substrates were used for absorption measurements. Silicon wafers were used for refractive index measurements. For corona poling, an indium-tin-oxide (ITO) coated conductive glass plate was used as an electrode.

SHG measurement during corona-poling with heating :

A corona discharge poling process of spin-coated films on ITO glass substrates was used to non-centrosymmetrically align the chromophores. The experimental set-up is shown in figure 2. The sample stage employs a stainless needle at high static potential that is positioned about 2 cm above a grounded ITO substrate onto which the copolymer film was coated. The sample is positioned on temperature variable hot stage in a stainless chamber that allows an inert atmosphere. The sample is arranged at 45° to the incident 1.064 μm Nd-YAG laser (Spectra Physics Model 3800S) which focused on the sample with p-polarization. The sample was heated at the rate of 1.0 °C/min with an electric field of 3 - 6 kV and a current of 2 - 4 μA. The fundamental wave was blocked by IR cut filters and a 532 nm interference filter. The second harmonic signal was detected by a photomultiplier tube and amplified.
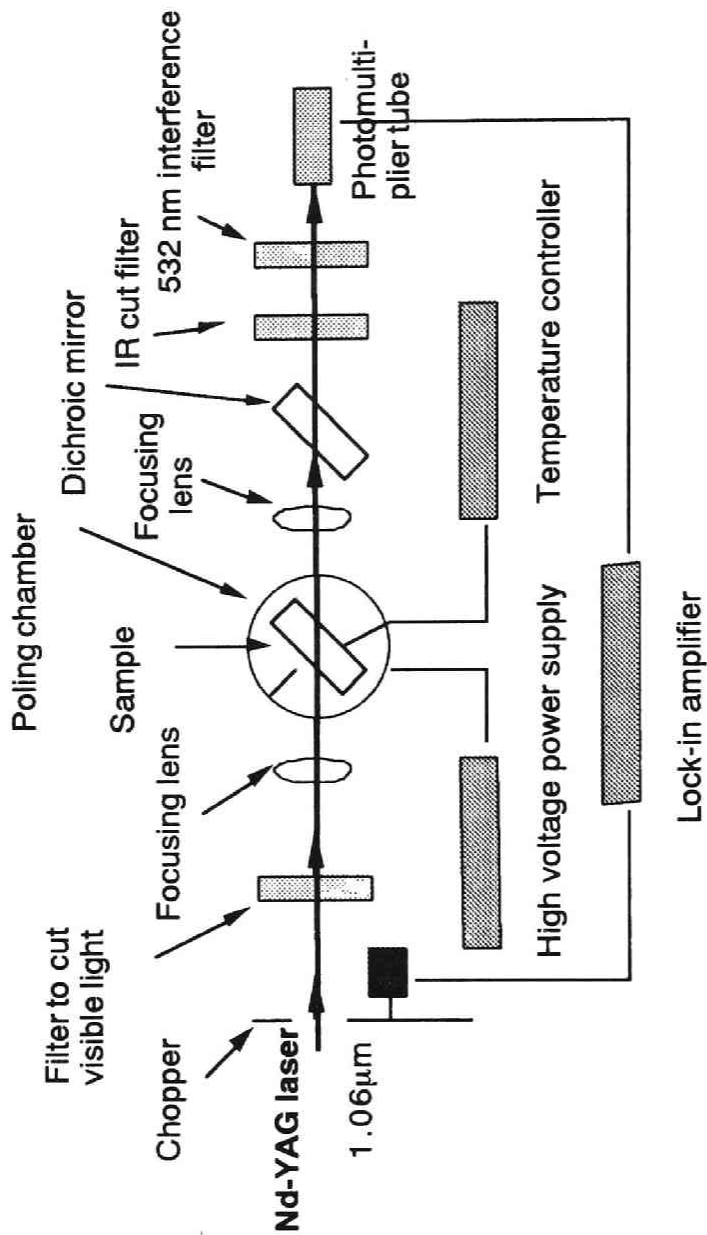
Figure 2. Schematic drawing of experimental setup for second harmonic generation measurement at various temperatures during corona poling.

114

Results and Discussion

Preparation and properties of crosslinkable NLO copolymers :

The methacrylate copolymers **1a - 1d**, studied in this chapter are based on methyl methacrylate, a nonlinear optical active azobenzene monomer and a crosslinkable 2-butenyl monomer (figure 1). The copolymers were synthesized by a free radical polymerization using AIBN as the initiator. All the synthesized copolymers were completely soluble in organic solvents such as benzene or chloroform, indicating that no crosslinking occurred during copolymerization. The results of GPC, DSC and refractive index investigations of copolymers **1a - 1d** are summarized in Table 2. The molecular weights and molecular weight distributions were measured by GPC calibrated

Table 2. Molecular weight, glass transition temperature and refractive index of copolymers **1a - 1d**.

Polymer	$Mn \times 10^{-3}$ [a]	$Mw \times 10^{-3}$ [a]	Mw/Mn [a]	Tg (°C) [b]	RI [c]
1a	263	496	1.88	120 [d]	1.598
1b	176	415	2.36	97 [e]	1.600
1c	146	392	2.69	87 [e]	1.603
1d	272	559	2.05	82 [e]	1.606

a) Determined by GPC, polystylene standards, UV detection.

b) Determined by DSC, heating rate : 10 °C/min.

c) Refractive index at 632.8 nm

d) Second heating after rapidly quenching with liquid nitrogen.

e) First heating.

with polystyrene standards. All copolymers had a mono-modal distribution. The number average molecular weights were in the order of 150,000 - 270,000 g/mol and the weight average molecular weights in the order of 400,000 - 560,000 g/mol. All polymers are amorphous. The glass transition temperatures (Tg) depend on copolymer composition and are dominated by the 2-butenyl methacrylate content. Tg decreases with increasing amount of 2-butenyl methacrylate. Refractive indices of copolymers are much higher than PMMA (n=1.49 at 632.8 nm). This is a consequence of the strong absorption at 478 nm associated with the NLO chromophore. For copolymers with similar content of NLO side groups, the refractive indices increase with increasing amount of 2-butenyl groups.

Thermal pre-crosslinking :

Copolymers with 2-butenyl side group **1b** - **1d** can be thermally crosslinked in inert atmosphere without decomposition at temperatures between 150 - 180 °C. Depending on time and temperature, the crosslink density can be varied. Films which are slightly swellable or completely non-swellable in chloroform are obtained. In an experiment under the same conditions, copolymer **1a**, which contains no 2-butenyl side group, was afterwards still fully soluble in chloroform. This indicates that the copolymer crosslinking reactions occur through the 2-butenyl carbon-carbon double bond. Table 3 lists glass transition temperatures of pre-crosslinked films after curing at various conditions. The glass transition temperatures of the pre-crosslinked systems depend on the curing time and are 2 - 7 °C higher compare to the starting copolymers. With increasing curing time a slight increase in Tg was observable. The Tg signal generally broadens with increasing

Table 3. Glass transition temperatures of thermally crosslinked copolymers **1b** and **1d** for different curing times at curing temperatures of 150 °C and 180 °C.

Curing time (hr)	Glass transition temperature (°C)			
	1b		**1d**	
	$CT^{a)}$=150	$CT^{a)}$=180	$CT^{a)}$=150	$CT^{a)}$=180
0	97	97	82	82
3	97	98	82	82
7	98	100	82	85
16	102	105	85	89
24	102	b)	88	b)

a) Curing temperature (°C)

b) not clearly detectable

curing time and was no more clearly detectable for film cured at 180 °C for 24 h.

It is possible to lower the curing temperature and to enhance the curing speed by the addition of a free radical initiator such as AIBN. The crosslinking density can be controlled by the amount of the initiator, the curing temperature and curing time. Copolymer films of **1b** - **1d** with 2 - 15 wt% AIBN were cured at 70 °C, 100 °C and 130 °C. Almost independent of the initiator concentration, no crosslinking occured below 70 °C. All films were still soluble in chloroform. The copolymers **1b** - **1d** doped with 4 wt% of AIBN crosslinked at 100 °C, became already insoluble in chloroform after curing for 30 minutes. At a curing temperature of 130 °C, the crosslink reaction was faster. The fact

that the samples exposed to 70 °C are still not crosslinked reveals that the crosslink reaction with AIBN occurs above Tg of the doped polymer. DSC measurements on these pre-crosslinked films did not show well defined glass transitions.

Photochemical pre-crosslinking :

The photoreaction of 2-butenyl methacrylate containing copolymers doped with benzophenone derivatives yield also crosslinked polymers. [20,21] Two benzophenone photoinitiators **2a** and **2b** were used in this study and are shown in figure 3. Benzophenone **2a,** represents a mono-functional photoinitiator, whereas **2b** is a bi-functional one. The pre-crosslinking density can be adjusted by exposure time and concentration of photoinitiator. Absorption spectra of films of **1b** and **1b** doped with 10 wt% of **2a** or **2b** on a quartz substrate are shown in figure 4. The absorption maxima of the copolymers are at 478 nm and the absorption minimum is around 350 to 375 nm. Due to the small n-π^* absorption of benzophenone derivatives, absorbance of doped films around 360 nm is slightly higher than that of the non-doped films. It is interesting that optically clear films with no phase separations up to 50 wt% of **2b** could be prepared by spin coating.
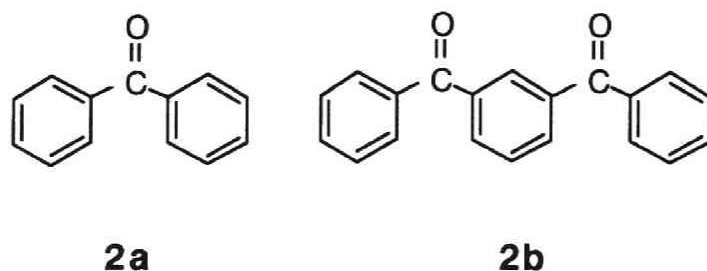
2a   **2b**

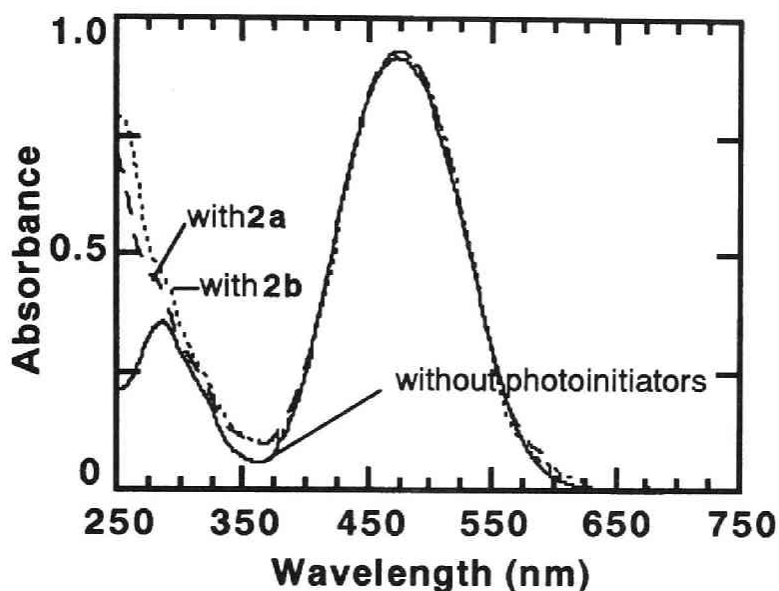**Figure 3.** Chemical structure of photoinitiators **2a** and **2b**.

Figure 4. Absorption spectra of spin-coated films of
1b on a quartz substrate (film thickness: 1.0-1.1 μm).
(Photoinitiator concentration was 10% w/w.)

Films of **1b** - **1d** doped with 30 wt% **2a** or **2b** were mainly studied. The benzophenone derivatives act as plastitizer and lower Tg at this concentration near room temperature. After seven hour irradiation at 30 - 35 °C (at 366 nm with 100W Hg lamp), the films became completely insoluble and non swellable in chloroform. After this exposure most of the benzophenone photoinitiator has reacted. In some experiments the non-reacted benzophenone derivative was removed by sublimation prior to corona poling. After the removal of benzophenone **2a**, no specific carbonyl vibration at 1661 cm^{-1} of IR spectra was observed. In the case of films with the bifunctional benzophenone **2b**, peak at 1661 cm^{-1} was still observable, indicating that the photoinitiator is covalently incorporated on one side.

119

Corona poling and SHG measurements :

Second harmonic generation (SHG) was measured simultaneously to the corona poling process while heating the samples as film on an ITO glass substrate between room temperature and 140 °C. The corona poling field was about 4 - 6 kV/2 - 3 μA. Thermally and photochemically pre-crosslinked films of **1b** - **1d** with different crosslinking degree were investigated. The results were compared with the non pre-crosslinked copolymers.

The SHG intensity of the non-crosslinked films of copolymers **1a** - **1d** started to increase already at room temperature when an electric field was applied. This means that NLO chromophores are mobile at room temperature although the glass transition of the copolymers is much higher (82 - 120 °C). The maximum SHG values of the copolymers were found at 98 °C for **1a,** 76 °C for **1b,** 63 °C for **1c** and 58 °C for **1d,** respectively. These values are about 15 - 20 °C below Tg of the copolymers. Above these temperatures, the SHG intensity decreased. This decrease is due to the mobility of the side group chromophores around Tg. Film damage at higher temperature with high electric fields also occured in some cases. These observations confirm that corona poling is most effective below Tg. [23)]

For the thermally pre-crosslinked copolymers SHG intensity started to increase at temperatures above room temperature. The onset temperature is depending on the curing temperature, curing time and the content of 2-butenyl side groups. As an example, figure 5 shows the intensity of SHG signals from films of **1b** pre-crosslinked at 180 °C for 4 h and 16 h compared to the non pre-crosslinked **1b.** During poling, the temperature was increased with about 1 °C/min. The onset temperature of the SHG signal shifts to higher values with longer curing times. The higher crosslink
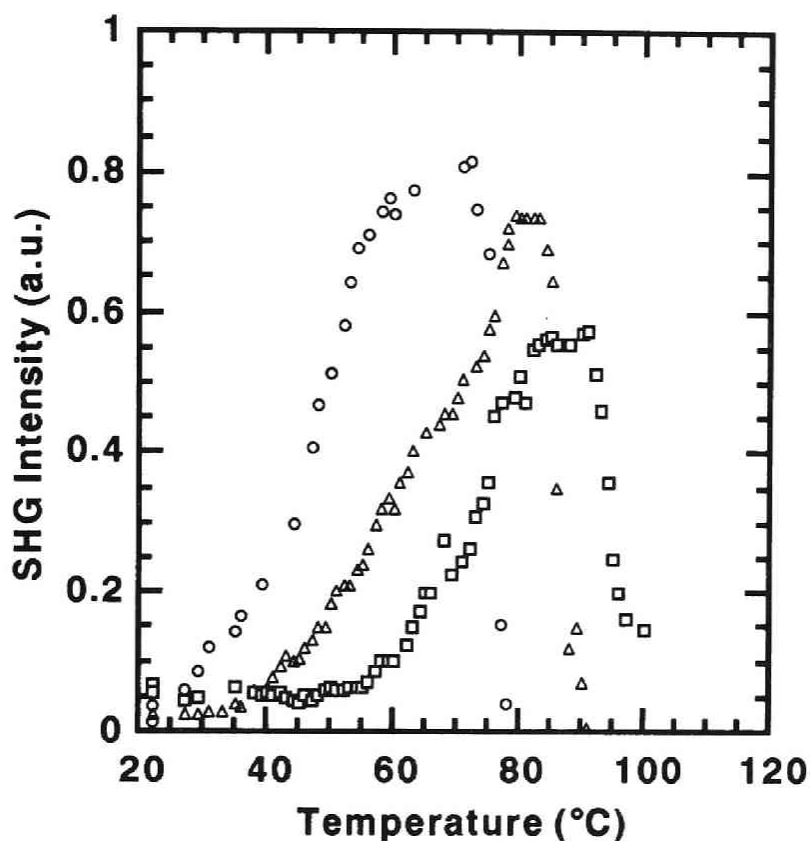
Figure 5. Intensity of SHG signal versus temperature for
thermally crosslinked films of **1b** (heating rate: 1 °C/min)
Curing temperature is 180 °C. Cured time; O: 0h, △ : 4h,
□ : 16h.

density restricts the mobility and does not allow the alignment of
the chromophores below an onset temperature. The maximum
SHG intensity for these systems seems to drop with increasing pre-
crosslinking. This can be attributed to the restricted mobility of
the chromophores in a higher crosslinked environment. Further
increase in temperature results in a decay of the SHG intensity and
damage of the film is observed.

121

The same experiments were performed with photo-chemically pre-crosslinked films of **1b** - **1d** doped with 30 wt% **2b.** UV light at a wavelength of 366 nm and an intensity of 3 - 5 mW/cm^2 was used. It is possible to remove unreacted **2b** from the film at 95 °C for 1 h under a reduced pressure. The results of
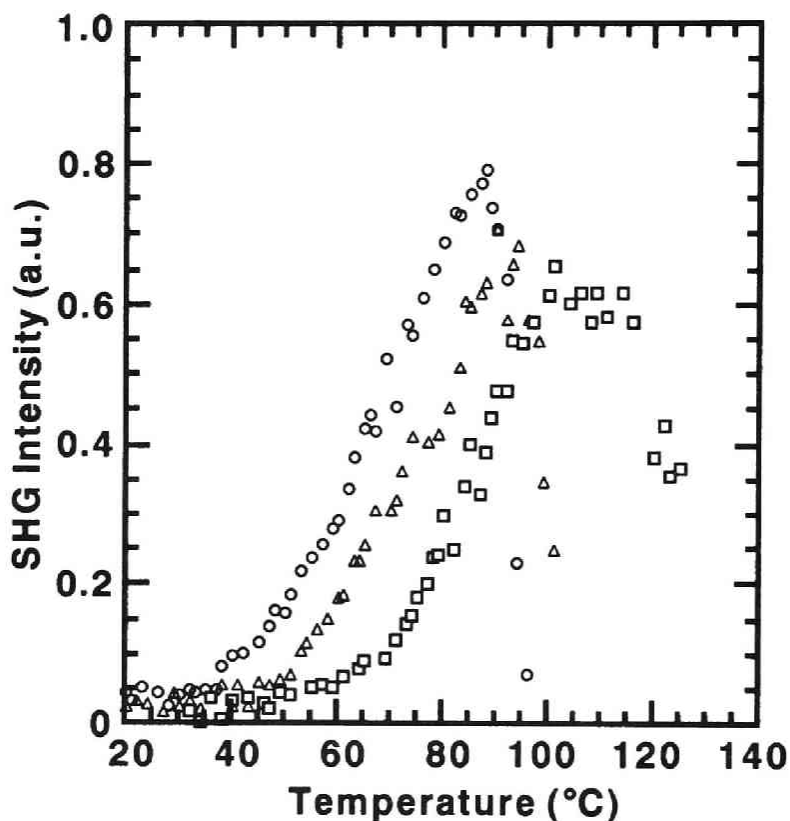

Figure 6. Intensity of SHG signal versus temperature for photochemically crosslinked films of **1b** doped with 30 wt% of **2b** (heating rate: 1 °C/min). ; exposure time ; O: 1h,△ : 4h, □ :16h.

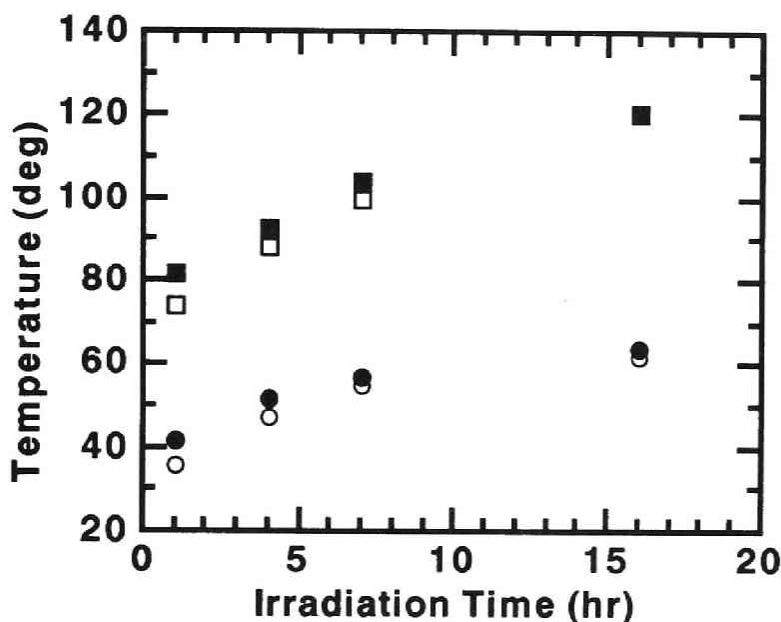(Unreacted **2b** was removed by sublimation after exposure.)

Figure 7. Onset temperature of SHG signal for photo-crosslinked films of **1b** (●) and **1d** (O) and temperature of maximum SHG signal for photocrosslinked film of **1b** (■) and **1d** (□) as a function of exposure time. Film thickness was $1.5 \sim 2.0\ \mu m$.
(Unreacted **2b** was removed by sublimation after exposure.)

SHG measurements are shown in figure 6. A non-irradiated film of **1b** aligned at room temperature when the corona field was applied. The onset temperatures of irradiated films are around 50 - 65 °C and increase with irradiation time. If the benzophenone, which acts as plastitizer, is not removed, the SHG onset temperatures is about 15 - 20 °C lower and the temperature of maximum SHG intensity is also 20 - 40 °C lower.

The onset temperatures and the temperatures of maximum SHG signal intensity for copolymers **1b** and **1d** are plotted in

figure 7 as a function of the irradiation time. In these experiments 30 wt% of **2b** was used and the unreacted amount was removed after exposure. The onset temperatures as well as the maximum temperatures for the SHG signal increased with increasing the irradiation time. The lower glass transition of **1d** compared to **1b** is also reflected, particularly at short irradiation times.

Alignment stability :

Thermally and photochemically pre-crosslinked films were corona poled at a few degrees below the determined maximum SHG intensity temperature and cooled slowly to room temperature in the presence of the corona field. A film of **1b** cured at 180 °C for 7 h was used for this experiments as an example for the thermally pre-crosslinked case. As photochemically pre-crosslinked film, **1b** with 30 wt% of **2b** irradiated for 7 h was used. For both samples, the SHG intensities did not change after poling for more than 4 weeks at room temperature. In comparison the SHG intensity of the non-crosslinked film already decayed to half of its original value after two weeks. The alignment stability of the NLO chromophore is related to the onset temperature of SHG intensity. The differences of the glass transition temperature of the non-crosslinked and crosslinked copolymers which are within 10 °C, can not solely explain the stability difference. In addition, the formed network structure and the local environment of the aligned chromophores seem to be important factors for the alignment stability.

Conclusions

Non-centrosymmetrically aligned copolymers with disperse red 1 side groups as NLO chromophore and 2-butenyl side group is as a crosslinkable unit display SHG. In order to stabilize the SHG signal, these polymers can be pre-crosslinked prior to corona poling thermally at temperatures between 150 - 180 °C or around 100 °C with the aid of a free radical initiator and photochemically by UV irradiation if benzophenone derivatives are added. The glass transition temperatures are a function of the copolymer content of 2-butenyl methacrylate and the crosslink density.

Investigations of the SHG signal intensity during the corona poling process revealed that the signal intensity and stability can be optimized if the copolymers are pre-crosslinked prior to the corona poling process. NLO chromophores are mobile at room temperature in the non-crosslinked films, although the glass transition temperature is between 82 - 120 °C. The onset temperature of the SHG signal shifts to higher values for films with increasing pre-crosslink density. The higher crosslink density restricts the mobility and does not allow the alignment of the chromophores below this onset temperature. Films poled at optimized pre-crosslinking and poling temperature showed no decay of the initial SHG intensity after storing for four weeks at room temperature.

References

1) For reviews, see for example : a) P. N. Prasad and D. R. Urich (Eds.) *"Nonlinear Optical and Electroactive Polymers"* Plenum Press (1988), b) P. N. Prasad and D. J. Williams (Eds.) "Nonlinear Optical Effects in Molecules and Polymers" John Wiley & Sons (1991), c) R. Lytel, G. F. Lipscomb, M. Stiller, J. I. Thackara, and A. J. Ticknor, *Nonlinear Optical Effects in Organic Polymers*, J. Messier et al. eds., Kluwer Academic Publishers (1989), p.277, d) D. R. Ulrich, *Mol. Cryst. Liq. Cryst.*, **189**, 3 (1990).

2) S. Ducharme, J. C. Scott, R. J. Twieg, and W. E. Moerner, *Phys. Rev. Lett.*, **66**, 1846 (1991).

3) a) R. Lytel, G. F. Lipscomb, M. Stiller, J. I. Thackara, and A. J. Ticknor, *Nonlinear Optical Effects in Organic Polymers*, J. Messier et al. eds., Kluwer Academic Publishers (1989), p.277, b) D. R. Ulrich, *Mol. Cryst. Liq. Cryst.*, **189**, 3 (1990).

4) Y. Nonaka, S. Kunioka, R. Aizawa, O. Sugihara, T. Kinoshita, Y. Koike, and K. Sasaki, *Proc. CLEO* C TuP4 136 (1991).

5) Y. Shuto, M. Amano and T. Kaino, *Jpn. J. Appl. Phys.*, **30**, 320 (1991).

6) D. R. Robello, *J. Polym Sci., part A : Polym. Chem.*, **28**, 1 (1990).

7) M. Amano, T. Kaino, F. Yamamoto, and Y. Takeuchi, *Mol. Cryst. Liq. Cryst.*, **182A**, 81 (1990).

8) M. Eich, A. Sen, H. Looser, G. C. Bjorklund, J. D. Swalen, R. Twieg, and D. Y. Yoon, *J. Appl Phys.*, **66**, 2559 (1989).

9) K. D. Singer, M. G. Kuzyk, W. R. Holland, J. E. Sohn, S. J. Lalama, R. B. Comizzoli, H. E. Katz, and M. L. Schilling, *Appl. Phys. Lett.*, **53**, 1800 (1988).

10) D. Jungbauer, B. Reck, R. Twieg, D. Y. Yoon, C. G. Willson, and J. D. Swalen, *Appl. Phys. Lett.*, **56**, 2610 (1990).

11) M. Eich, B. Reck, D. Y. Yoon, C. Grant, and G. C. Bjorklund, *J. Appl. Phys.*, **66**, 3241 (1989).

12) K. D. Singer, M. G. Kuzyk, T. Fang, W. R. Holland and P. A. Cahill, *Organic Molecules for Nonlinear Optics and Photonics*, J. Messier, F. Kazyar and P. Prasad. eds., NATO ASI Series E. **Vol 194** 105 (1991)

13) S. Allen, D. J. Bone, N. Carter, T. G. Ryan, R. B. Sampson, D. P. Devonald and M. G. Hutchings, *Organic Materials for Nonlinear Optics II*. R. A. Hann and D. Bloor eds., Redwood Press Ltd, Melksham, Wiltshire (1991), p235.

14) K. D. Singer, M. G. Kuzyk, T. Fang, W. R. Holland and P. A. Cahill, *Organic Molecules for Nonlinear Optics and Photonics*, J. Messier, F. Kazyar and P. Prasad. eds., NATO ASI Series E. **Vol 194** 105 (1991)

15) S. Allen, D. J. Bone, N. Carter, T. G. Ryan, R. B. Sampson, D. P. Devonald and M. G. Hutchings, *Organic Materials for Nonlinear Optics II*. R. A. Hann and D. Bloor eds., Redwood Press Ltd, Melksham, Wiltshire (1991), p235.

16) B. K. Mandal, J. Kumar, J.-C. Huang, and S. Tripathy, *Makromol. Chem., Rapid Commun.*, **12**, 63 (1991).

17) B. K. Mandal, J. Kumar, J.-C. Huang, and S. Tripathy, *Appl. Phys. Lett.*, **58**, 2459 (1991).

18) H. Müller, I. Müller, O. Nuyken, and P. Strohriegel, *Makromol. Chem., Rapid Commun.*, **13**, 289 (1992).

19) N. Kawatsuki, K. Pakbaz, and H.-W. Schmidt, *Makromol. Chem., Rapid Commun.*, **14**, 625 (1993).

20) a) N. Kawatsuki, and M. Uetsuki, *Appl. Opt.* **29**, 210 (1990), b) N. Kawatsuki, and M. Uetsuki, *"Polymers for Lightwave and Integrated Optics"*, L. A. Hornak ed., (Marcel Dekker, New York, 1992), p. 171.

21) Y. Ito, Y. Aoki, T. Matsuura, N. Kawatsuki, and M. Uetsuki, *J. Appl. Polym. Sci.*, **42**, 409 (1991).

22) Y. Ito, N. Kawatsuki, B. P. Giri, M. Yoshida, and T. Matsuura, *J. Org. Chem.*, **50**, 2893 (1985).

23) R. H. Page, M. C. Jurich, B. Reck, A. Sen, R. J. Twieg, J. D. Swalen, G. C. Bjorklund, and C. G. Willson, *J. Opt. Soc. Am.*, **B7**, 1239 (1990).

Chapter 6

New Photocrosslinkable Methacrylate Copolymers for Nonlinear Optical Applications

Abstract : New photocrosslinkable methacrylate copolymers bearing benzophenone and 2-butenyl side group were synthesized. These copolymers can be crosslinked by UV irradiation and become insoluble in organic solvents. For a NLO application of these copolymers, methacrylate monomer with NLO active side group was copolymerized with crosslinkable comonomers. This copolymer can also be crosslinked by UV light in corona-poling state and showed a stable alignment of NLO chromophore.

Introduction

Because of their great potential for integrated optical devices such as modulators, electro-optic (E-O) switches, frequency doublers and photorefractive applications, a lot of second-order nonlinear optical (NLO) polymers have been synthesized. [1,2] Compared to inorganic molecules, organic molecules generally have large second order hyperpolarizabilities and flat E-O responses well beyond one GHz. [1] Polymeric materials offer additional advantages in device fabrication, such as easy film preparation, which is important for waveguide formation.

129

The principal problem with second-order NLO polymers which are aligned by an external electric field, is the relaxation of the non-centrosymmetric structure. [3-5] One approach for solving this problem is the formation of a chemically crosslinked network during or after the poling process. Thermally crosslinkable NLO polymers were first reported a few years ago by *IBM group*. [6,7] They are based on multifunctional epoxy monomers and nitrophenylamine chromophores. Other thermally crosslinkable NLO polymer systems have been reported subsequently. [8,9] In thermally crosslinkable systems, it is difficult to optimize and influence the crosslinking rate simultaneously with the poling at the poling temperature. In the case of photocrosslinkable NLO-polymers, the crosslinking can be performed by irradiation at various temperatures during and/or after the poling process. Photocrosslinking additionally offers patternability by photolithographic techniques. Tripathy *et al* [10,11] studied photocrosslinkable host-guest NLO systems, based on the photoreaction of cinnamoyl esters. The same crosslinking reaction was also used in NLO side chain polymers. [12]

It is well known that phenyl carbonyl compounds photochemically react with non-conjugate carbon-carbon double bonds. [13] As described in chapters 1-3, photopatternable material composed of benzophenone derivatives and 2-butenyl side chain containing methacrylate derivatives has been used for preparation of optical grating devices. [14]

This chapter describes new photocrosslinkable NLO copolymers, which are based on methyl methacrylate, a photo-excitable benzophenone monomer, a nonlinear optical active 4'-[(2-hydroxyethyl)ethylamino]-4-nitroazobenzene (disperse red 1) side chain monomer and a crosslinkable 2-butenyl monomer. These copolymers can be crosslinked by UV light at 366 nm in the poled state and show a stable alignment of NLO chromophore.

Experimental

Materials :

Methyl methacrylate and methacryloyl chloride were used after distillation to remove the inhibitor. 4'-[(2-Hydroxyethyl)ethylamino]-4-nitroazobenzene, triethylamine and dioxane (Aldrich) were used as received. 2-Butenyl methacrylate without inhibitor was supplied by Kuraray Co., Ltd. and used without further purification. 2,2'-Azobis-(2-methylpropionitrile) (AIBN) (Eastman Kodak Co.) was recrystallized from ethanol and stored at 0 °C. Tetrahydrofuran (THF) was distilled over potassium and stored under argon. All other solvents and chemicals were used as received.

Monomer synthesis :
3-(Benzoyl)-phenyl methacrylate (**1**)

Under dry and inert atmosphere, a mixture of 14.0 g (0.07 mol) of 3-hydroxybenzophenone, 8.0 g of triethylamine, 20 mg of 2,6-di-*t*-butyl-4-methyl-phenol (inhibitor) and 250 ml of dry THF was cooled below 5 °C. 8.0 g (0.075 mol) of methacryloyl chloride was added dropwise while stirring. The reaction mixture was stirred for 2 h at 5 °C and 20 h at room temperature. The solution was poured into 200 ml of water and extracted with diethyl ether (3 X 100 ml). The combined ether phase was washed with saturated aqueous sodium chloride (300 ml) and water (300 ml) and dried over sodium bicarbonate. The solvent was removed at reduced pressure and resulting oil was purified by column chromatography over silica gel using dichloromethane as eluent. A clear viscous liquid was obtained.

Yield : 11.1 g (59%)

^{1}H-NMR: (CDCl$_3$): δ (ppm) = 2.03 (3H, s), 5.76 (1H, s), 6.34 (1H, s), 7.4 - 7.8 (9H, m).
IR (neat on NaCl): 1734, 1657, 1637, 1583 cm^{-1}.

4'-[(2-Methacryloxyethyl)ethylamino]-4-nitroazobenzene (**2**) was synthesized from 4'-[(2-Hydroxyethyl)ethylamino]-4-nitro-azobenzene and methacryloyl chloride by the same procedure as described in chapter 5.

Polymer synthesis :

Copolymers **3a - 3f**, **4a** and **4b** were obtained by free radical polymerization in dioxane solution with AIBN as initiator. In the case of copolymers **3a-3f** and **4a** the monomer concentration was between 40 to 50 w/v %, which corresponds to a molar concentration of 1.2-2.5 mol/l. For copolymer **4b**, the monomer concentration was 25 w/v % and 1.2 mol/l. The molar ratio of monomers to AIBN was about 1000:1. The monomer feed ratios of the different copolymerizations and preparative yields are summarized in Table 1. As an example, the procedure for copolymer **4a** is given below.

Copolymer **4a**

0.09 g (0.9 mmol) of methyl methacrylate, 0.77 g (5.5 mmol) of 2-butenyl methacrylate, 0.79 g (2.97 mmol) of **1**, 0.535 g (1.4 mmol) of **2** and 2.0 mg of AIBN were dissolved in 4.0 ml of dioxane. The reaction mixture was treated with a gentle stream of argon to eliminate oxygen. After sealing, the mixture was heated to 52 °C for 24 h. The resulting viscous solution was cooled and added dropwise into 300 ml of methanol to precipitate the copolymer. After two additional precipitations from dichloromethane solution into methanol, the copolymer was

continuously extracted with methanol until the methanol became colorless. The polymer was dried at 40 °C in vacuum for 48 h. Preparative yield: 1.3 g (59 %).

^{1}H-NMR (CDCl$_3$): δ (ppm) = 0.81~1.2 (m), 1.5~1.7 (m), 1.90 (brs, CH$_3$CH=CH-CH$_2$-O-), 3.56 (brs, OCH$_3$ + N-CH$_2$-CH$_3$), 3.64 (brs, N-CH$_2$-CH$_2$-O), 4.13 (brs, N-CH$_2$-CH$_2$-O), 4.36 (brs, O-CH$_2$-CH=CHCH$_3$), 5.5 (brs, O-CH$_2$-CH=CHCH$_3$), 5.7 (brs, O-CH$_2$-CH=CHCH$_3$), 6.83 (brs, aromatic of monomer **2**), 7.20~7.75 (m, aromatic of monomer **1**), 7.92 (brs, aromatic of monomer **2**), 8.29 (brs, aromatic of monomer **2**).

IR (film on NaCl, cm^{-1}) : 1731 and 1728 (carbonyl vibration of esters) , 1661 (carbonyl of monomer **1**), 1598 and 1586 (phenyl groups of monomer **1** and **2**), 1517, 966 (carbon - carbon double bond of 2-butenyl side group) .

Table 1. Monomer feed ratio and yield of copolymers
3a -3d, **4a** and **4b**

No.	Monomer feed ratio(mol %)[a) [monomers]					Yield (%)
	L	M	N	O	mol/l	
3a	90	0	10	0	2.5	45
3b	75	0	25	0	1.2	30
3c	50	0	50	0	1.2	25
3d	15	55	30	0	2.5	43
3e	25	25	50	0	1.2	32
3f	12.5	12.5	75	0	1.9	25
4a	8.5	23	46	22.5	2.0	59
4b	8.5	13	51	27.5	1.2	40

a) L : methyl methacrylate; M : 2-butenyl methacrylate
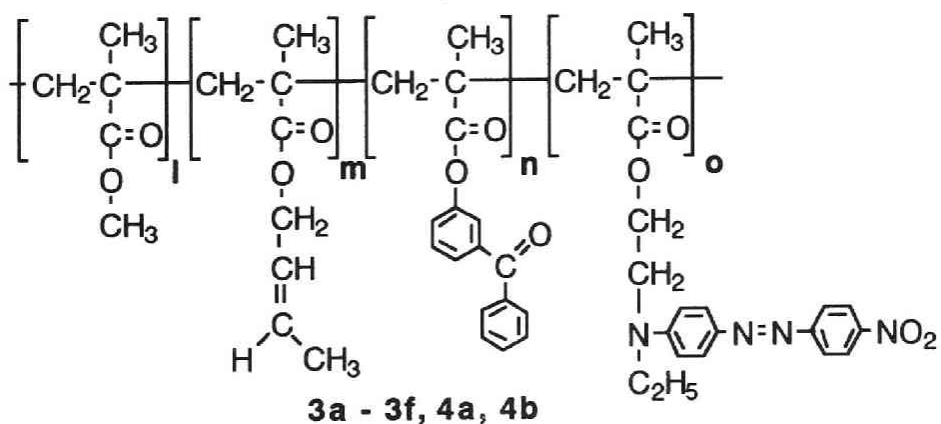
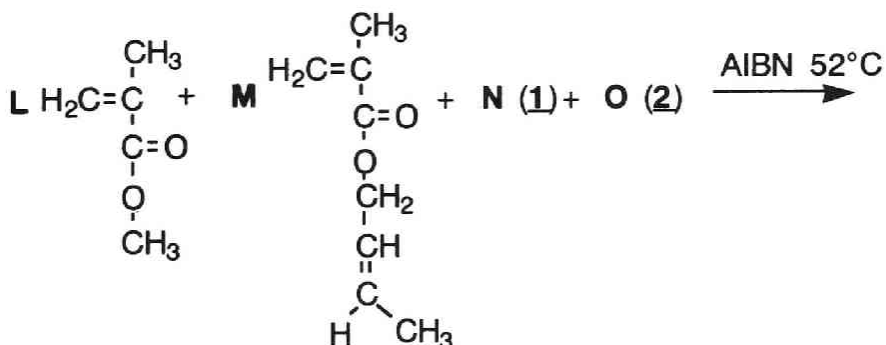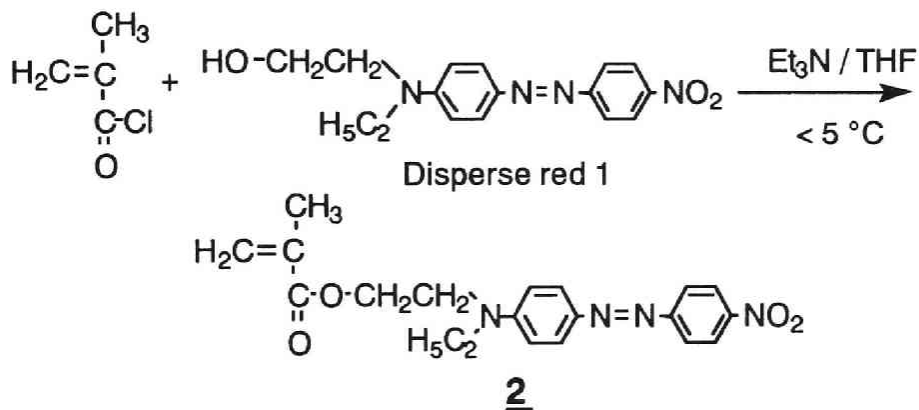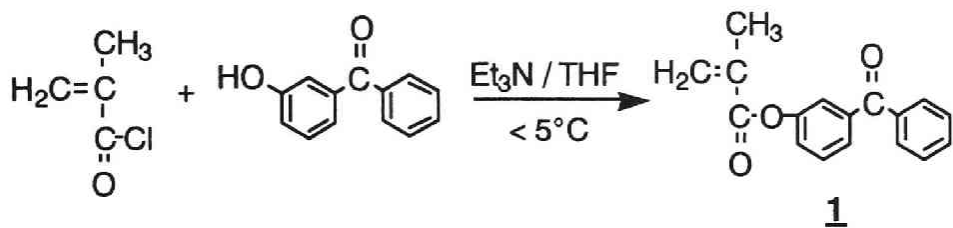 N : monomer **1** ; O : monomer **2** .

Characterization :

Differential scanning calorimetry data were obtained with a Mettler DSC 30 using a heating rate of 10 °C/min. The molecular weight and molecular weight distributions were measured with chloroform as eluent using a Spectra-Physics LC-GPC systems and a Spectra Physics UV-100 detector. The columns (Polymer Standards Service) were calibrated with polystyrene standards. UV-VIS spectra were measured with a Perkin Elmer Lambda-9 spectrometer. FT-IR spectra were recorded with a Perkin Elmer FT-IR 1600. NMR spectra were measured with a 400 MHz instrument from General Electric. Deuterated chloroform was used as a solvent. Copolymer composition was determined by NMR spectroscopy. For the determination of the crosslinking kinetics, thin films were prepared by spin-coating on a sodium chloride substrate from a benzene solution. The films were irradiated with filtered light of a UV lamp at 366 nm. In all experiments the light intensity was about 3-5 mW/cm^2. Conversion of the polymer to the crosslinked form was monitored by FT-IR using a similar method to that is described by Strohriegel *et al* [12]; the intensity of the carbonyl vibration at 1661 cm^{-1} of benzophenone unit of monomer **1** was used.

Results and discussion

Synthesis of copolymers :

The methacrylate copolymers studied in this chapter are based on methyl methacrylate, a photo-excitable benzophenone monomer **1**, a nonlinear optical active azobenzene monomer **2** and a crosslinkable 2-butenyl monomer (Scheme 1). Monomer **1** was synthesized from methacryloyl chloride and 3-hydroxybenzophenone. Disperse red 1 was reacted with

Et$_3$N / THF < 5°C

1

Et$_3$N / THF < 5 °C

HO-CH$_2$CH$_2$ ... N=N ... NO$_2$

Disperse red 1

2

L **M** + **N** (**1**) + **O** (**2**) AIBN 52°C

3a - 3f, 4a, 4b

Scheme 1

135

methacryloyl chloride to give the nonlinear optical active monomer **2**. The copolymers were synthesized by a free radical polymerization using AIBN as an initiator. All synthesized copolymers were completely soluble in organic solvents such as benzene or chloroform, indicating that no crosslinking occurred during copolymerization. The copolymer composition could be easily determined by proton NMR-spectroscopy, because each monomer unit showed separated signals. The results revealed that the benzophenone monomer **1** had a higher reactivity than the other monomers. The molecular weights and molecular weight distributions were measured by GPC and compared to polystyrene. All copolymers had a mono-modal distribution. The number average molecular weights were on the order of 200,000 - 370,000 g/mol and the weight average molecular weights on the order of 475,000 - 960,000 g/mol. Methyl methacrylate polymerized with the same initiator concentration and under the same conditions yielded poly-(methyl methacrylate) with similar molecular weight. The data of the NMR, GPC and DSC investigations of copolymers **3a - 3f**, **4a** and **4b** are summarized in Table 2. The copolymerization results demonstrate that under these conditions, the nitro- or azo- groups of disperse red do not interfere with the copolymerization and that the 2-butenyl side groups does not crosslink.

Photocrosslinking reaction of copolymers 3a-3f, 4a and 4b :

The copolymers **3a - 3f**, **4a** and **4b** were photochemically crosslinked with UV light at a wavelength of 366 nm. This wavelength was selected to minimize photo-bleaching of the NLO chromophore during crosslinking. The type of crosslinking reactions of the copolymers **3d - 3f**, **4a** and **4b** with the benzophenone unit and the 2-butenyl side group are the same as

Table 2. Copolymer composition, molecular weight and glass transition temperature of coplymers **3a-3f**, **4a** and **4b**.

| No.	Copolymer composition[a]				Molecular weight [b]			Tg (°C)[c]
	l [a]	m[a]	n[a]	o[a]	MnX10^{-3}	MwX10^{-3}	Mw/Mn	
3a	79.5	0	20.5	0	197	475	2.4	113
3b	49.5	0	50.5	0	301	691	2.3	105
3c	25.7	0	74.3	0	275	636	2.3	103
3d	8.0	38.3	53.7	0	196	457	2.3	73
3e	8.9	9.9	81.2	0	369	959	2.6	94
3f	4.3	5.3	90.4	0	342	668	2.0	98
4a	8.3	43.6	36.9	12.2	337	939	2.8	82
4b	8.4	39.5	29.8	22.3	-[d]	-[d]	-[d]	89

a) Determined by NMR.

b) Determined by GPC, polystylene standards, CHCl$_3$ as eluent, UV(260nm) detection.

c) Determined by DSC, 1st run.

d) Molecular weight > 1000 x 10^3 (out of range for the GPC column separation)

reported for similar copolymers containing these structures. [14,15] The photocrosslinking process probably occurs by two pathways as illustrated in Scheme 2. The excited benzophenone side group can react directly with the carbon - carbon double bond of the 2-butenyl side group to form an oxetane ring.
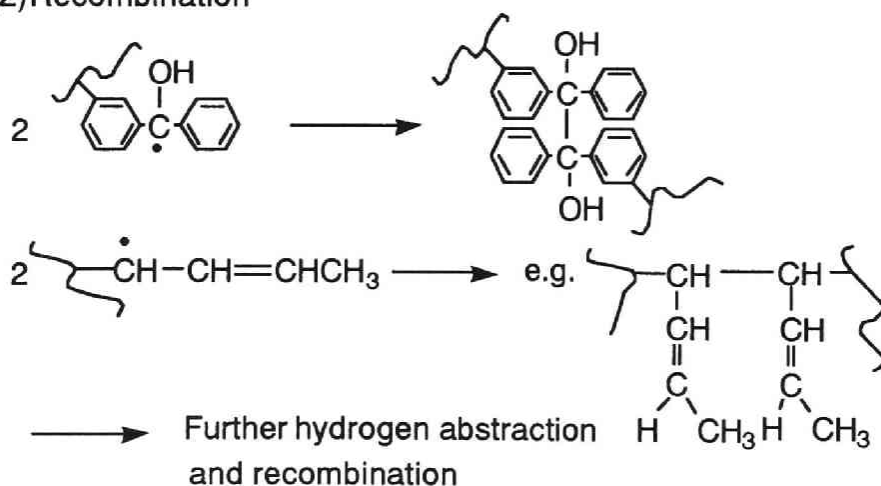
Oxetane formation:

excited benzophenone
side group
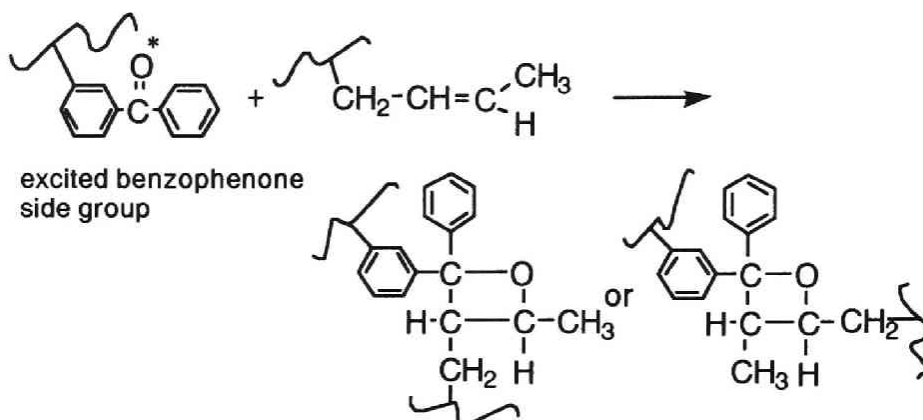
Recombinations of radicals:

(1) Hydrogen abstraction of benzophenone from 2-butenyl side group

excited benzophenone side group

Ketyl radical   Allyl radical

(2) Recombination
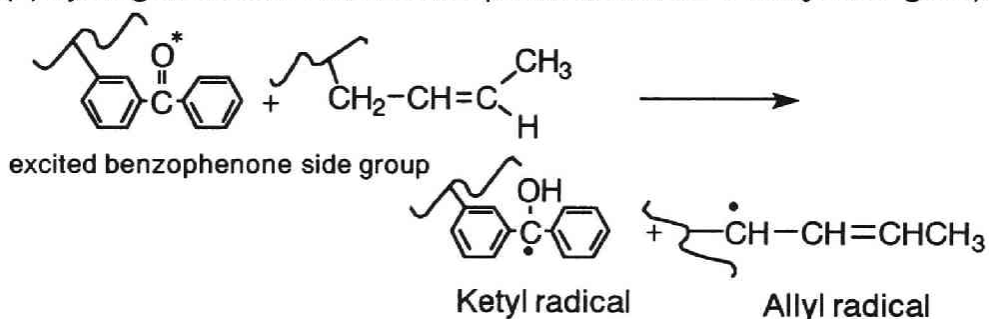
→ Further hydrogen abstraction
and recombination

Scheme 2

138

The excited benzophenone side group can also abstract a hydrogen from the 2-butenyl group, resulting in a ketyl radical and an allyl radical. Two ketyl radicals can recombine to form a pinacol crosslink. A new absorption around 3500 cm^{-1} in the FT-IR spectrum suggests this pinacol formation. Allyl radicals can also crosslink by recombination. These structures are capable of further hydrogen abstraction and recombination processes. Recombination between the ketyl radical and the allyl radical may also occur and other photo-induced reactions are possibly occured.

The photoreaction of the copolymers **3a** - **3f** was monitored by FT-IR spectroscopy, utilizing the vibrations at 1661 cm^{-1} for the carbonyl of the benzophenone unit, and at 967 cm^{-1} for the carbon - carbon double bond of the 2-butenyl side group. Both peaks decrease with irradiation time. The pinacol formation is detectable by the new peak around 3500 cm^{-1} for the hydroxyl vibration. Figure 1 shows IR spectra of a thin film of copolymer **3d** for different irradiation times. The photoreaction is slower for copolymers **3a** - **3c**. The pinacol formation, which requires a hydrogen abstraction, is much faster in copolymers **3d** - **3f** containing the 2-butenyl methacrylate comonomer. This result is demonstrated in figure 2 for copolymers **3b** and **3d**. Both copolymers have similar concentrations of monomer **1**. After two hours of irradiation of copolymer **3d** more than 50 % of the benzophenone side groups have reacted. The reaction seems to continue with further irradiation. In contrast, the photoreaction of copolymer **3b** is much slower because it cannot form the oxetane and the availability of abstractable hydrogen is limited. After UV-irradiation copolymers **3d** - **3f** became completely insoluble and showed very little swelling in organic solvents, whereas copolymers **3a** - **3c** became only partially insoluble.
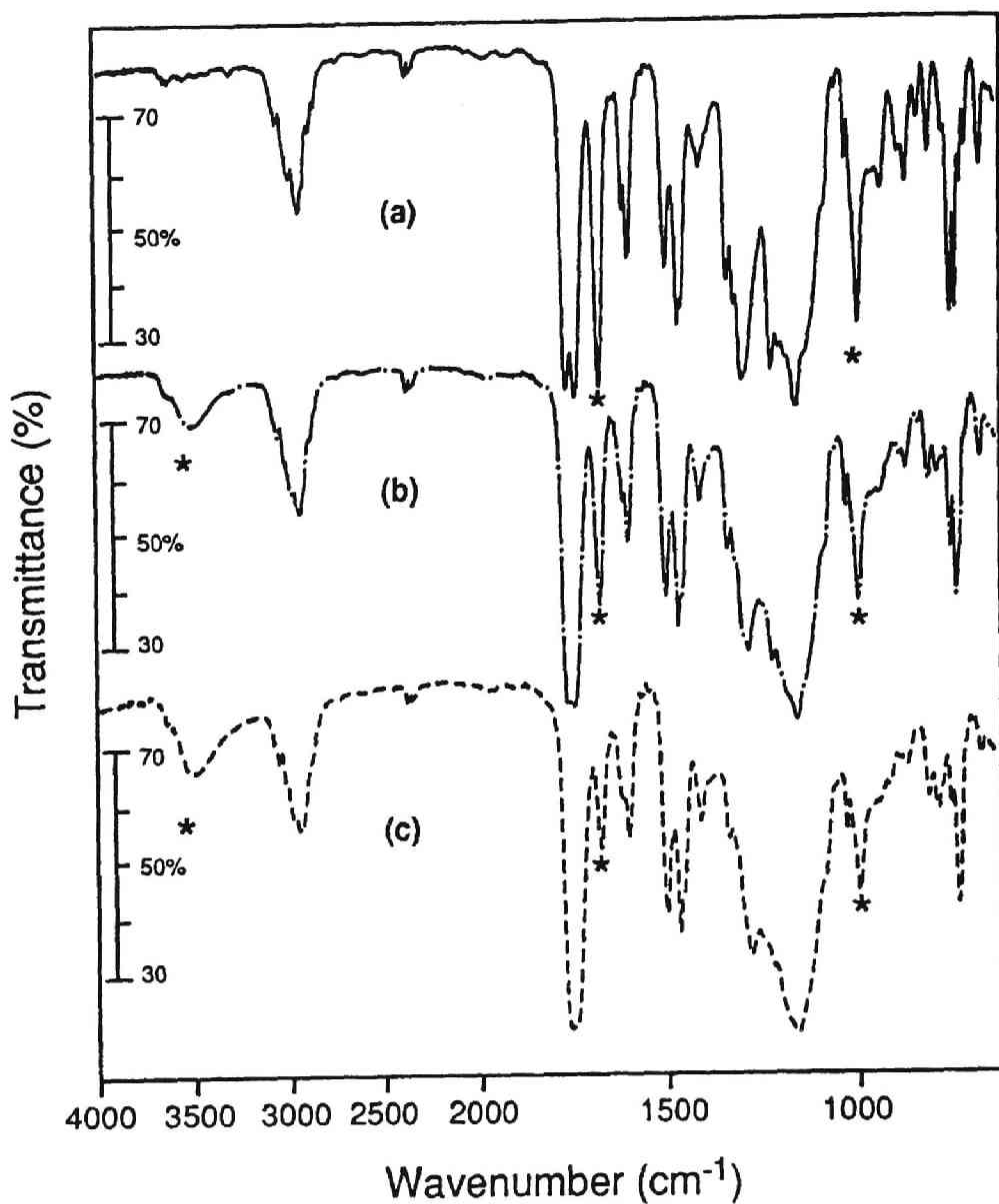
Figure 1. The FT-IR spectra of the photocrosslinked film of copolymer **3d**. The peaks mentioned in the text are indicated with asterisk. (Substrate : NaCl, Film thickness was about 0.2 mm.) Irradiation time : 0 h (a), 1 h (b), 4 h (c).
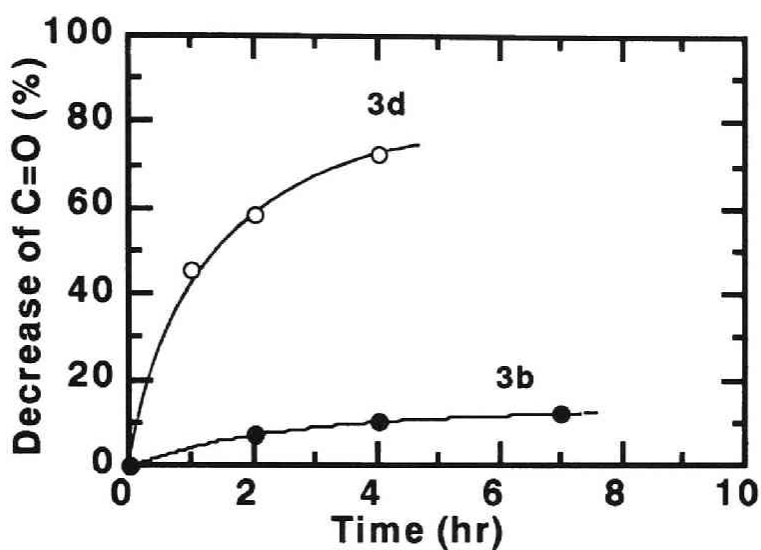
Figure 2. Time-conversion plot of photocrosslinking of copolymer**3b** (•) and**3d** (o) (determined by FT-IR, decrease of carbonyl vibration at 1661 cm^{-1}).
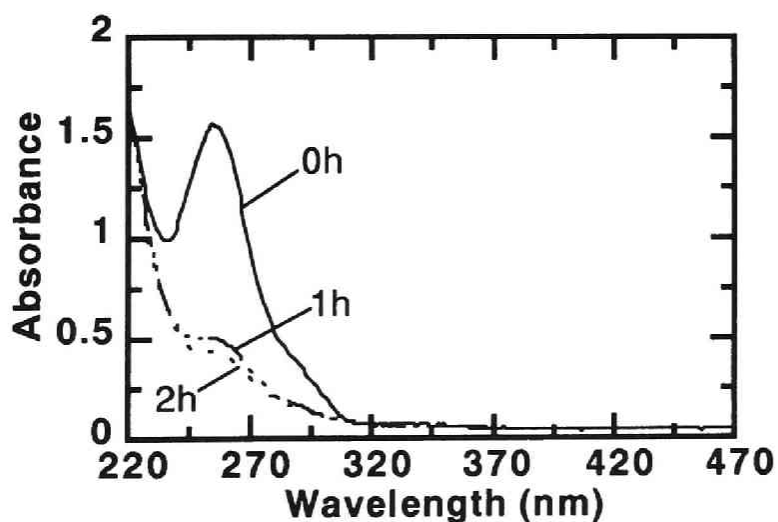

Figure 3. UV-VIS spectra of the photocrosslinked film (substrate : quartz) of copolymer **3d** after the irradiation of 0 h, 1 h, and 2 h.

Photocrosslinking was also monitored by the UV-VIS spectroscopy of thin films on a quartz substrate. Figure 3 compares absorption spectra of copolymer **3d** irradiated by UV light for various times. The n-π* absorption of the benzophenone segment around 360 nm is very small compared to the π-π* absorption at 258 nm. The photo reaction of the benzophenone unit can be monitored by following the π-π* absorption of the benzophenone side group, which decreases with increasing exposure.
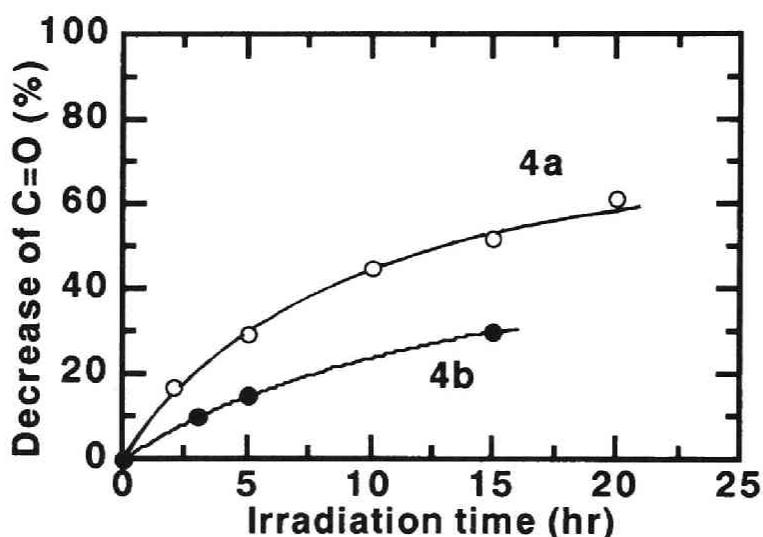

Figure 4. Time-conversion plot of photocrosslinking of copolymer **4b**(•) and **4a** (o) (determined by FT-IR, decrease of carbonyl vibration at 1661 cm^{-1}).

The photocrosslinking reactions of the azobenzene containing copolymers **4a** and **4b** are much slower. This is a consequence of the absorption of azobenzene chromophore, which competes with the energy absorption of benzophenone side groups at 366 nm. Figure 4 shows the kinetics of the photoreaction (disappearance of benzophenone carbonyl unit) for both

copolymers. The kinetics behavior reflects the copolymer composition of NLO- chromophore and benzophenone side group. As expected, the reaction kinetics of **4b**, which contains a lower amount of monomer **1** and more monomer **2**, are slower.

Corona-poling and second harmonic generation of copolymer 4a :

Thin films of copolymer **4a** were spin-coated on ITO substrates. The non-centrosymmetric alignment of the chromophores was obtained by corona poling at 60 °C for 30 min. The sample was crosslinked by exposure to UV radiation during cooling to room temperature under the electric field. Figure 5 shows absorption spectra of an unpoled film of **4a**, an uncrosslinked film after poling and a crosslinked poled film. Due
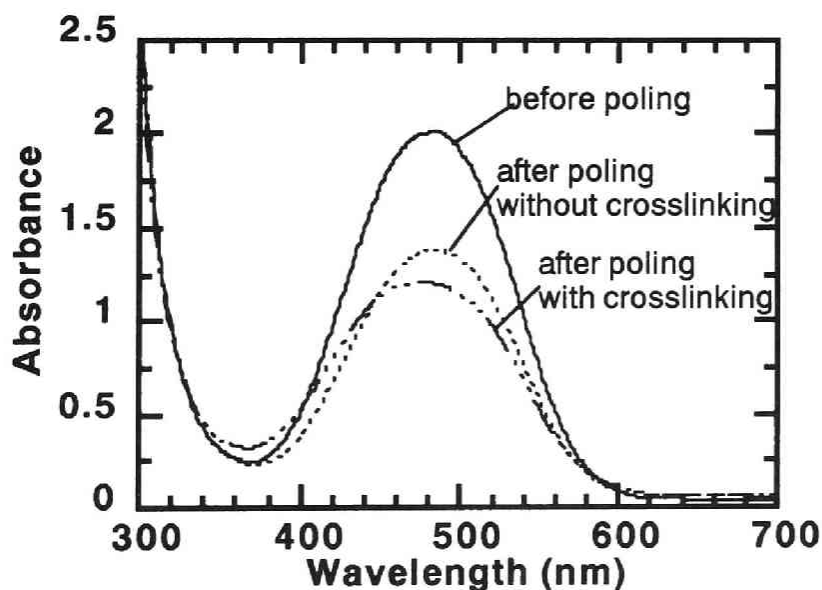

Figure 5. Absorption spectra of film of copolymer **4a** on ITO glass : before poling, corona-poled without crosslinking and corona-poled with crosslinking.

(Film thickness 1.2 μm. Irradiation time 2 h. Poling field : 4.6 kV/ 2.5 μA for 30 min at 60 °C)

143

to the alignment of NLO chromophores perpendicular to the substrate, the absorbance is reduced for both poled films. In the case of the uncrosslinked poled film, the absorption maximum is shifted to longer wavelength. This effect was also observed for other poled NLO polymers. [16]   In the case of the crosslinked and poled film, the absorbance is further reduced and slightly shifted to a shorter wavelength. The additional decrease in absorbance can be attributed to some photo-bleaching or *trans-cis* photo-isomerization of diazo group during exposure.

It is possible to monitor the stability of the chromophore alignment by absorption spectroscopy. The absorption intensity will increase if the chromophores relax. [16]   The crosslinked, poled film of **4a** did not change its absorption after storing 4
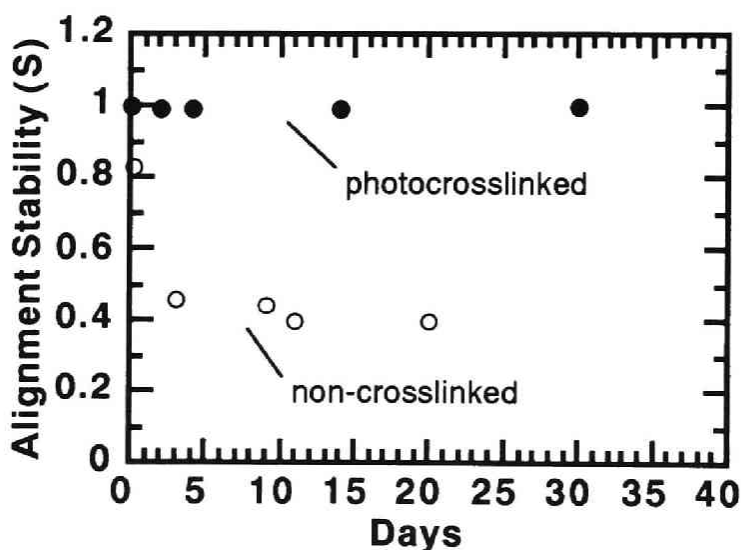

Figure 6. Alignment stability S of corona-poled co-polymer **4a** : S=(Ainitial-Astored)/(Ainitial-Apoled), Ainitial, Apoled and Astored show absorbance before poling, just after poling and after storing at r.t.,respectively

144

weeks at 25 °C as shown in figure 6. In comparison the absorption of the non-crosslinked poled film increased to almost half of its original value during this period.

The poled films of copolymers **4a** and **4b**, both uncrosslinked and crosslinked, show a signal for second harmonic generation and an electro-optical (EO) effect. Second order EO coefficiencies are in the order of 10 - 50 pm/V by the interferometric method, [17] depending on copolymer and poling/crosslinking conditions.

Conclusions

New photocrosslinkable copolymers with 2-butenyl and benzophenone side groups were synthesized. For an application of these copolymers, crosslinkable NLO copolymers with disperse red 1 side group were also synthesized. These copolymers are photocrosslinked at 366 nm UV light and become insoluble in organic solvents. Photocrosslinking reaction was measured by FT-IR and UV-VIS spectra. NLO copolymers can be crosslinked in a poled state and show a stable alignment of NLO chromophore at room temperature for more than one month.

References

1) For reviews , see for example : a) P. N. Prasad and D. R. Urich (Eds.) *"Nonlinear Optical and Electroactive Polymers"* Plenum Press (1988), b) P. N. Prasad and D. J. Williams (Eds.) "Nonlinear Optical Effects in Molecules and Polymers" John Wiley & Sons (1991), c) R. Lytel, G. F. Lipscomb, M. Stiller, J. I. Thackara, and A. J. Ticknor, *Nonlinear Optical Effects in Organic Polymers*, J. Messier et al. eds., Kluwer Academic Publishers (1989), p.277, d) D. R. Ulrich, *Mol. Cryst. Liq. Cryst.*, **189**, 3 (1990).

2) S. Ducharme, J. C. Scott, R. J. Twieg, and W. E. Moerner, *Phys. Rev. Lett.*, **66**, 1846 (1991).

3) H. L. Hampsh, J. Yang, G. K. Wong, and J. M. Torkelson, *Macromolecules* **21**, 526 (1988).

4) K. D. Singer, M. G. Kuzyk, W. R. Holland, J. E. Sohn, S. J. Lalama, R. B. Comizzoli, H. E. Katz, and M. L. Schilling, *Appl. Phys. Lett.*, **53**, 1800 (1988).

5) E. Eich, A. Sen, H. Looser, G. C. Bjorklund, J. D. Swalen, R. Twieg, and D. Y. Yoon, *Appl. Phys. Lett.*, **66**, 2559 (1989).

6) M. Eich, B. Reck, D. Y. Yoon, C. Grant, and G. C. Bjorklund, *J. Appl. Phys.* **66**, 3241 (1989).

7) D. Jungbauer, B. Reck, R. Twieg, D. Y. Yoon, C. G. Willson, and J. D. Swalen, *Appl. Phys. Lett.*, **56**, 2610 (1990).

8) K. D. Singer, M. G. Kuzyk, T. Fang, W. R. Holland and P. A. Cahill, *Organic Molecules for Nonlinear Optics and Photonics*, J. Messier, F. Kazyar and P. Prasad. eds., NATO ASI Series E. **Vol 194** 105 (1991).

9) S. Allen, D. J. Bone, N. Carter, T. G. Ryan, R. B. Sampson, D. P. Devonald and M. G. Hutchings, *Organic Materials for Nonlinear*

Optics II. R. A. Hann and D. Bloor eds., Redwood Press Ltd, Melksham, Wiltshire (1991), p235.

10) B. K. Mandal, J. Kumar, J.-C. Huang, and S. Tripathy, *Makromol. Chem., Rapid Commun.,* **12**, 63 (1991).

11) B. K. Mandal, J. Kumar, J.-C. Huang, and S. Tripathy, *Appl. Phys. Lett.,* **58**, 2459 (1991).

12) H. Müller, I. Müller, O. Nuyken, and P. Strohriegel, *Makromol. Chem., Rapid Commun.,* **13**, 289 (1992).

13) N. J. Turro, "Modern Molecular Photochemistry", Benjamin/Cummings, Menlo Park, CA, (1978).

14) a) N. Kawatsuki, and M. Uetsuki, *Appl. Opt.* **29**, 210 (1990), b) N. Kawatsuki, and M. Uetsuki, *" Polymers for Lightwave and Integrated Optics "*, L. A. Hornak ed., (Marcel Dekker, New York, 1992), p. 171.

15) Y. Ito, Y. Aoki, T. Matsuura, N. Kawatsuki, and M. Uetsuki, *J. Appl. Polym. Sci.,* **42**, 409 (1991).

16) R. H. Page, M. C. Jurich, B. Reck, A. Sen, R. J. Twieg, J. D. Swalen, G. C. Bjorklund, and C. G. Willson, *J. Opt. Soc. Am.,* **B7**, 1239 (1990).

17) H. Ono, K. Misawa, K. Minoshima, A. Ueki, and T. Kobayashi, submitted in J. Appl. Phys.

Chapter 7

Synthesis and Characterization of Aromatic Polyesters with Dicyanovinyl Substituents

Abstract : The synthesis, characterization and structure-property relations of aromatic polyesters with dicyanovinyl substituents are presented. Two comparable series of polyesters based on 3,4-dihydroxybenzylidenemalononitrile and 3,4-dihydroxy-5-methoxybenzylidenemalononitrile were prepared. As aromatic diacid components, terephthalic acid, phenylterephthalic acid, isophthalic acid and 2-phenylisophthalic acid were used. The polyesters were prepared by solution polycondensation. GPC investigations revealed the existence of substantial amounts of defined cyclic products. These cycles could be isolated by preparative GPC. The polyesters are soluble in common low boiling organic solvents, particularly the phenyl substituted ones. The polyesters are amorphous and have glass transition temperatures between 140 °C and 170 °C. The absorption maxima are in the range of 306 and 322 nm. The cut-off wavelength is between 400 to 428 nm. The polyesters with methoxy substituent have generally the absorptions at longer wavelength. The refractive index of thin films of these polyesters were between 1.61 and 1.63 at 632.8 nm.

Introduction

The past decade has witnessed an enormous growth in interest and research activities in the design, synthesis and structure-property relations of specially functionalized polymers for optical, electro-optical and electronical applications. Outstanding examples for these developments include areas such as photo-resists, side-chain liquid crystal polymers, photo-conducting and electrically conducting polymers, as well as polymers for waveguide and nonlinear optical applications. [1] In all cases, the special materials properties and functions are based on a carefully designed chemical structure, facilitating control and optimization of the desired properties. Along these lines, aromatic polymers which contain strong electron acceptor groups are of general interest for several of the areas mentioned above. [2]

This chapter presents synthetic aspects and characterization of wholly aromatic polyesters with dicyanovinyl substituents. Aromatic polyesters are generally used as temperature resistant amorphous or liquid crystalline engineering thermoplastics with applications mainly in the structural and coating area. [3] The dicyanovinyl substituent is increasingly utilized, as an alternative to nitro and cyano substituents in the design of donor-π-acceptor chromophores for nonlinear optical effects. [4] This is based on the stronger electron acceptor function in addition to the enhanced hyperpolarizability through the olefinic double bond. [5] The large permanent dipole moment of the dicyanovinyl group helps also to achieve the necessary non-centrosymmetric alignment by an applied external electrical field either by plate poling or by corona discharge. [6] In order to process such polymers to thin and optically clear films by casting or spin-coating techniques, a sufficient solubility in common organic solvents and an amorphous structure of the polymers are required.

Two structurally comparable polyester series (figure 1) based on two catechol derivatives with dicyanovinyl substituents were prepared. As aromatic diacid constituent terephthalic acid, phenylterephthalic acid, isophthalic acid and 2-phenylisophthalic acid were used. The aim of this chapter is to present and discuss the monomer synthesis, polymer synthesis and the influence of different chemical modifications on thermal, solution and optical properties. Special considerations are made in the design of the polyesters, in order to obtain organo-soluble polymers with high glass transition temperatures and short cut-off wavelengths.
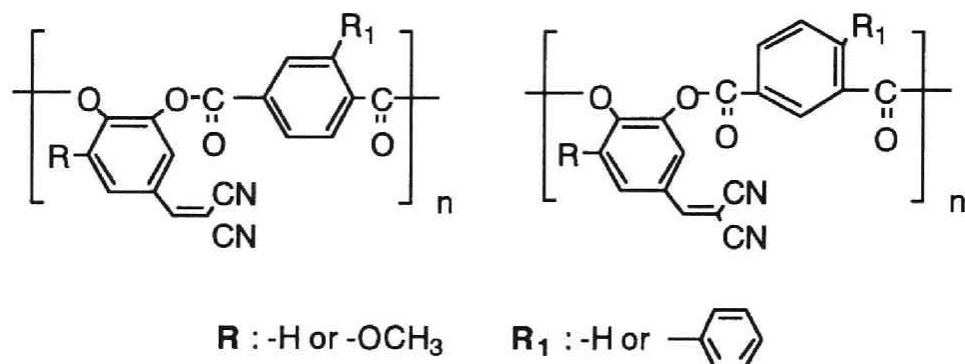

R : -H or -OCH₃   R₁ : -H or ⟨benzene ring⟩

Figure 1. Chemical structure of dicyanovinyl substituted aromatic polyesters based on catechol units and terephthalic acid or isophthalic acid units.

Experimental

Materials :

3,4-Dihydroxybenzaldehyde, 5-iodovanilin, 2-bromo-*m*-xylene, bromo-*p*-xylene, iodobenzene, thionylchloride, 4-*t*-butylbenzoyl chloride and triethylamine (99+%) (Aldrich) were

used as received. Terephthaloyl chloride and isophthaloyl chloride (Aldrich) were recrystallized from hexane under dry conditions. Phenyl terephthaloyl chloride was synthesized according to a previously described procedure by Land *et al* and Hatke *et al* and recrystallized from dry hexane. [7] Tetrahydrofuran (THF) was distilled over potassium and stored under argon. All other solvents and chemicals were used as received.

Monomer synthesis :

3,4-Dihydroxybenzylidenemalononitrile (1)

To a solution of 10.0 g (72.5 mmol) of 3,4-dihydroxybenzaldehyde and 6.0 g (91 mmol) of malononitrile dissolved in 50 ml methanol, 10 drops of piperidine were slowly added. After a few hours, the solid was precipitated. After 20 hours this solid was filtered by suction, washed with small amounts of methanol and dried *in vacuum*. The monomer was purified prior to polymerization by sublimation at 190 - 200 °C / 1 -2 mmHg.

Yield : 10.1 g (75%) ; m.p. 228 °C (decomposition) ; (lit.: 221 °C [8]).

^{1}H-NMR (DMSO-d_6): δ (ppm) = 6.93 (1 H, d,J = 8.3 Hz) ; 7.34 (1H, dd J1= 2.0 Hz, J2 = 8.3 Hz, 1H) ; 7.54 (1H, d, J = 2.0 Hz,) ; 10.0~10.2 (1H).

IR (KBr): 3646, 3285, 2237, 1614, 1594, 1571 cm^{-1}.

3,4-Dihydroxy-5-methoxybenzaldehyde (2) was prepared according to a method by Banerjee *et al* [9] and purified by recrystalization from benzene.

Yield : 45% ; m.p. 132 -134°C (lit .:133 -134 °C [9]).

^{1}H-NMR (DMSO-d_6): δ (ppm) = 3.84 (3H, s); 7.01 (1H, s) ; 9.3 - 9.6 (2H, br); 9.54 (1H, s).

3,4-Dihydroxy-5-methoxybenzylidenemalononitrile (3)

To a solution of 3.6 g (21.4 mmol) of **2** and 1.45 g (22.0 mmol) of malononitrile in 15 ml methanol, a few drops of piperidine were added. The mixture was stirred for 15 hours. The precipitate was filtered by suction, washed with a small amount of ethanol and dried *in vacuo*.

Yield : 4.5 g (98%); m.p. : 238 - 241 °C (decomposition)

^{1}H-NMR (DMSO-d_6): δ (ppm) = 3.76 (3H, s) ; 7.17 (1H, s) ; 7.25 (1H, s) ; 8.18 (1H, s) ; 9.7 -10.1 (2H, br).

IR (KBr): 3301, 2239, 2218, 1603, 1566 cm^{-1}.

2,4-Dimethylbiphenyl (4)

To a mixture of 51 g (0.25 mol) of iodobenzene, 0.8 g of dichloro[1,3-bis(diphenylphosphino)-propane]nickel(II) and 90 ml of dry diethyl ether under nitrogen, a solution of 0.27 mol of 2,4-dimethylphenylmagnesium bromide in 95 ml of diethyl ether was added dropwise for 1 hr. During the addition, the reaction mixture was cooled in an ice bath. After the addition was completed the reaction mixture was allowed to warm up to room temperature and refluxed for 20 h. The reaction mixture was poured into 300 ml of ice water. The aqueous layer was extracted two times with diethyl ether. The combined organic phases were dried over magnesium sulfate. The solvent was removed by evaporation. The product was isolated by vacuum distillation at 75~76 °C , 0.02 mmHg. (lit.: 145 °C,12 mmHg [10]).

Yield; 27.0 g (59%).

^{1}H-NMR (CDCl$_3$): δ (ppm) = 2.22 (3H, s); 2.36 (3H, s); 7.05 - 7.18 (3H, m); 7.25 - 7.38 (5H, m).

2-Phenyl-isophthalic acid (5)

11.0 g (60 mmol) of 2,4-dimethylbiphenyl was dissolved in a mixture of 210 ml of pyridine and 21 ml of water. After addition of 27 g of potassium permanganate the mixture was refluxed. Over a period of 5 h, 63 g of potassium permanganate and 140 ml of water were added in portions to the mixture, while the mixture was refluxed. The reaction mixture was refluxed for additional 15 h. The formed mangane dioxide was filtered off and the washed with hot water. The combined filtrates were acidified with hydrochloric acid. The white precipitated solid was washed several times with water and dried *in vacuum* at 80°C. The crude product was recrystallized from acetic acid.

Yield: 9.5 g (67%); m.p.: 245 - 246 °C (245-246 °C [11]).

2-Phenyl-isophthaloyl dichloride (6)

8.0 g (33 mmol) of 2-phenyl-isophthalic diacid (5) were dissolved in 60 ml of thionyl chloride and 1 ml of *N,N*-dimethylformamide was added. After refluxing for 24 h, the excess thionyl chloride was removed by distillation. The diacid dichloride was purified by distillation at 137 °C under 0.2 mmHg.

Yield:7.6 g (83%).

^{1}H-NMR (CDCl$_3$): δ (ppm) = 7.35 - 7.38 (2H, m); 7.42 - 7.47(3H, m); 7.58 (1H, d, J = 8.7 Hz); 8,32 (1H, d, J = 8.7 Hz); 8.63 (1H, s).

IR (neat): 1756,1597 cm^{-1}.

Polymer synthesis :

The dicyanovinyl substituted catechol derivatives **1** and **3** were reacted under the same conditions with terephthaloyl dichloride, phenylterephthaloyl dichloride, isophthaloyl dichloride and 2-phenylisophthaloyl dichloride **6**, resulting in the polyester

series **7a** - **7d** and **8a** - **8d** (Scheme 3). As an example, the general procedure for the polycondensation is given for polyester **7d**.

Polyester 7d

1.200 g (5.55 mmol) of 3,4-dihydroxy-5-methoxy-benzilidenemalononitrile **3** and 1.549 g (5.55 mmol) of phenylterephthaloyl dichloride were dissolved in 30 ml of dry THF under nitrogen. To this solution 1.2 g (11.9 mmol) of triethylamine was added in one portion. The reaction mixture was allowed to stir for 21 h at room temperature. This solution was then dropped into methanol to precipitate the polymer. After two times of reprecipitation from THF solution into methanol and the polymer was extracted with methanol under reflux for a few days. The polyester was dried at 60 °C in vacuum.
Yield: 1.4 g (68 %).
^{1}H-NMR (CDCl$_3$): δ (ppm) = 3.65 (3H, brs), 7.08 (4H, brs), 7.34 (1H, brs), 7.81 (2H, brs).
IR (film on NaCl): 3026, 2229, 1754, 1602, 1579, 1503 cm^{-1}.

Polyesters **7a**, **7c** and **8a** were found to be insoluble in the reaction medium and precipitated during the reaction. These polymers were purified by washing with methanol and extraction with hot methanol for a few days. The extraction procedure, which was used in all samples, removed not only residual reactants and solvent, but also fractions of oligomers and cyclic products. Consequently, the yields of the isolated polymers were found to be in the following range: **7a** (70 %), **7b** (66 %), **7c** (54 %), **8a** (71 %), **8b** (70 %), **8c** (45 %) and **8d** (60 %).

Endcapping procedure: (polyester 10)

2.347 g (10.857 mmol) of diol **3**, 3.000 g (10.748 mmol) of phenyl terephthaloyl dichloride, 3.23 g (32 mmol) of triethylamine and 60 ml of THF were reacted at room temperature for 22 h. Then 1.96 g (10 mmol) of 4-*t*-butylbenzoyl chloride and 1 g of triethylamine was added to the reaction mixture following by stirring for 48 h. The color of reaction mixture turned from dark yellow to light yellow. After the reaction, the solution was dropped into methanol to precipitate the polymer. The polymer was twice redissolved in THF and reprecipitated, before it was dried under vacuum.

Yield: 3.1 g (68 %).

^{1}H-NMR (CDCl$_3$): δ (ppm) = 0.9 - 1.0 (m, very small, according to *t*-butyl end groups), 3,65 (brs), 7.08 (brs), 7.34 (brs), 7.81 (brs).

IR (film on NaCl): 3027, 2229, 1754, 1602, 1579, 1503 cm^{-1}.

Characterization:

Solubility tests were conducted with polymer concentrations of 4% (w/v) at room temperature. Differential scanning calorimetry data were obtained with Mettler DSC 30 using a heating rate of 10 °C/min. Before the second heating curve was recorded, the samples were rapidly quenched with liquid nitrogen. Thermogravimetric analysis was performed on a Mettler TA 50 apparatus using a heating rate of 20 °C/min under nitrogen atmosphere. The molecular weight and molecular weight distributions were measured in chloroform as eluent using a Spectra-Physics LC systems GPC and Spectra UV-100 detector. The columns (Polymer Standards Service) were calibrated with polystyrene standards of known molecular weight. Preparative GPC was also done in order to separate the low molecular weight

oligomers, cyclic products and polymers, using a column of Merck-Merckogel OR-PVA 6000, UV-100 detector and THF as a solvent. UV-VIS spectra were measured by Perkin-Elmer Lambda-9 spectrometer. FT-IR spectra were recorded with a Perkin Elmer FT-IR 1600. Refractive indices were measured by Metricon Prism coupler Model-2010 at 632.8 nm with spin-coated thin film on silicon substrate.

Results and discussion

Monomer Synthesis :

Aromatic dicyanovinyl derivatives can be easily synthesized by the condensation of aldehydes with malononitrile in a *Knoevenagel* reaction. [12] The different reactions to the dicyanovinyl containing catechol derivatives, 3,4-dihydroxy-benzylidenemalonitrile **1** and 3,4-dihydroxy-5-methoxy-benzylidene-malononitrile **3**, which contains the electron-withdrawing dicyanovinyl substituent and a methoxy substituent as electron donor, are summarized in Scheme 1.

As substituted aromatic diacid dichloride monomers, phenyl-substituted terephthaloyl dichloride and phenyl-substituted isophthaloyldichloride were used. In analogy to the synthetic route of phenylterephthaloyl dichloride described by Land *et al,* [7] 2-phenylisophtaloyl dichloride **6** was prepared (Scheme 2). The first step involves a transition metal catalyzed biaryl coupling reaction under typical *Kumada* conditions. [13] 2,4-Dimethylbiphenyl **4** was prepared by reacting iodobenzene with 2,4-dimethyl-phenylmagnesium bromide and dichloro[1,3-bis(diphenyl-phosphino)-propane] nickel (II) as catalyst. The isolated 2,4-dimethylbiphenyl was oxidized to 2-phenylisophthalic
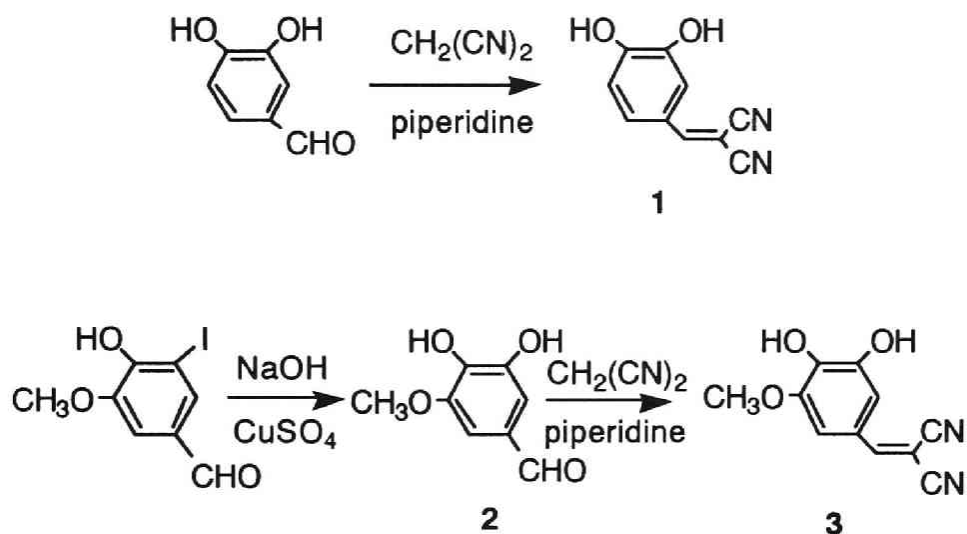
Scheme 1. Synthesis of dicyanovinyl catechol derivatives **1** and **3**.
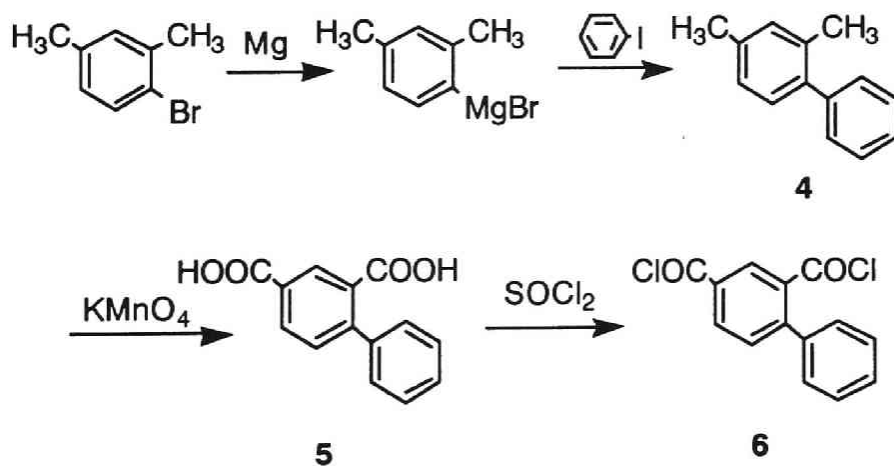
Scheme 2. Synthesis of phenyl-substituted isophthaloyl dichloride **6**.

acid **5** with potassium permanganate in pyridine as solvent. The diacid was converted with thionylchloride to 2-phenyl-isophtaloyl dichloride **6** and purified by vacuum distillation.
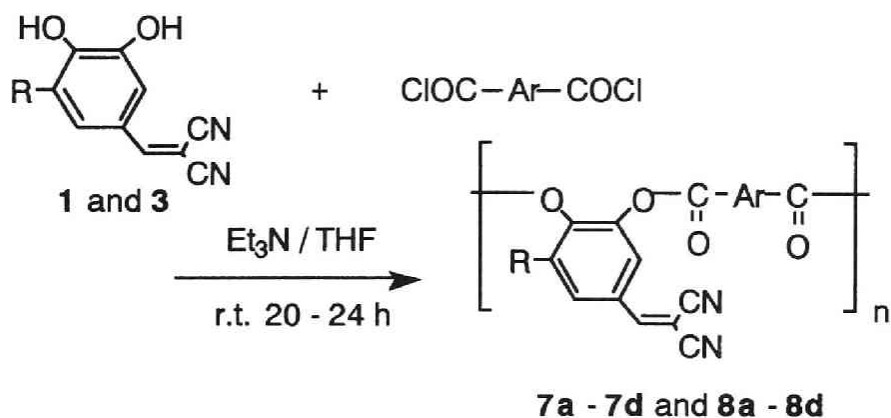
Polycondensation :

The polycondensation of the dicyanovinyl substituted catechol derivatives **1** and **3** with the aromatic diacid dichlorides was performed in a typical low-temperature solution polycondensation with triethylamine as base. As aromatic diacid chlorides, terephthaloyl dichloride, phenylterephthaloyl dichloride, isophthaloyl dichloride and 2-phenylisophthaloyl dichloride were used. Scheme 3 summarizes the polycondensation reaction and the chemical structures of the resulting polyester series **7a - 7d**, based on terephthalic acid moieties and **8a - 8d**, based on isophthalic acid moieties. The solubility of catechol derivatives **1** and **3** is relatively low in chloroform, tetrachloroethane or aromatic solvents. Both diol monomers are soluble in more polar solvents such as THF, DMF or ethanol. Consequently, THF was used as solvent for the polycondensation reactions.

Polyesters **7a**, **7c** and **8a** were found to be insoluble in the reaction medium and precipitated during the reaction. All other polyesters resulted homogeneous solutions. These polyesters were purified by precipitation and extraction with hot methanol for a few days. The extraction procedure further removed not only residual reactants and solvent, but also fractions of oligomers and cyclic products. As a result, the yields were typically in a 60 to 70% range.

Solubility :

The solubility behavior of the synthesized polyester series demonstrates the influence of chain stiffness and substitution with

Scheme 3. Polycondensation of catechol derivatives **1** and **3** with aromatic diacid chlorides and chemical structures of polyesters **7a** - **7d** and **8a** - **8d**.

No.	R	Ar	No.	R	Ar
7a	H		**8a**	H	
7b	H	Ph	**8b**	H	Ph
7c	OCH$_3$		**8c**	OCH$_3$	
7d	OCH$_3$	Ph	**8d**	OCH$_3$	Ph

phenyl groups. The results of solubility tests which were conducted at concentration of 4 percent by weight are summarized in Table 1. Polyester series **7a** - **7d** based on terephthalic acid moieties shows the effect of the lateral phenyl substituent on the solubility. Both polyesters **7a** and **7c** are not soluble in low boiling organic solvents such as chloroform and

THF, whereas the phenyl substituted polyesters **7b** and **7d** are soluble. Series **8a** - **8d** which is based on isophthalic acid is more soluble than series **7a** - **7d**. This is a consequence of the higher chain flexibility due to meta-linkage in the isophthalic acid units. With exception of polymer **8a**, which is only partially soluble in chloroform and THF, all other polyesters of this series are soluble. A good solvent for all synthesized polyesters is DMF. The polymers are as a result of their polar nature insoluble in non-polar aromatics such as benzene. This solubility profile enables thin film preparation by spin-coating from low boiling solvents, as well opens the possibility of multi-layer structures with other polymers.

Table 1. Solubility of dicyanovinyl- substituted aromatic polyesters **7a** - **7d** and **8a** - **8d**.

Polymer	Solubility [a]			
	CHCl₃	THF	DMF	benzene
7a	-	-	±	-
7b	+	+	+	-
7c	-	-	+	-
7d	+	+	+	-
8a	±[b]	±[b]	+	-
8b	+	+	+	-
8c	+	+	+	-
8d	+	+	+	-

a) determined for a 4% (w/v) solution

b) only low molecular weight portion was soluble

GPC investigations :

Gel permeation chromatography (GPC) investigations on chloroform soluble polyesters revealed a multi-modal distribution with sharp and isolated peaks in the low molecular weight region. It will be demonstrated later, that these peaks are caused by the formation of a substantial amounts of cyclic products. The determined molecular weights of these peaks were in good agreement with cycles consisting of two and three monomer units. The determined molecular weight for the linear polyesters fractions were in the range of 4000 - 8000 g/mol.

Figure 2 compares the GPC-chromatograms of structurally isomeric polyesters **7d** and **8d**. For both polyesters the isolated
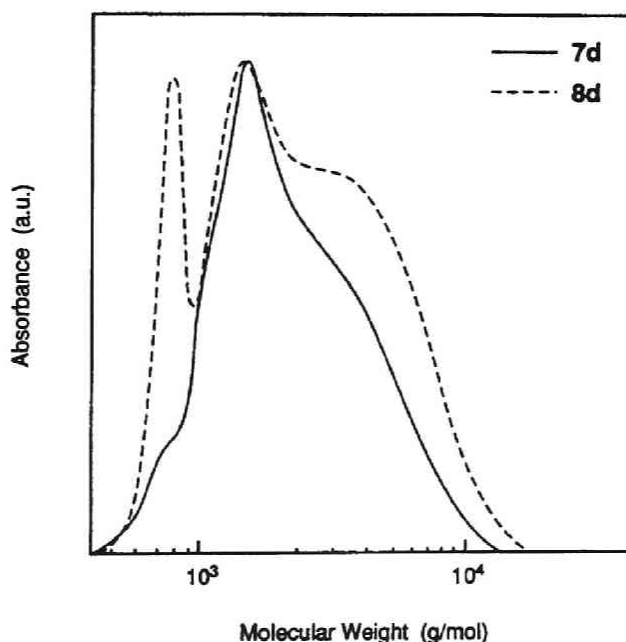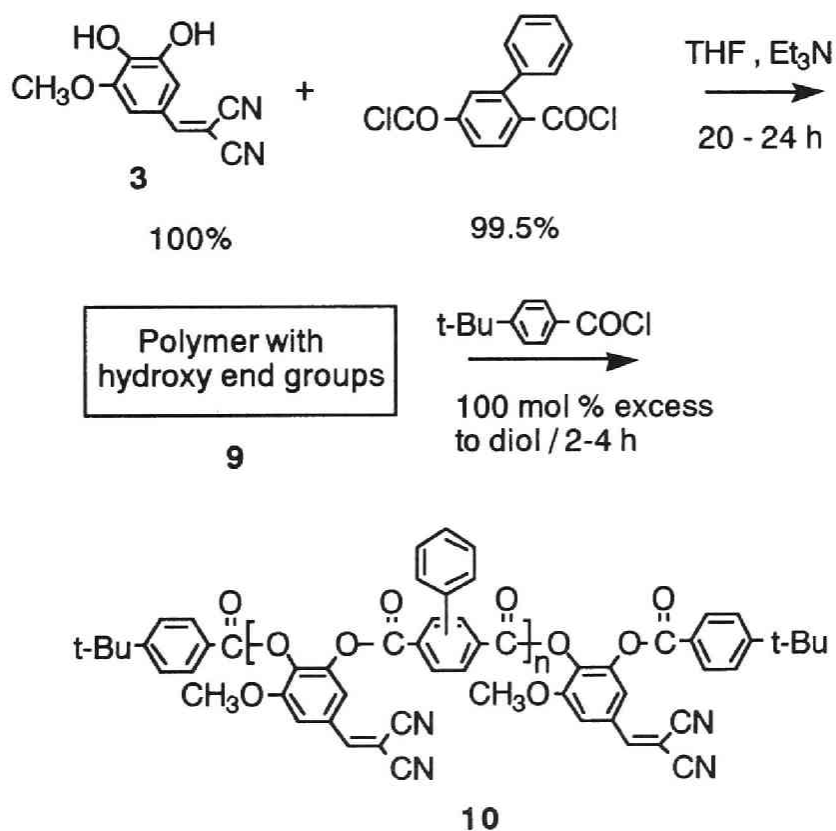

Figure 2. GPC chromatogram of aromatic polyester **7d** and **8d**, after extraction with methanol.

peaks in the low molecular weight region were found at the same position. Polyester **8d** derived from phenylisophthalic acid displays two distinct peaks corresponding to the cyclic products with two and three monomer units. A monomer unit consists of one diacid and one diol moieties. In polyester **7d** the amount of the cycle based on two monomer units is much smaller and only indicated as shoulder. This difference is a reflection of the conformational flexibility in combination to steric hindrance of the oligomeric chain during polycondensation, thus influencing the probability of the cycle formation. Polyester **8a** has in addition to the *ortho*-diol component a *meta*-diacid component which promotes to a larger extent the formation of two monomer unit containing cycle. The *para*-diacid unit does not allow the formation of the two monomer unit cycle so easily.

To proof the existence of the cyclic structures and to distinguish from linear oligomers, the polyester based on 3,4-dihydroxy-5-methoxybenzylidenemalononitrile **3** and phenyl-terephthaloyl dichloride was synthesized with a slight excess of the diol monomer (Scheme 4). The resulting polyester with hydroxy end groups **9** was end-capped with a large excess of 4-*t*-butyl-benzoyl chloride. Figure 3a shows the GPC-chromatogram of the *t*-butyl end-capped polyester **10**. The peak marked with **a** results from the diol monomer which reacted on both hydroxy groups with *t*-butylbenzoyl chloride. The peak position is identical with that determined for the model compound prepared in a separate reaction. Also, the sharp peaks in the low molecular weight region are present. The polyester was fractionated by preparative GPC with THF as eluent. Figure 3b shows the chromatograms of different isolated fractions. Fraction **b** corresponds to the cyclic product consisting of two monomer units and fraction **c** to the cyclic product of three monomer units. ^{1}H-NMR investigations on both fractions confirmed the cyclic structure. No signals of the *t*-

butyl group as well as signals from other endgroups were detectable. FT-IR investigations confirmed also this result. Fraction **d** consists mainly of the linear polyester **10** with *t*-butyl endgroups.

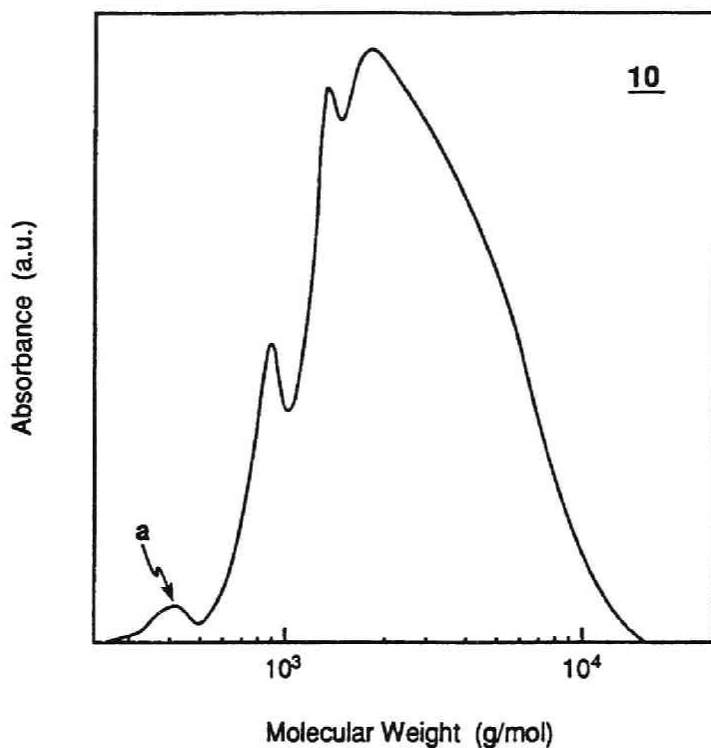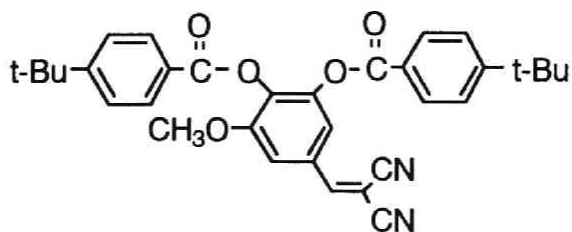**Scheme 4.** End-capping reaction with 4-*t*-butylbenzoyl chloride, resulting to the end-capping polyester **10**.

Figure 3. **(a)** GPC chromatogram of reaction mixture of end-capping reaction with *t*-butylbenzoyl chloride of polyester **10**: Peak **a** corresponds to the compound below.
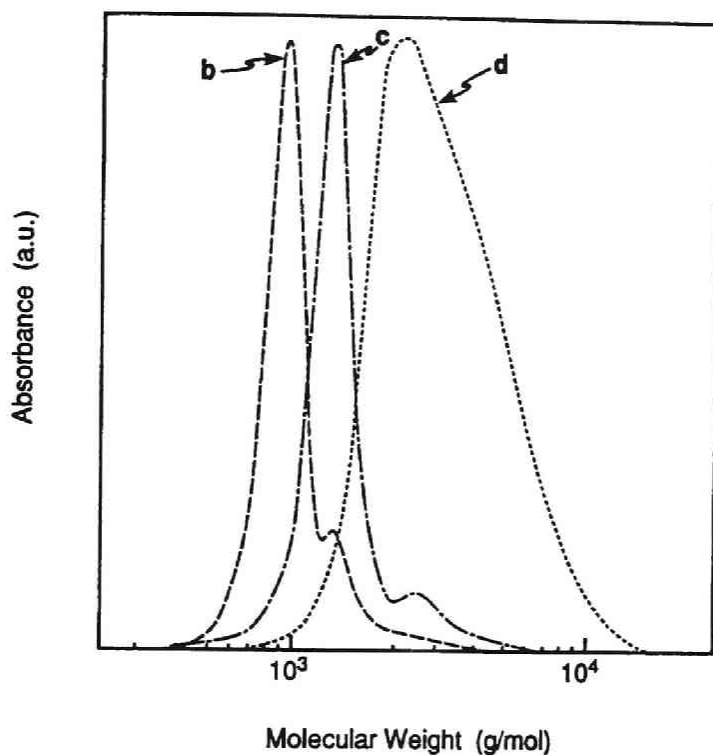
Figure 3. (b) GPC chromatogram of fractions
of polyester **10** separated by preparative GPC :
    b: cycle consisting of two monomer units.
    c: cycle consisting of three monomer units.
    d: endcapped polymer **10.**

Thermal properties :

    The synthesized polyesters were investigated with respect to
their thermal properties by differential scanning calorimetry
(DSC) and thermogravimetric analysis (TGA). The results are
summarized in Table 2 and DSC curves of **7a - 7d** and TGA of
7d are illustrated in figures 4 and 5, respectively.

165

Table 2. Thermal properties of dicyanovinyl substituted aromatic polyesters **7a - 7d** and **8a - 8d**.

No.	$Tg^{a)}$ (°C)		$TGA^{c)}$ (°C)
	1st	$2nd^{b)}$	
7a	143	143	388
7b	145	149	404
7c	148	154	373
7d	153	158	390
8a	145	149	405
8b	154	154	391
8c	_d)	157	390
8d	_d)	173	392

a) determined by DSC (heating curve : 10 °C/min)

b) Samples were quenched from 250 °C after
   1st heating.

c) determined by TGA: peak temperature of 1st
   derivative.

d) not clearly

DSC measurements demonstrate the amorphous character of the polyesters. A glass transition was observed for all polymers in the first and second heating curve in a temperature range between 140 °C and 175 °C. Figure 4 show the second heating curves of quenched samples for polyester series **7a - 7d**. DSC curves of series **8a - 8d** are similar to series **7**. The glass transition temperatures depend on degree of substitution and bulkiness of the lateral side group. Tg increases with increasing size and number of substituents. In all cases the phenyl substituted polymers have higher glass transition temperatures compared to the polyesters

without phenyl groups. Also a slight increase is observable with increasing chain flexibility. The fact that the polyesters do contain certain amounts of cycles may also have an influence on the observed glass transition temperature. As an example for the thermal stability, the TGA curves of polyester **7d** in nitrogen atmosphere are presented in figures 5. Up to temperatures of almost 300 °C no weight loss is detectable. In all cases the degradation takes place in one step. The minimum of the first derivative falls in all cases between 390 and 405 °C.
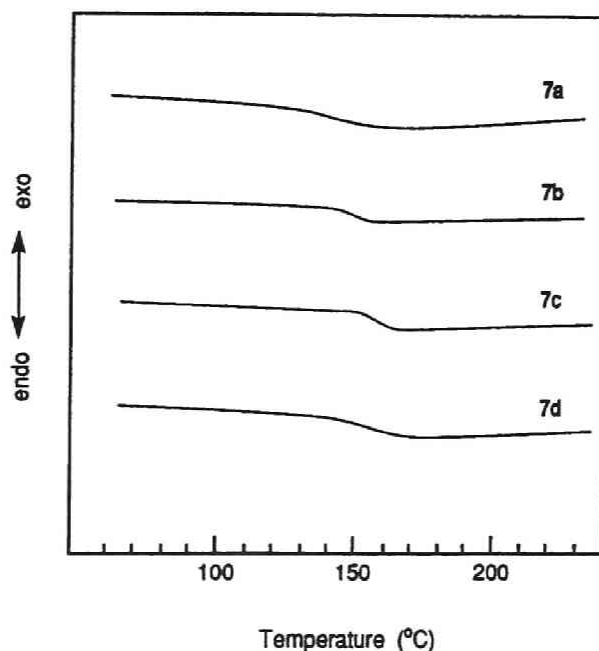

Figure 4. Differential scanning calorimetry (DSC) curves of dicyanovinyl substituted aromatic polyesters **7a-7d** (second heating, heating rate of 10 °C/min).
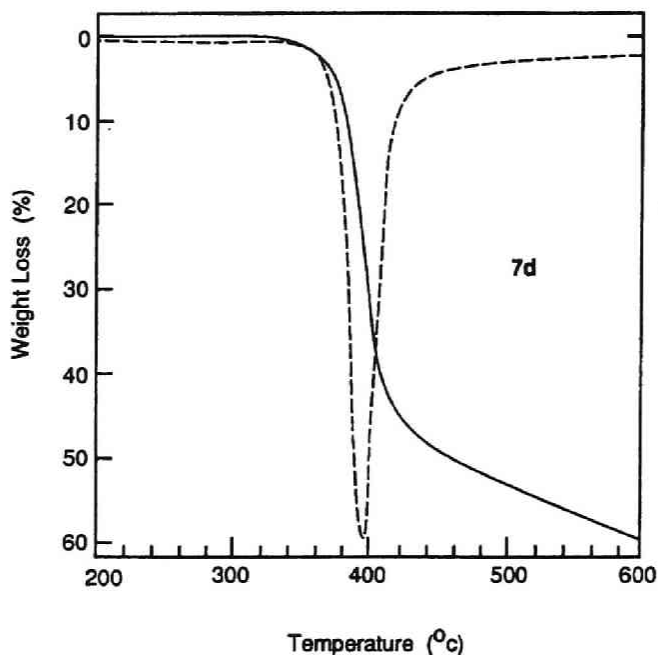
Figure 5. TGA curve of aromatic polyester **7d** with a heating rate of 20 K/min under nitrogen.

Optical Properties :

The optical properties of the chloroform-soluble polyesters were investigated in solution and as thin films on quartz or silicon substrates. A summary of UV-VIS spectroscopy data in chloroform solution and on a quartz substrate is given in Table 3. The films on substrates were prepared by spin coating from chloroform solution and had a thickness of 0.3 - 0.7 μm. All films are amorphous, of uniform thickness, optically clear, and transparent in the visible region. Absorption spectra of films of **7b, 7d, 8b, 8c** and **8d** on quartz substrate are shown in figures 6 and 7. The difference in chemical structures is reflected in various

Table 3. Absorption properties of dicyanovinyl-substituted aromatic polyesters **7a-7d** and **8a-8d**.

Polymer	Solution[a]		Film[b]	
	λ_{max}(nm)	ε[c]	λ_{max}(nm)	$\lambda_{cut-off}$(nm)[d]
7b	314	18000	316	400
7d	317	18400	322	428
8b	310	23000	306	396
8c	316	25000	322	420
8d	309	20100	310	418

a) measured in chloroform solution

b) on quartz substrate: thickness 0.3 - 0.7μm

c) caluculated per monomer unit

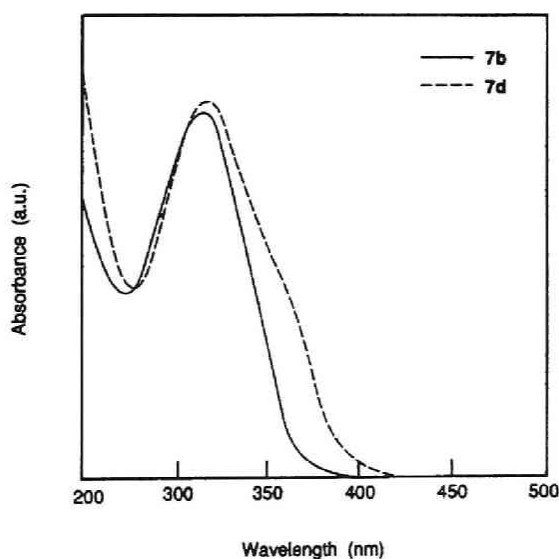d) at zero absorption of under 1 μm thickness film

Figure 6. Absorption spectra of spincoated polyesters of **7b** and **7d** on a quartz substrate (thickness, 0.3-0.7 μm).
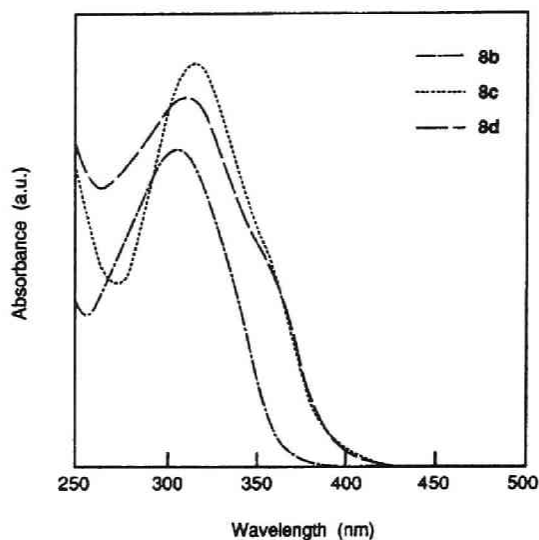
Figure 7. Absorption spectra of spincoated polyesters of **8b**, **8c**, and **8d** on a quartz substrate (thickness, 0.3-0.7 μm).

aspects in the absorption spectra. The conformation and conjugation of the polyester backbone, which is a segment of the chromophore, has an influence on the absorption spectra. The absorption maxima in solution and as film are for the polymers with terephthaloyl units (**7b** and **7d**) at a higher wavelength, compared to the isomeric polymers with isophthaloyl units (**8b** and **8d**). The same trend is observed for the cut-off wavelength. A comparison of **8c** with **8d** indicates that the phenyl substituent in *ortho*-position to the carbonyl group twists the planar ester group out of conjugation. Therefore, **8d** has a lower absorption maxima than **8c**. Compared to the polyesters **7b** and **7d**, the absorption spectra of the polymers with methoxy substituent (**8b**, **8c** and **8d**) show a recognizable shoulder and a bathochromic shift. The cut-off wavelength of the methoxy substituted polymers is higher

170

compared to the polymers without the methoxy substituent. All this demonstrates the effect of the methoxy group as an additional electron donor.

Refractive indices of the spin-coated films were measured by a prism coupling method on silicon substrates at 632.8 nm. Values of 1.63 were obtained for polyesters without methoxy substituent (**7b** and **8b**), and of 1.61 for polyesters with methoxy substituent (**7d** and **8d**). These values are relatively high for organic polymers, in particular compared to acrylate based polymers. The relative high refractive index is due to the large amount of aromatic structures in these polyesters.

The synthesized polyesters possess as a consequence of the dicyanovinyl substituent strong dipole moments. This permits the alignment of the dipoles to a non-centrosymmetric structure by an external electric field near the glass transition temperature. The alignment can be conserved for certain time, but relaxes back. In first qualitative experiments it could be demonstrated that corona poled thin films on ITO glass substrate are capable of indicating second harmonic generation (SHG) of the Nd-YAG laser (1.06 μm). SHG intensity of corona poled thin films of **7d** was in the order of 1/10 of quartz. The values for SHG and the stability strongly depend on the polymer structure and the poling conditions.

Conclusions

3,4-Dihydroxybenzylidenemalononitrile and 3,4-dihydroxy-5-methoxy-benzylidenemalononitrile can be prepared in high yields with malononitrile by a *Knoevenagel* reaction. These monomers were used for preparation of aromatic polyesters with dicyanovinyl substituents. These diol monomers are also interesting starting materials to prepare dimethacrylates for crosslinked systems by free radical reactions. GPC investigations revealed the existence of substantial amounts of defined cyclic products consisting of two and three monomer units. These cycles could be isolated by preparative GPC and characterized. The polyesters with phenyl substituents are soluble in common low boiling organic solvents. The polyesters are amorphous and have glass transition temperatures between 140 °C and 170 °C. Films of uniform thickness, optically clear and transparent in the visible region could be prepared by spin coating. The absorption maxima and cut-off wavelength, which are controlled by the chemical structure, are in the range of 306 to 322 nm and 400 to 420 nm, respectively. The polyesters with methoxy substituent have generally absorptions at longer wavelength. The refractive index was measured as 1.61 and 1.63 at 632.8 nm. Qualitative experiments demonstrated that corona poled thin films on ITO glass substrate display second harmonic generation (SHG) of the Nd-YAG laser (1.06 μm).

References

1) For reviews: a) L. F. Thompson, C. G. Willson and M.J. Bowden (Eds.) *"Introduction to Microlithography"* ACS Symposium Series, **219** (1988), b) M. J. Bowden and S. R. Turner (Eds.) *"Electronic and Photonic Applications of Polymers"* ACS Advances in Chemistry Series, **218** (1988), c) P. N. Prasad and D. J. Williams (Eds.) *"Nonlinear Optical Effects in Molecules and Polymers"*, John Wiley & Sons (1991), d) S. R. Marder, J.E. Sohn and G. D. Stucky (Eds.) *"Materials for Nonlinear Optics"*, ACS Symposium Series **455** (1991), e) P. N. Prasad and D. R. Ulrich (Eds.) *"Nonlinear Optical and Electroactive Polymers"*, Plenum Press (1988), f) C. B. McArdle (Ed.) *"Side Chain Liquid Crystal Polymers"*, Blackie (1989).

2) a) H. W. Gibson, *Polymer,* **25,** 3 (1984), b) J. E. Mulvaney and R. A. Brand, *Macromolecules,* **13,** 244 (1980), c) F. Fuso, A. Buyle Padias and H. K. Hall, Jr. , *Macromolecules,* **24,** 1710 (1991).

3) a) H. H. Yang, "Aromatic High Strength Fibers", John Wiley & Sons, New York (1989), b) R.B. Seymour and G. S. Kirshenbaum (Eds.) *"High Performance Polymers",* Elsevier, New York (1986), c) R. B. Seymour *"Engineering Polymer Sourcebook"*, McGraw-Hill Publishing Company (1990).

4) a) K. D. Singer, M. G. Kuzyk, W. R. Holland, J. E. Sohn, S. J. Lalama, R. B. Comizzoli, H. E. Katz, and M. L. Schilling *Appl. Phys. Lett.,* **53,** 1800 (1988), b) M. L. Schilling, H. E. Katz, and D.I. Cox , *J. Org. Chem.* **53,** 5538 (1988), c) Z. Ni, T. M. Leslie, A. Buyle Padias, and H. K. Hall, Jr., *Macromolecules,* **24,** 2100 (1991), d) G. Gadret, F. Kajzar and P. Raimond, *Proceedings SPIE* **1560,** 226 (1991), e) Y. Shuto, M. Amano and T. Kaino, *Proceedings SPIE* **1560,** 184 (1991).

173

5) H. E. Katz, K. D. Singer, J. E. Sohn, C. W. Dirk, L. A. King and H. M. Gordon, *J. Am. Chem. Soc.,* **109,** 6561 (1987).

6) a) R. H. Page, M. C. Jurich, B. Reck, A. Sen, R. J. Twieg, J. D. Swalen, G. C. Bjorklund and C. G. Wilson, *J. Opt. Soc. Am. B.,* **7,** 1239 (1990), b) S.J. Bethke, S. G. Grubb, H.L. Hampsch and J.M. Torkelson, *Proceedings SPIE* **1216,** 260 (1990), c) G. Knabke, H. Francke and W. F. X. Frank, *J. Opt. Soc Am. B* **6,** 761 (1989), d) J. I. Thackara, G. F. Lipscomb, M. A. Stiller, A. J. Ticknor and R. Lytel *Appl. Phys. Lett.* **52,** 1031 (1988).

7) a) H .T. Land, W. Hatke, A. Greiner, H.- W. Schmidt and W. Heitz, *Makromol. Chem.,* **191,** 2005 (1990), b) W. Hatke, H.-W. Schmidt and W. Heitz, *J. Polym. Sci., Part A: Polym. Chem.* **29,** 1387 (1991).

8) K. W. Rosenmand and T. Boehm, *Ann.,* **437,** 125 (1924).

9) S. K. Banerjee, M. Manolopoulo and J. M. Pepper, *Can. J. Chem.,* **40,** 2175 (1962).

10) R. Chapurlat and J. Dreux, *Bull. Soc. Chim. France,* 349 (1962).

11) K. Alder, J. Haydn, K. Neufang, G. Hansen and W. Gerhard, *Ann.,* **586,** 110 (1954).

12) G. Jones, *Org. React.,* **15,** 204 (1967).

13) K. Tamao, A. Minato, N. Miyake T. Matsuda, Y. Kiso and M. Kumada, *Chem. Lett.,* 133 (1975).

LIST OF PUBLICATIONS

Chapter 1.   (a) M. Uetsuki and N. Kawatsuki
Microoptics News **6** (3) 165 - 170 (1988).

(b) N. Kawatsuki, R. Watanabe, T. Tokuhara, M. Uetsuki, S. Nagata and H. Ichimura
Submitted to *J. Appl. Polym. Sci.*

Chapter 2.   Y. Ito, Y. Aoki, T. Matsuura, N. Kawatsuki and M. Uetsuki
J. Appl. Polym. Sci., **42** (2) 409 - 415 (1991).

Chapter 3.   N. Kawatsuki and M. Uetsuki
Appl. Opt., **29** (2) 210 - 215 (1990).

Chapter 4.   N. Kawatsuki and M. Uetsuki
Jpn. J. Appl. Phys. part 1, **29**, (11), 2420 - 2423 (1990).

Chapter 5.   N. Kawatsuki, H.-W. Schmidt and K. Pakbaz
J. Appl. Polym. Sci., **50** (9), 1575 - 1582 (1993).

Chapter 6.   (a) N. Kawatsuki, K. Pakbaz and H.-W. Schmidt
Polym. Prep., Am. Chem. Soc., **34**, (1) 713-714 (1993).

(b) N. Kawatsuki, K. Pakbaz and H.-W. Schmidt
Makromol. Chem., Rapid Communication, **14**, 625 - 632 (1993).

Chapter 7. (a) N. Kawatsuki and H.-W. Schmidt
Polym. Prep., Am. Chem. Soc., **33** (1) 984-985
(1992).

(b) N. Kawatsuki, M. Dörr and H.-W. Schmidt
J. Polym. Sci. Part A: Polym. Chem., **31**, 1013-1021
(1993).

The following papers and reviews which are not included in this thesis have been published by the author *et al.*

(1)   Y. Ito, N. Kawatsuki and T. Matsuura
Tetrahedron Lett., **25** (26) 2801 - 2804 (1984).

(2)   Y. Ito, N. Kawatsuki and T. Matsuura
Tetrahedron Lett., **25** (40) 4525 - 4528 (1984).

(3)   Y. Ito, N. Kawatsuki, B. P. Giri, M. Yoshida and T. Matsuura
J. Org. Chem., **50** (16) 2893 - 2904 (1985).

(4)   N. Kawatsuki and M. Uetsuki
"Polymers for lightwave and integrated optics", L. A. Hornak ed. Marcel Dekker, p 171 - 193 (1992).

(5)   M. Uetsuki and N. Kawatsuki
"Handbook for optical materials ", p 889 - 917, Realize INC. (1992).